



# ENERGINET

## Geophysical Surveys For Danish Offshore Wind 2030 - Hesselø South

Title	Geophysical and Geological Survey Report For Hesselø South
Number	BE5376H-711-01-RR
Revision	3.0

3.0	20/02/2024	For Client Review	JWA/SKA	EVA	AMO/LRO
Revision	Date	Description of Revision	Author	Checked	Approved

## REVISION HISTORY

The screen version of this document is always the CONTROLLED COPY. When printed it is considered a FOR INFORMATION ONLY copy, and it is the holder's responsibility that they hold the latest valid version.

The table on this page should be used to explain the reason for the revision and what has changed since the previous revision.

Rev.	Date	Reason for revision	Changes from previous version
1.0	22/09/2023	For Client review	N/A
2.0	19/12/2023	Addressing Client comments	Ref. Deliverable_Register_DOW2030_WPA&C_HS_rev00 (version 1).xlsx
3.0	20/02/2024	Client comments	Ref. Deliverable_Register_DOW2030_WPA&C_HS_Geoxyz comments_20231222_rev01.xlsx

## TABLE OF CONTENTS

<i>Revision History</i> .....	2
<i>Definitions and abbreviations</i> .....	9
<b>1 PURPOSE OF THE DOCUMENT</b> .....	<b>10</b>
<b>2 EXECUTIVE SUMMARY</b> .....	<b>11</b>
<b>3 INTRODUCTION AND BACKGROUND</b> .....	<b>15</b>
3.1 Project overview .....	15
3.1.1 Geological site survey.....	16
3.1.2 Geophysical site survey .....	16
3.1.3 Area of investigation – Hesselø South.....	17
3.1.4 Existing infrastructure .....	18
3.2 Scope of work.....	18
3.2.1 Objectives .....	18
3.2.2 Line Planning .....	18
3.2.3 Parties Involved .....	22
3.3 Reference documentation .....	23
<b>4 GEODETIC PARAMETERS AND TRANSFORMATIONS</b> .....	<b>25</b>
4.1 Horizontal datum .....	25
4.2 Vertical reference.....	25
4.3 Time Reference .....	25
<b>5 SURVEY RESOURCES</b> .....	<b>27</b>
5.1 Survey Vessels.....	27
5.2 Equipment And Software.....	27
<b>6 TECHNICAL QUERIES AND CHANGES TO SURVEY SCOPE</b> .....	<b>30</b>
<b>7 DATA PROCESSING AND INTERPRETATION METHODS</b> .....	<b>31</b>
7.1 Multibeam Echosounder.....	31
7.1.1 Data acquisition.....	31
7.1.2 MBES methodology .....	31
7.1.3 Backscatter methodology.....	34
7.1.4 Data quality assessment.....	35
7.2 Side Scan Sonar .....	38
7.2.1 Data acquisition.....	38
7.2.2 SSS data processing .....	38
7.2.3 Data quality assessment.....	44
7.3 Magnetometer .....	47
7.3.1 Data acquisition.....	47

---

7.3.2	Magnetometer data processing .....	48
7.3.3	Data quality assessment.....	51
7.3.4	Magnetometer dataset profile example .....	52
7.3.5	Magnetic residual anomaly grid .....	53
7.3.6	Magnetic analytic anomaly grid .....	54
7.4	Sub-Bottom Profiler .....	54
7.4.1	Data acquisition.....	54
7.4.2	Data processing .....	55
7.4.3	Data quality assessment.....	55
7.5	2D UHR Seismics .....	56
7.5.1	Data acquisition.....	56
7.5.2	Data processing .....	56
7.5.3	Data quality assessment.....	56
7.6	Seabed Sampling .....	58
<b>8</b>	<b>RESULTS AND INTERPRETATION .....</b>	<b>61</b>
8.1	Classification criteria .....	61
8.1.1	Slope classification criteria .....	61
8.2	Bathymetry.....	61
8.3	Seabed Surface Classification: Geology .....	69
8.4	Seabed Surface Classification: Morphology.....	72
8.4.1	Boulder field identification criteria .....	76
8.5	Seabed Surface Classification: Man-made features .....	76
8.5.1	Archaeological findings .....	76
8.5.2	Wrecks.....	76
8.5.3	Metallic objects .....	79
8.5.4	Cables and ropes .....	80
8.5.5	Pipelines .....	82
8.5.6	Other man-made objects .....	82
8.5.7	Items related to fishing activity.....	82
8.5.8	Seabed disturbances .....	83
<b>9</b>	<b>SUB-SURFACE GEOLOGY .....</b>	<b>84</b>
9.1	Regional geological history .....	84
9.1.1	Pre-Quaternary Geology .....	84
9.1.2	Quaternary Geology .....	84
9.1.3	Late Glacial and Holocene .....	84
9.2	Soil Unit Interpretation .....	85
9.2.1	Shallow Geological Overview .....	85



---

9.2.2	Stratigraphy and general arrangement of units.....	85
9.2.3	Quaternary Deglaciation History.....	86
9.2.4	Shallow geological installation constraints .....	96
9.2.5	Sub-surface acoustic velocity model .....	101
<b>10</b>	<b>COMPARISON BETWEEN SEABED AND SUB-SEABED FINDINGS.....</b>	<b>103</b>
<b>11</b>	<b>CONCLUSIONS .....</b>	<b>104</b>
<b>12</b>	<b>OVERVIEW OF THE DIGITAL DELIVERABLES .....</b>	<b>107</b>
12.1	Geological survey .....	107
12.2	Geophysical survey .....	108
<i>REFERENCES.....</i>		<i>111</i>
<b>APPENDIX A.</b>	<b>Hesselø South – UHR Seismic Processing Report.....</b>	<b>112</b>
<b>APPENDIX B.</b>	<b>Surficial Geotechnical Ground-Truthing Report .....</b>	<b>113</b>

## LISTS OF TABLES AND FIGURES

Table 1: Abbreviations used in this document .....	9
Table 2: Coordinates of Hesselø South survey area .....	17
Table 3: Summary of Hesselø South survey area .....	18
Table 4: Client specifications and survey overview .....	21
Table 5: Reference documents .....	23
Table 6: Project Reports .....	24
Table 7: Datum parameters .....	25
Table 8: Projection parameters .....	25
Table 9: Survey vessel specifications .....	27
Table 10: GOV survey equipment specifications .....	27
Table 11: GOVI survey equipment specifications .....	28
Table 12: Primary software list .....	29
Table 13: TQ clarifications and outcomes .....	30
Table 14: MBES system settings .....	31
Table 15: MBES client specifications .....	31
Table 16: Loading MBES data in Qimera .....	32
Table 17: MBES positioning verification .....	32
Table 18: MBES data de-spiking and processing .....	32
Table 19: MBES data quality control .....	32
Table 20: MBES target picking .....	33
Table 21: SSS system settings .....	38
Table 22: SSS specifications .....	38
Table 23: Importing SSS data into SonarWiz .....	39
Table 24: Navigation correction in SonarWiz .....	39
Table 25: SSS signal processing .....	39
Table 26: SSS infill assessment .....	39
Table 27: SSS contact picking .....	39
Table 28: SSS mosaic creation .....	42
Table 29: SSS seabed classification .....	42
Table 30: MAG system settings .....	47
Table 31: MAG client specifications .....	47
Table 32: Magnetometer navigation processing .....	48
Table 33: Magnetometer altitude processing .....	48
Table 34: Magnetometer data QC .....	49
Table 35: Magnetometer background calculation .....	49
Table 36: Magnetometer residual field calculation .....	49
Table 37: Magnetometer dynamic range calculation .....	49
Table 38: Magnetometer target picking .....	50
Table 39: SBP client specifications .....	54
Table 40: SBP data import and data QC .....	55
Table 41: Client 2D UHR specifications .....	56
Table 42: Slope classification .....	61

Table 43: Acoustic characteristics of the sediment types within the Hesselø South site .....	69
Table 44: Morphological interpretation .....	73
Table 45: Boulder field classification .....	76
Table 46: Summary of man-made objects.....	76
Table 47: Wrecks within Hesselø South survey area.....	77
Table 48: Shallow geological units.....	86
Table 49: Overview of the digital deliverables for the geological survey .....	107
Table 50: Overview digital deliverables for the geophysical survey .....	108
Figure 1: Project location for Hesselø South, the Baltic Sea .....	15
Figure 2: Overview of Hesselø South.....	17
Figure 3: Hesselø South geological survey line plan.....	19
Figure 4: Hesselø South geophysical survey line plan .....	20
Figure 5: Hesselø South geophysical survey updated line plan .....	21
Figure 6: Parties involved in the project.....	23
Figure 7: General MBES data processing workflow.....	34
Figure 8: TVU coverage map.....	35
Figure 9: THU coverage map .....	36
Figure 10: Backscatter data across the Hesselø South survey area .....	37
Figure 11: Example of stripe effect on the backscatter mosaic in Hesselø South .....	37
Figure 12: Automated boulder detection progress.....	41
Figure 13: Automatic correct boulder detection vs false positive boulder detection .....	42
Figure 14: SSS data processing workflow .....	43
Figure 15: Pycnocline influence on the SSS data in the Data View (top), Coverage Overview (bottom), and the SVP chart (insert).....	44
Figure 16: SSS coverage map.....	45
Figure 17: Pycnocline effect on the outer range of the SSS data (left) and trimmed-cleaned SSS data after Far field transparency function in SonarWiz (right) .....	46
Figure 18: SSS data example HS_B02_SSS_GO6_0523 (MMO ID 107) .....	47
Figure 19: Magnetometer processing workflow .....	51
Figure 20: Data example showing comparison between raw and filtered altitude values.....	52
Figure 21: Data example of a signal strength profile (line 1542_-5376_C_KG_GO5_1623V_-MAG) .....	52
Figure 22: MAG profile example, line C_HS_G06_L534S) .....	53
Figure 23: MAG residual anomaly grid across the survey area .....	53
Figure 24: MAG analytic anomaly grid across the survey site.....	54
Figure 25: Example of UHR data of high quality and good utility in Hesselø South site .....	57
Figure 26: UHR data example showing useful data (good area) and low quality data (bad area) due to the presence of gas.....	57
Figure 27: UHR data example showing dropped shots .....	58
Figure 28: Proposed surficial geotechnical ground-truthing sampling locations within the Hesselø South area .....	60
Figure 29: Bathymetry across Hesselø South area .....	62

---

Figure 30: Bathymetry profiles based on selected line plan segments and a profile across the broad channel feature (A-B) .....	63
Figure 31: Bathymetry and slope map of the broad channel in the western central part of the survey area	65
Figure 32: Bathymetry and slope map of a boulder field in the southern part of the survey area .....	66
Figure 33: Slope map of the three wrecks found within the survey area .....	67
Figure 34: Slope map of a smaller elevated feature in the southeastern part of the survey area .....	68
Figure 35: Wentworth Scale – classifying sediment particles .....	70
Figure 36: EMODNET Folk substrate classification .....	71
Figure 37: Seabed surface geology classification .....	72
Figure 38: Seabed surface morphology classification .....	73
Figure 39: Overview of wreck 1 .....	77
Figure 40: Overview of wreck 2 .....	78
Figure 41: Overview of wreck 3 .....	79
Figure 42: Overview of metallic targets found within the survey site .....	80
Figure 43: Overview of soft rope targets found within the survey site .....	81
Figure 44: Example of an MMO identified as soft rope (HS_B05_SSS_GO6_1587) .....	81
Figure 45: Overview of other man-made targets within the survey site .....	82
Figure 46: MMO related to fishing activities (HS_B05_SSS_GO6_1648) .....	83
Figure 47: Geological schematic, general arrangement of units.....	86
Figure 48: SBP data example, line L028 (location shown in Figure 50), Unit I ponded against glacial ridge ..	88
Figure 49: SBP data example, line X_07 (location shown in Figure 50), Unit I within channel .....	88
Figure 50: Thickness and distribution of Unit I Holocene deposits .....	89
Figure 51: SBP data example, line L_047 (location shown in Figure 50), Unit I, typical.....	89
Figure 52: UHR data example, line L_006 (location in Figure 54), glacial/late glacial delta and till ridge .....	91
Figure 53: UHR data example, line L_008 (location in Figure 54), late glacial character and till ridge .....	91
Figure 54: Thickness and distribution of Unit II late glacial deposits .....	92
Figure 55: Interaction of till ridge, Unit II thickness and Unit I distribution/Unit II outcrop.....	92
Figure 56: Thickness and distribution of Unit III Glacial deposits .....	94
Figure 57: UHR data example, line L051A (location in Figure 56), Unit III, till platform/ice-contact facies....	94
Figure 58: Depth BSB to H30 (bedrock).....	95
Figure 59: UHR data example, line X05 (location shown in Figure 58), Unit IV, south of the area.....	96
Figure 60: UHR data example, line L04 (location shown in Figure 58), Unit IV, north-west of the area .....	96
Figure 61: SBP data example, line L_014, Unit I, rare point diffraction .....	98
Figure 62: Boulder Factor, Quaternary.....	98
Figure 63: Gas, SBP geological survey .....	100
Figure 64: SBP data example, line X013 (location in Figure 63), Unit II, gas .....	100
Figure 65: UHR data example, line X17C (location in Figure 63), Unit II, gas .....	101



## DEFINITIONS AND ABBREVIATIONS

Throughout this document the abbreviations are listed in Table 1. Where abbreviations used in this document are not included in this list, it may be assumed that they are either equipment brand names or company names.

**Table 1: Abbreviations used in this document**

Abbreviation	Definition	Abbreviation	Definition
2D	Two Dimensional	ka BP	kilo annum [thousand years] Before Present
3D	Three Dimensional	MBES	Multibeam Echosounder
AS	Analytical Signal	mE	Metres East
BSB	Below Seabed	mN	Metres North
BSL	Below Sea Level	MRU	Motion Reference Unit
CPT	Cone Penetration Test	MSL	Mean Sea Level
dB	Decibel	NMEA	National Maritime Electronics Association
DGNSS	Differential Global Navigation Satellite System	nT	Nanotesla
DTM	Digital Terrain Model	QC	Quality Control
ECR	Export Cable Route	RES	Residual Magnetic Field
EGN	Empirical Gain Normalisation	SBP	Sub-Bottom Profiler
EPSG	European Petroleum Survey Group	SEGY	Society of Exploration Geophysicists Y format
ETRF2000	European Terrestrial Reference Frame 2000	SIMOPS	Simultaneous Operations
ETRS89	European Terrestrial Reference System 1989	SP	Shot Point
FMGT	Fledermaus Geocoder Toolbox	SSS	Side Scan Sonar
GIS	Geographic Information System	SVP	Sound Velocity Profile
GOIV	Geo Ocean IV	THU	Total Horizontal Uncertainty
GOV	Geo Ocean V	TPU	Total Propagated Uncertainty
GRS80	Geodetic Reference System 1980	TVU	Total Vertical Uncertainty
HS	Hesselø South site	TWT	Two Way Time
Hz	Hertz	UHR	Ultra-High Resolution
IHO	International Hydrographic Organisation	USBL	Ultra-Short Baseline
INS	Inertial Navigation System	UTM	Universal Transverse Mercator
IOGP	International Association of Oil and Gas Producers	UXO	Unexploded Ordnance
ITRF	International Terrestrial Reference Frame	ZDA	NMEA-0813 Date Time Message String (UTC, day, month, year, and local time zone offset)



## **1 PURPOSE OF THE DOCUMENT**

This report focuses on the geological and geophysical surveys, detailing the geophysical and geological results for the Hesselø South survey site. This report will detail the findings from the five sensors used to investigate the Hesselø South area, giving a detailed overview of the survey site, as well as listing any hazards that are likely to affect the scope or objectives of the survey, or potential later installation works.

## 2 EXECUTIVE SUMMARY

Hesselø South			
Survey dates	Geological survey	Start	14/01/2023
		End	11/04/2023
	Geophysical survey	Start	28/01/2023
		End	10/03/2023
Sensors	Multibeam Echo Sounder (MBES), Side Scan Sonar (SSS), Magnetometer (MAG), Sub-Bottom Profiler (SBP), 2D Ultra-High Resolution seismic (2D UHR)		
Coordinate system	Datum	European Terrestrial Reference System 1989 (ETRS89)	
	Projection	UTM Zone 32 N (EPSG: 25832)	
<b>Bathymetry</b>			
Depth	16.6 m MSL – 35.3 m MSL		
Site topography	<p>A broad channel feature crosses the western side of the site, approximately delineated by the 27.0 m MSL contours. This feature is between 750 m and 3000 m wide and runs approximately north-south. Seabed levels within the channel range from approximately 25.0 m MSL to a maximum of 35.3 m MSL, at its narrowest part. To the east of the narrow channel feature, seabed levels undulate very gently between approximately 21.0 m MSL and 30.0 m MSL. Levels initially shoal very gently eastwards, towards a broad, low ridge feature, which stands approximately 3.0 m above the surrounding seabed. To the east of the low ridge feature, seabed levels deepen very gently towards the east and north-east. To the west of the broad channel feature, seabed levels deepen very gradually towards the east, or east-northeast.</p>		
Slope angles	<p>Typical slope gradients across the survey area range from &lt;math&gt;&lt;0.1^\circ - 3.2^\circ&lt;/math&gt;. The highest slope values (very steep slopes; &gt;15°) are related to the edges of seabed features such as boulders and wrecks, as well as on the sides of localised ridges and smaller elevated features.</p>		
<b>Seabed surface: Geology</b>			
<p>The seabed sediments across much of the northern/north-eastern and southern sections of the site comprise a series of large, irregular outcrops of till/Diamicton, partially covered by large, irregular areas of sands and muddy sands (silty, clayey sands), with finer grained, muddy sands (silty/clayey sands) becoming more prevalent towards the south and west. A curved area of outcropping Quaternary clay and silt is present within the eastern section of the meandering channel feature, which runs across much of the northern section of the site.</p> <p>The seabed across the central, western section of the site comprises an expanse of muddy sands (silty/clayey sands), with occasional, irregular areas of sands and/or areas of gravels and coarse sands. Smaller, less extensive areas of Till/Diamicton are also present in the southern/south-western section of the site, together with several small areas of sands and a larger, irregular area of gravels and coarse sands.</p>			

**Hesselø South**

**Seabed surface: Morphology**

Boulder fields are visible in the southwestern and central part of the site. The high-density boulder fields (Class 2) generally coincide with outcropping/subcropping areas of Till/diamicton, with the intermediate density boulder fields (Class 1) surrounding the Class 2 boulder fields.

Sandwaves are seen in the southwestern part of the survey area. These features are orientated E-W, NW-SE and SW-NE and have wavelengths between 20 m and 130 m, with heights between 0.1 and 1.0 m. Subordinate ripples are present between the sandwaves. These features are similarly orientated and have wavelengths between 0.5 m and 2 m.

Extensive fishing activity, including numerous well-preserved trawl marks are seen, mainly in the northern half part of the area, as well as within the channel feature.

Six areas containing numerous, roughly circular, small depressions, between 0.1 m and 0.4 m deep and up to 5.0 m across, occur in the central-eastern part of the site. These six areas vary between 60 m and 1500 m in width and length. Similar features are seen along a SW-NE line in the southeastern part of the site, possibly related to fishing, surveying or construction activities. An isolated depression, with an approximate radius of 6 to 8 m and 1.5 m depth, occurs in the southern part of the site. Disturbed seabed areas, possibly of anthropogenic origin (fishing, survey, construction activities) are also present.

An irregular, NW – SE orientated seabed mound, approximately 65 m long and up to 2.0 m high, is present in the central part of the site.

An area of unknown features is present in the northern part of the site. These are visible in the MBES data but are not recognizable in the SSS dataset. They could be interpreted as possible sandwaves, but no other evidence of other bedforms such as ripples is present. Alternatively, they could be possible erosional features/ice sculpted areas and a seabed expression of the H05 erosional surface, in an area where Unit II – periglacial-glaciomarine sediments are covered by a thin layer of Unit I Holocene deposits. The interpretation of those features is uncertain.

**Seabed surface: Man-made features and site-specific hazards**

Wrecks	3
Metallic objects	450
Other contacts	464
Rope/wire	8
Cables	0
Pipelines	0

**Sub-seabed soil units**

Unit I	Holocene deposits
Unit II	Late Glacial deposits
Unit III	Glacial deposits
Unit IV	Bedrock (likely Cretaceous Chalk, and/or Jurassic clastics)

## Hesselø South

### 2D UHRS: Geology

The geological foundation zone extends to ~70 m below seabed, with the rocks and sediments interpreted with reference to the supplied GEUS desk study. There is generally a good correspondence between the shallow geology imaged in this project's sub-seabed data and the desk study. In general, the area has a glacial to post-glacial sequence of relatively recent sediments over much older bedrock. The recent sediments are generally 40-50 m thick, though locally these recent sediments are interpreted to be much thicker.

The Holocene Unit (Unit I) comprises post-glacial silty, sandy CLAY, which is less than 1.5 m thick over large parts of the site. Unit I includes a thin veneer of sandier seabed sediments. The Holocene sediments are widely distributed over the study area, but are very thin or absent (unmapped) over an east-west trending glacial/glacio-marine ridge across the centre of the area and in the far south-west, where till is close to the seabed. Small pockets of Holocene may occur in these areas and a <0.2 m thick seabed veneer may be present.

The Holocene deposits are thickest over a north-south trending 1-2 km wide zone situated in the central southern part of the area. Here the deposits partially infill a channel which is still apparent at the seabed and are up to 18 m thick and commonly over 5 m thick. The sediments are best developed on the western side of the axis of the channel and subdue the complex morphology at the base of the Holocene. The channel appears to have its origin during the late glacial/glaciomarine period, it does not correspond with any feature at the top of the bedrock. Here, some of the bedded deposits included within Unit II (the Late Glacial division) may correspond with the earliest Holocene sediments.

The Holocene unit (Unit I) has seismic characteristics indicating that it is very soft/weak and may contain diffuse gas.

The Late Glacial deposits (Unit II) are very complex, due to the area's range of environmental conditions during the Late Weichselian and earliest Holocene. Some intervals show laminations, indicative of clays and silts, others may represent sandy beach-type deposits. The interval is mapped with H2O at its base. This is generally at the top of deposits which show clear signs of ice contact, true glacial deposits.

In the extreme south-west, the Unit II glaciomarine sediments pinch out over a great thickening of the subcropping tills. Taken together, these two intervals form a delta-like complex of deposits sourced from the south (the landward direction), the lower deposits of the Glacial deposits (Unit III) show a greater, more direct, influence of ice, while the later Unit II deposits retain intervals of preserved bedded facies suggesting limited ice contact.

Further north the Unit II deposits thin over an east to west trending till (Unit III) ridge. North of the till ridge the glaciomarine deposits crop out and form a high. It is possible that the glaciomarine deposits to the north of the till ridge were pushed against the deeper till ridge during a later ice advance, perhaps by part of the Baltic Ice Stream. Unit II deposits in this area tend to have a more chaotic internal structure than those south of the till ridge.

Glacial deposits (Unit III) occur through most of the study area, only being absent over very small parts of the north of the site. Unit III is interpreted to be deposited in association with the last major ice advance

## Hesselø South

over the area. The till forms a relatively thin blanket over central and northern areas where it is less than 10 m thick. The till is arranged in a thick platform to the east and thickens considerably to the south where it is at or close to outcrop and comprises the entire post bedrock sequence. There is an east-west trending till ridge running across the site, just south of centre. This ridge generates an approximate 20 m thickness increase in Unit III and a similar reduction in the thickness of Unit II. The desk study indicates that this till ridge is the Sjællands Odde ice marginal ridge.

The upper part of Unit III is generally a glacial till, which has been subjected to direct ice contact. The ice-contact facies may comprise a clay-prone diamicton, which is likely to contain subordinate silt, sand, gravel, cobbles and boulders and will be overconsolidated. Consolidation levels may significantly vary over short distances. Seismically, the ice contact facies is structureless with a very irregular upper surface, which probably forms a series of ridges.

Unit III may contain numerous cobbles and boulders.

The GEUS desk study shows that the Grenå-Helsingborg Fault runs west-north-west to east-south-east through the centre of the area, in the approximate position of the Sjællands Odde ice marginal ridge. Numerous bedrock faults can be made out in the UHR and are mapped on a line-by-line basis. The desk study indicates that the bedrock will likely comprise Cretaceous carbonates and/or Jurassic clastics. These ancient faults were reactivated during the Jurassic/Cretaceous and, in this area, generated subsidence.

The top of the bedrock is generally 40-50 m below seabed, exceeding 60 m and reaching 80 m in the east of the area and over small parts of the far south-west and north. Unit IV may have strength variations, may be weathered at the upper truncation surface, and may locally be weakened by faulting and micro fractures.

### 3 INTRODUCTION AND BACKGROUND

#### 3.1 PROJECT OVERVIEW

Following a decision in the Danish Parliament in 2022, Denmark is on the path to establish offshore energy infrastructure in the Danish inner sea (Kattegat) to connect further offshore wind energy to the Danish mainland. The regional location of the project is shown in Figure 1.



**Figure 1: Project location for Hesselø South, the Baltic Sea**

The offshore elements of the project comprise the following main parts:

- An offshore windfarm in Kattegat (Hesselø South)
- Offshore platforms for substations
- Export cable between offshore wind farms and the Danish mainland

The Danish Energy Agency has instructed the Client to initiate site investigations, environmental and metocean studies for the abovementioned main project elements.

The Client has awarded GEOxyz a contract for a geophysical survey of the Kattegat and Danish Baltic Sea project components, denoted in green in Figure 1.

The scope of the project includes the following work packages:

- Work Package A – Geological site survey
- Work Package C – Geophysical site survey

The scope of Work Package A and C includes the following:

### 3.1.1 Geological site survey

A geophysical site survey comprising Multi Beam Echo Sounder (MBES) including backscatter, Sub Bottom Profiler (SBP) and 2D UHR seismic system is to be performed to map the subsurface geological soil layers. Bathymetry should be mapped along the survey lines, as should the shallow geology.

The functional requirements of this work package are to:

- Map all major geological layers and structures to at least 100 m below seabed.
- Locate structural complexities or geohazards within the shallow geological succession such as faulting, accumulations of shallow gas, buried channels, soft sediments, hard sediments, mobile sediments etc.

### 3.1.2 Geophysical site survey

A full coverage geophysical site survey comprising MBES including backscatter, SSS, magnetometer, and SBP to map the bathymetry, static and dynamic elements of the seabed surface, and the subsurface geological soil layers to at least 10 m below the seabed. Grab sampling is also required to support the interpretation of the seabed surface geology.

The functional requirements of this work package are to carry out a detailed mapping of the seabed surface to provide:

- Accurate bathymetric data and charts in the surveyed areas.
- The morphology and natural features of the seabed surface such as megaripples, sandwaves, boulders, outcropping geology, seaweed and reefs.
- Possible man-made features such as wrecks, debris, fishing gear, trawl marks, anchor scars and objects of potential archaeological interest.
- Identification of features of potential conservation interest including but not limited to; sandbanks, gravel reef, cobble reef, rocky reef and biogenic reef structures.

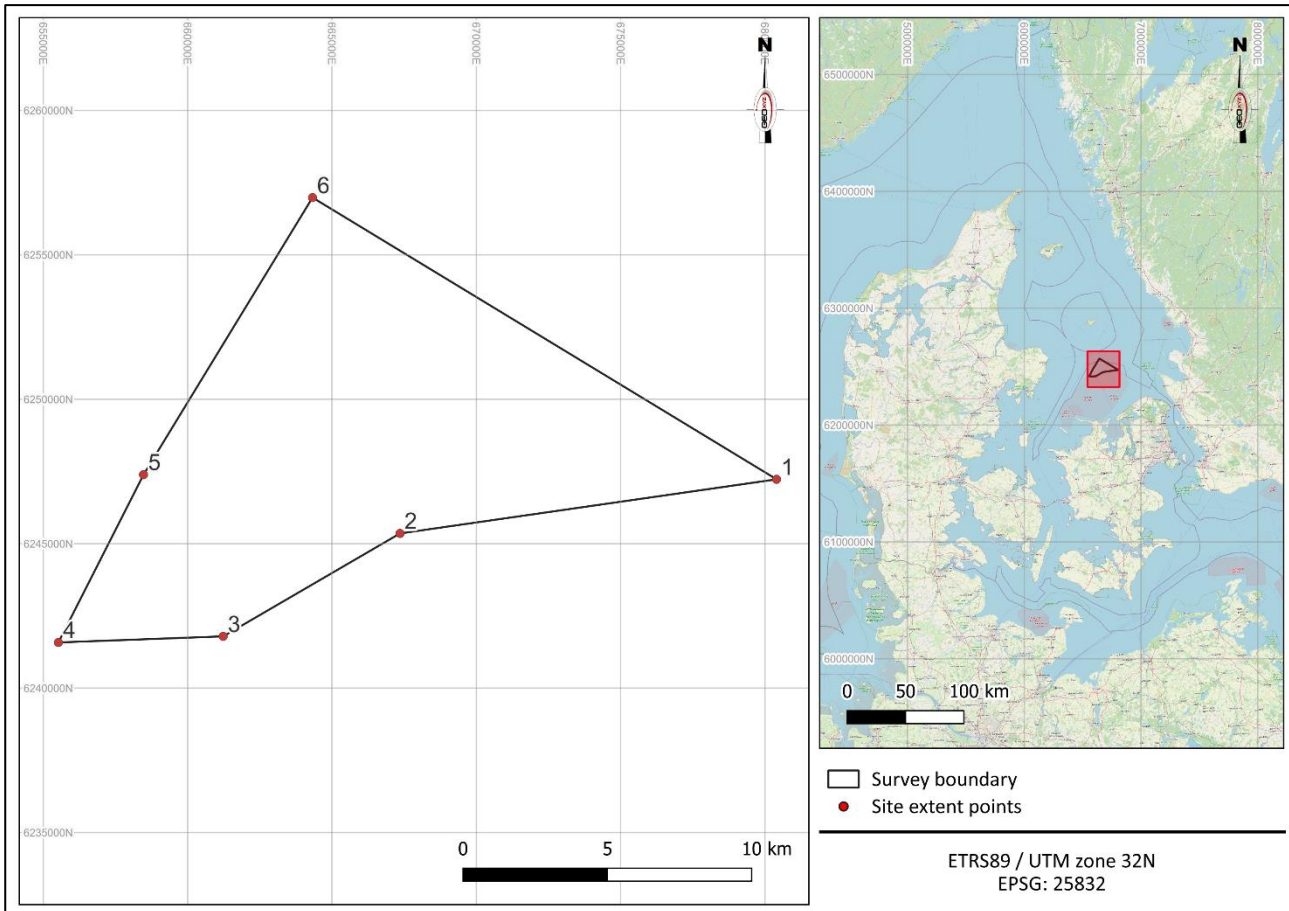
Mapping of the upper part of the seabed subsurface is required to a sufficient level of detail to:



- Locate structural complexities or geohazards within the shallow geological succession such as faulting, accumulations of shallow gas, buried channels, soft sediments, hard sediments, high boulder density, mobile sediments etc.

### 3.1.3 Area of investigation – Hesselø South

The Hesselø South survey site is located in the Kattegat Region off the eastern coast of Denmark (Figure 2). A summary of coordinates and the site extents are displayed in Figure 2, Table 2, and Table 3.



**Figure 2: Overview of Hesselø South**

**Table 2: Coordinates of Hesselø South survey area**

Point ID	Easting EUREF89 Zone 32N (m)	Northing EUREF89 Zone 32N (m)	Longitude EUREF89	Latitude EUREF89
1	680400	6247230	11°55.099' E	56°20.121' N
2	667356	6245357	11°42.383' E	56°19.400' N
3	661231	6241793	11°36.317' E	56°17.608' N
4	655523	6241583	11°30.781' E	56°17.610' N
5	658472	6247391	11°33.847' E	56°20.679' N
6	664326	6256983	11°39.884' E	56°25.724' N

**Table 3: Summary of Hesselø South survey area**

Site	Region	Survey Area Extent (km <sup>2</sup> )
Hesselø South	Kattegat	166

### 3.1.4 Existing infrastructure

No existing infrastructure was found crossing the Hesselø South survey area.

## 3.2 SCOPE OF WORK

The scope for the geological and geophysical surveys was undertaken across 2 vessels, Geo Ocean V and Geo Ocean VI. The vessels were mobilised at the end of 2022 and the surveys were undertaken in 2023. The surveys achieved full coverage in the areas of investigation and mapped the bathymetry, the static and dynamic elements of the seabed surface, and the sub-surface geological soil layers to at least 100 m below seabed.

### 3.2.1 Objectives

The results of the survey will be used as basis for:

- Initial marine archaeological site assessment.
- Planning of environmental investigations.
- Planning of initial geotechnical investigations.
- Decision of foundation concept and preliminary foundation design.
- Assessment of installation conditions for foundations and inter-array cables.
- Site information enclosed the tender for the offshore wind farm concession.

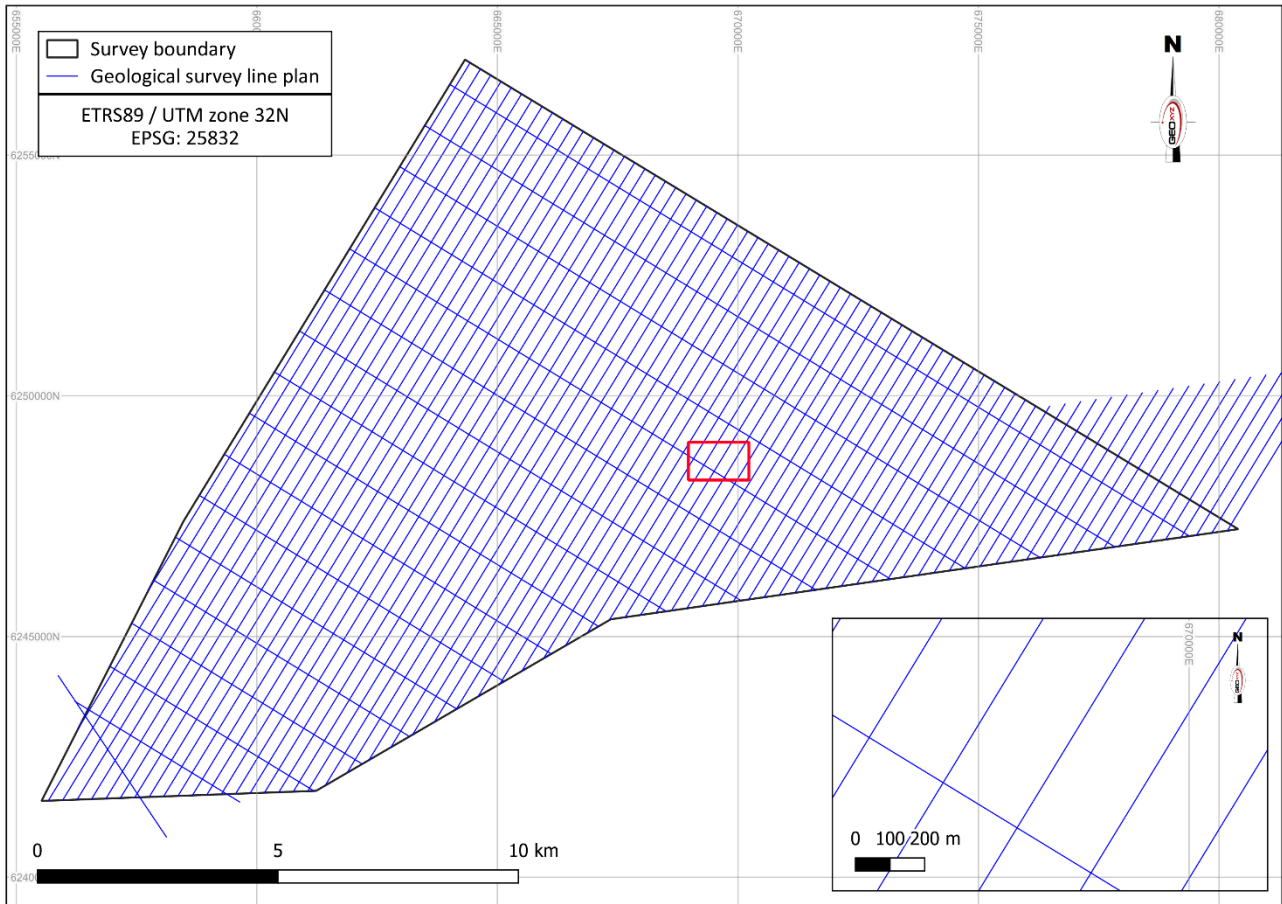
To accomplish these aims GEOxyz:

- Acquired high resolution bathymetric data to ascertain water depth and changes in topography across the sites using multibeam echosounder (MBES) data.
- Acquired high frequency (900 kHz) side scan sonar (SSS) data to identify seabed objects and features.
- Acquired low frequency (300 kHz) side scan sonar (SSS) data to distinguish seabed sediments.
- Acquired magnetometer data to identify cables, pipelines, potential UXOs and other ferrous objects on and below the seabed.
- Acquired high-resolution and 2D ultra high-resolution seismic data, in order to locate structural complexities or geohazards within the shallow geological succession, such as faulting, accumulations of shallow gas, buried channels, soft sediments, hard sediments, high boulder density estimation, mobile sediments, etc.

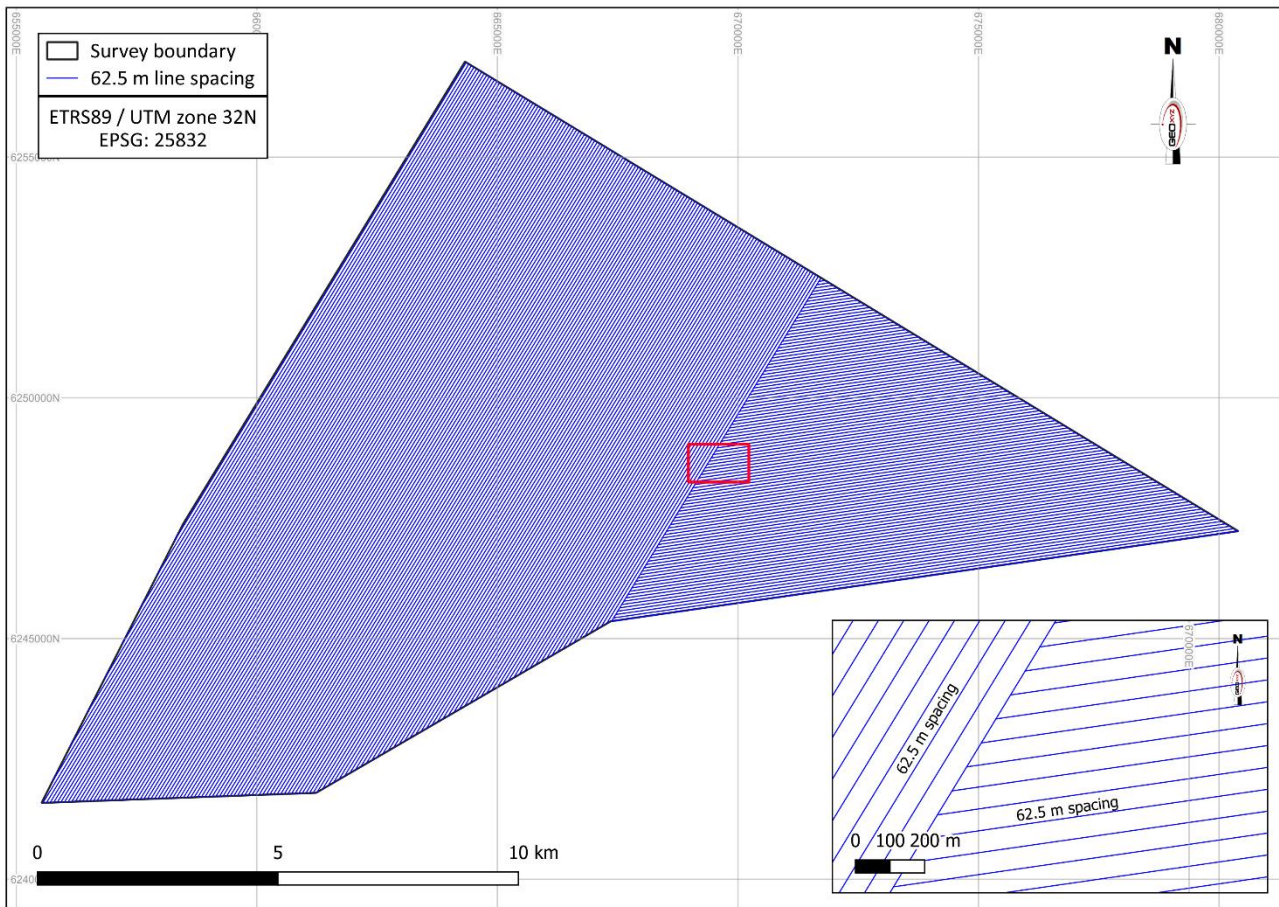
### 3.2.2 Line Planning

For the geological, the survey lines comprised of main lines spaced at 250 m, and cross lines spaced every 1000 m. Survey lines that were shorter than 4 km were extended outside the survey area to obtain this minimum length. Orientation of survey lines were determined to acquire main lines predominantly along the long axis of the site where this is apparent. Figure 3 shows a schematic diagram of the line plan for the geological survey.

For the geophysical survey, the original survey lines were spaced at 62.5 m apart, oriented predominantly along the long axis of the site where this is apparent. Figure 4 shows a schematic diagram of the line plan for the geophysical survey.

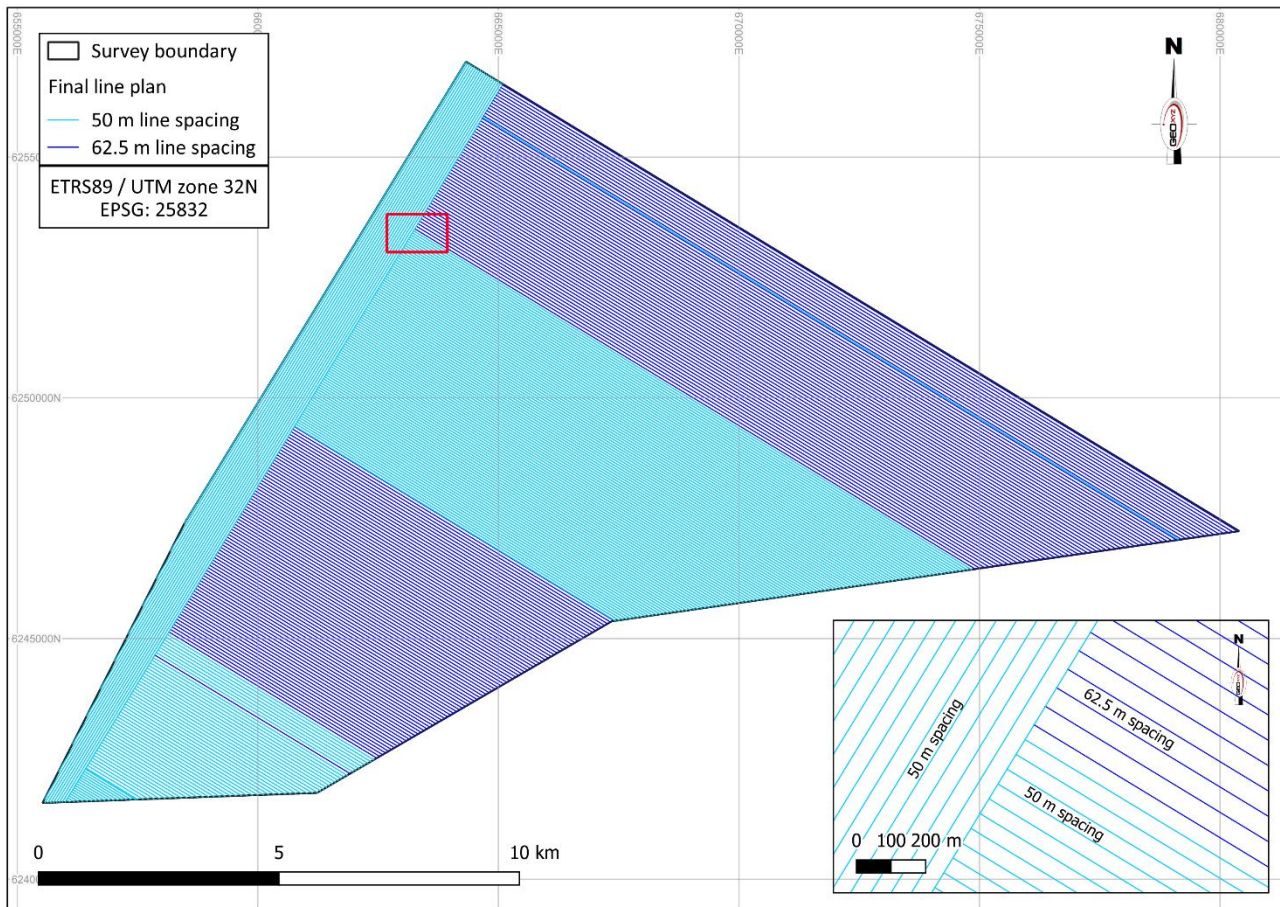


**Figure 3: Hesselø South geological survey line plan**



**Figure 4: Hesselø South geophysical survey line plan**

Due to the presence of a pycnocline and the conditions in the area, the line plan was adapted to make acquisition more efficient. The survey lines in the updated line plan were spaced between 50 and 62.5 m, and have a different orientation. The final line plan for the geophysical survey is displayed in Figure 5.



**Figure 5: Hesselø South geophysical survey updated line plan**

The client specification and survey overview are detailed in Table 4.

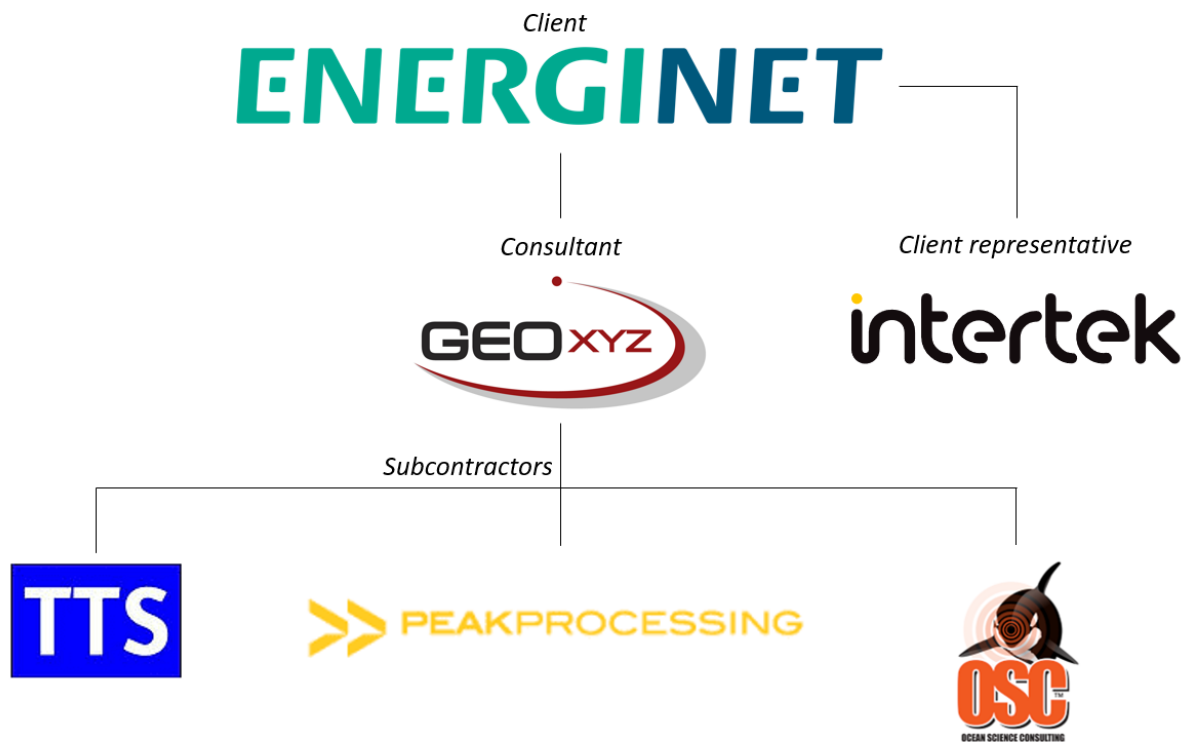
**Table 4: Client specifications and survey overview**

Equipment	Specification	Survey Requirement
<b>Vessels</b>	Multi-vessel operations	Geo Ocean V (GOV) and Geo Ocean VI (GOVI)
<b>Line Planning</b>	Main Lines WPA	Spaced at 250 m
	Cross Lines WPA	Spaced at 1000 m
	Main Lines WPC	Spaced at 50 - 62.5 m
	Cross Line WPC	none
<b>MBES Bathymetry/ Backscatter</b>	Data density	16 hits/m <sup>2</sup> on 99 % of site
	Standard Deviation	0.20 m on 95 % of the site
	MBES Mode	Equidistant
	Gridded	0.25 m cell size
	Coverage	100 %
<b>Side Scan Sonar</b>	Resolution sufficient for detecting seabed object/features	0.5 m (length, width and height)
	Towing altitude	8 - 12 % of range (optimised for data quality)
	Positional accuracy	± 2 m (using vessel course-over-ground and USBL)

Equipment	Specification	Survey Requirement
	Operating mode	High Definition Mode
	Range	70 m
	Coverage	200 %
<b>Magnetometer</b>	Seabed altitude	≤ 3.0 m
	Measurement sensitivity	0.02 nT
	Sampling frequency	≥ 10 Hz
	Noise level	≤ 2 nT
	Coverage (in areas of operation)	100 %
<b>Sub-Bottom Profiler</b>	Penetration	10 m
	Vertical resolution	0.3 m
	System	Innomar SES 2000 or similar
<b>2D Ultra High Resolution</b>	Fundamental frequency	Between 1 and 3 kHz
	Vertical resolution	0.3 m to 40 m depth; 0.5 m to 100 m depth
	Minimum Penetration	100 m
	Fire rate	2 pulses/second
	Feather angle	<12° during 95 % of the shots
	Streamer depth	As per last PEP rev 1.4: 1.0 m ±0.5 m (although primarily determined by weather and data quality)
	Other acquisition parameters (dropped channels, noise threshold etc)	Source depth: 0.4 m ± 0.1 m. Noise thresholds: <ul style="list-style-type: none"> <li>- Random noise: 7 µB (10 µB near/far traces &amp; depth controller locations.</li> <li>- Coherent Noise ahead/astern: 15 µB.</li> <li>- Coherent noise abeam: 5µB.</li> </ul> Dropped bad shots threshold: No dead channels in the near 6 channels and a maximum of 2 non-consecutive dead channels from channel 6 to the far channel. Dropped/bad channels threshold: ≤ 2 channels.
	Variable energy levels	Between 100 and 1000 Joules
	System	A suitable multi-channel and multi-element hydrophone streamer with depth control plus depth measurement for continuous monitoring and recording of streamer depth

### 3.2.3 Parties Involved

The parties involved in the project are represented by the organogram given in Figure 6.



**Figure 6: Parties involved in the project**

### 3.3 REFERENCE DOCUMENTATION

Key project documentation from the Client is listed in Table 5.

**Table 5: Reference documents**

Ref.	Document Number	Title	Owner
1.	22/02940-1	Scope of Services – Lot 1	Client
2.	22/02940-2	Scope of Services – Enclosure 1 – Technical Requirements	Client
3.	22/02940-5	Scope of Services – Enclosure 2 – Standards of Deliverables	Client
4.	22/02940-3	Scope of Services – Enclosure 3 – HSE Requirements	Client
5.	22/02940-4	Scope of Services – Enclosure 4 – Quality Management Requirements	Client
6.	16/19566-2	Requirements to TSG	Client
7.		TQ system (Energinet SharePoint site)	Client

Details on the conducted calibrations prior to the start of the survey and the operational aspects of the survey, including resources, event logs, etc., can be found in the Mobilisation and Calibration Report and the Operations Report, respectively. Information on the methodology and workflow on the datasets is outlined in the Processing Report. This report presents the interpreted results of the geophysical and geological datasets of the survey for the Hesselø South site.

Table 6 lists all the reports delivered as part of this survey, with this report highlighted in **bold**.

**Table 6: Project Reports**

Ref.	Report Document Number	Title	Type of Report
8.	BE5376H-711-MCR-01	Mobilisation and Calibration Report Geo Ocean V	Mobilisation and Calibration Report
9.	BE5376H-711-MCR-02	Mobilisation and Calibration Report Geo Ocean VI	Mobilisation and Calibration Report
10.	BE5376H-711-OR-01	Operations Report geological survey	Operations Report
11.	BE5376H-711-OR-03	Operations Report geophysical survey	Operations Report
12.	<b>BE5376H-711-01-RR-1.0</b>	<b>Hesselø South Geophysical Report – Geological and Geophysical Survey</b>	<b>Results Report</b>



## 4 GEODETIC PARAMETERS AND TRANSFORMATIONS

### 4.1 HORIZONTAL DATUM

The datum parameters for the survey are described in Table 7 and the projection parameters are given in Table 8.

**Table 7: Datum parameters**

Parameter	Details
Name	European Terrestrial Reference System 1989 (ETRS89)
EPSG Datum Code	6258
EPSG Coordinate Reference System	4258
Spheroid	GRS80
EPSG Ellipsoid Code	7019
Semi-Major Axis	6378137.000
Semi-Minor Axis	6356752.314140
Flattening	1/298.2572221010
Eccentricity Squared	0.00669428002290

**Table 8: Projection parameters**

Parameter	Details
EPSG Coordinate Reference Code	25832
EPSG Map Projection Code	16032
Projection	UTM
UTM Zone	32N
Central Meridian	9° East
Latitude of Origin	0°
False Easting	500000.00 m
False Northing	0.00 m
Scale Factor at Central Meridian	0.9996
Units	Metres

### 4.2 VERTICAL REFERENCE

The vertical datum for the project is Mean Sea Level (MSL) as defined by the Technical University of Denmark geoid model DTU21MSL. Height data was acquired relative to the ellipsoid and reduced to the project vertical datum. All reported depths in the current report are related to DTU21MSL.

### 4.3 TIME REFERENCE

The time frame set up in all survey systems on board the vessel as well as the reported time in any official form and document is provide in Coordinated universal time (UTC).



Online displays, overlays and logbooks are annotated in UTC as well as the daily progress report (DPR) and the Daily Processing Progress report (DPPR).

The synchronisation of the survey system is controlled by the ZDA NMEA time and date and the pulse per second (PPS) issued by the primary positioning system.

## 5 SURVEY RESOURCES

### 5.1 SURVEY VESSELS

For the geological and geophysical surveys, the survey vessels Geo Ocean V (GOV) and Geo Ocean VI (GOVI) were utilised to complete the work across the survey site. Both vessels are 54 m and equipped to perform a range of subsea surveys in the offshore renewables, and the oil and gas industries. Additionally, they can both operate 24 hours/day and can remain at sea for up to four weeks. The specifications of the GOV and GOVI are summarised in Table 9.

**Table 9: Survey vessel specifications**

Feature	Geo Ocean V	Geo Ocean VI
Owner:	GEOxyz	GEOxyz
Flag:	Luxembourg	Luxembourg
Length:	53.8 m	53.8 m
Width:	13.0 m	13.0 m
Draught:	4.0 – 4.8 m	4.8 m
Speed:	10 knots (cruising)	11 knots (cruising)
Main Propulsion:	Hybrid propulsion CP-propeller	Hybrid propulsion CP-propeller
Endurance:	28 days	28 days
Accommodation:	24	24
Positioning:	DGPS, HiPaP351 USBL	DGPS, HiPaP352P USBL NAVIS NavDP 4000
A-Frame:	10t Stern	13t Stern
Image of the vessel		

### 5.2 EQUIPMENT AND SOFTWARE

Details on the survey equipment used for this project onboard the GOV and GOVI are listed in Table 10 and Table 11, respectively.

**Table 10: GOV survey equipment specifications**

System	Manufacturer – Model	Equipment Specifications
GNSS	Trimble BX992 & BD982 (2x G4 corrections)	RTK: < 0.05 m; DGNSS: <0.10 m
INS (motion, heading)	IXBlue Octans V SBG Apogee Navsight	H: 0.1°; R&P: 0.01°; Heave: 5 cm H: 0.01°, R&P: 0.03°, Heave: 5 cm

System	Manufacturer – Model	Equipment Specifications
SVP	Valeport Swift	0.02 m/s
MBES	Kongsberg EM2040 Dual Rx, Dual ping	Freq: 200 – 400 kHz Focus: 0.4° x 0.7° at 400 kHz
USBL	Kongsberg HiPAP 351P	0.02 m range detection accuracy or < 0.3% of slant range
Magnetometer	Geometrics G882	Accuracy: < 2 nT throughout range. Freq: up to 40 Hz
SSS	2x Edgetech 4200 (300/600 kHz)	Horizontal beamwidth: 0.5° @ 300 kHz, 0.26° @ 600 kHz Resolution Across Track: 3 cm @ 300 kHz, 1.5 cm @ 600 kHz
SBP	Innomar SES-2000 Medium	2-22 kHz 1-5 cm resolution

**Table 11: GOVI survey equipment specifications**

System	Manufacturer – Model	Equipment Specifications
GNSS	2x Trimble BX992 (1 x XP2 and 1 x G4 corrections)	RTK: < 0.05 m; DGNSS: <0.10 m
INS (motion, heading)	IXBlue Hydrins SBG Apogee Navsight	H: 0.01°; R&P: 0.01°; Heave: 5cm H: 0.01°, R&P: 0.03°, Heave: 5cm
SVP	Valeport Swift	0.02 m/s
MBES	Kongsberg EM2040 MKII Dual head, Dual swath	Freq: 200 – 400 kHz Focus: 0.4° x 0.7° at 400 kHz
USBL	Kongsberg HiPAP 352P	0.02 m range detection accuracy or < 0.3% of slant range
Magnetometer	Geometrics G882	Accuracy: < 2 nT throughout range. Freq: up to 40 Hz
SSS	2x Edgetech 4200 (300/600 kHz)	Horizontal beamwidth: 0.5° @ 300 kHz, 0.26° @ 600 kHz Resolution Across Track: 3 cm @ 300 kHz, 1.5 cm @ 600 kHz
SBP	Innomar SES-2000 Medium	2-22 kHz 1-5 cm resolution

The primary software that was used to acquire and process the data is listed in Table 12.

**Table 12: Primary software list**

Type	Software	Related equipment
Acquisition	QPS QINSY	Navigation, MBES, GNSS, SSS, MAG
	Edgetech Discover	SSS Edgetech
	Innomar SESwin	SBP
Processing	Beamworx Autoclean	MBES
	QPS Qimera	MBES
	QPS FMGT	Backscatter
	Sonarwiz	SSS
	Oasis Montaj	MAG
	Kingdom or Silas	SBP
	ProMAX	2D UHR (processing)
	Kingdom	2D UHR (Interpretation)
	QGIS / AutoChart / ArcGIS	SSS, MBES, MAG, SBP

## 6 TECHNICAL QUERIES AND CHANGES TO SURVEY SCOPE

Geological, oceanographic, and technical site limitations resulted in necessary adjustments to the survey scope. These survey scope adjustments were made as Technical Queries (TQs) and were checked and validated by the Energinet (Client) and by GEOxyz. Table 13 outlines the project specific TQs related to the geological and geophysical surveys.

**Table 13: TQ clarifications and outcomes**

TQ ID	Subject	Conclusion
TQ - 004	SBP Interpretation	Where homogeneous geology is interpreted on SBP lines of the geophysical survey, interpretations are performed on every 2nd line
TQ - 009	Boulder Field Criteria geophysical survey	Picking criteria within in boulder fields targets: Boulders $\geq 2$ m in any direction & "Non-geological contacts" $\geq 0.5$ m in any direction
TQ - 010	SSS nadir coverage	SSS Coverage of 200% acquired at entire site, except area affected by pycnocline effects

## 7 DATA PROCESSING AND INTERPRETATION METHODS

### 7.1 MULTIBEAM ECHOSOUNDER

#### 7.1.1 Data acquisition

The system settings and client specifications for the project are listed in Table 14 and Table 15, respectively.

**Table 14: MBES system settings**

Kongsberg EM2040 (DH/DSW)	Head 1 port	Head 2 stbd
Survey speed	Average 4 knots	
Frequency	400 kHz	400 kHz
Bottom sampling	High Density Dual Swath (1024 beams)	
Range	50 m	
Power	Maximum	
Pulse length	Auto	
Patch test roll	<i>TX -0.205°, RX -40.005°</i>	<i>TX -0.270°, RX 42.530°</i>
Patch test pitch	<i>TX 0.340°, RX 0.340°</i>	<i>TX 0.242°, RX 0.242°</i>
Patch test heading	<i>TX -2.238°, RX 177.762°</i>	<i>TX -2.345°, RX 177.655°</i>
Sector width	80°	80°
Ping rate	25 Hz – 30 Hz (maximum)	

**Table 15: MBES client specifications**

Item	Specification
Data density	16 hits/m <sup>2</sup> at 99 % of the site
Standard Deviation	0.20 m on 95 % of the site
MBES Mode	Equidistant
Grid	0.25 m cell size
Coverage	100 %

In TQ 008- MBES, it was requested and agreed to increase the MBES SD limit to 0.25 on 95 % of the site and to modify the hit count specifications to the following: A minimum of 99 % of site will show a hit count of at least 16 hits/m.

#### 7.1.2 MBES methodology

The objective of the MBES processing workflow was to create a final digital terrain model (DTM) that provided the most realistic representation of the seabed.

The processing workflow is comprised of four general steps, which are summarized in the tables below:

**Table 16: Loading MBES data in Qimera**

Step 1	Load MBES data into Qimera
Set Up Project	Load in RAW multibeam files (*.db) as recorded by QINSy in a new project Grid cell size 0.25 m * 0.25 m
QC of coverage	Check completeness of data by cross-referencing the imported files with the Survey Log

**Table 17: MBES positioning verification**

Step 2	Positioning
All verification during the Positioning control was performed by checking the data with the 95% confidence option	
SVP correction	Applying the last SVP done into the data set
Overall statistics	Run Standard Deviation statistics. The standard deviation must be < 0.25 m
Verify horizontal positioning and Total Horizontal Uncertainty (THU)	Create a dynamic surface at 0.20 m. A .xyz file with THU values can be exported or a static surface can be created with THU values in it. The surface needs to be updated and a new export can be done (for the 24 hours QA deliverables)
Verify vertical positioning and Total Vertical Uncertainty (TVU)	Create a dynamic surface at 0.20 m. A xyz with TVU values can be exported or a static surface can be created with TVU values in it. The surface needs to be updated and a new export can be done (for the 24 hours QA deliverables)
FAU export	FAU files export to finalise the processing in BeamWorx Autoclean processing software (separate export per head)

**Table 18: MBES data de-spiking and processing**

Step 3	Data de-spiking
Quality assessment and data correction/filtering	Refraction and vertical mismatch issues due to pycnocline to be assessed and filtered when possible. Outer ranges to be trimmed when data cannot be properly filtered.
Manual De-spiking	Remove remaining substantial spikes manually using the 2D and 3D views. Correct where necessary
Filter De-spiking	Filters applied to de-spike the data
Coverage reassessment (SD and Hit count)	Coverage and specifications reassessment after processing

**Table 19: MBES data quality control**

Step 4	Quality Control
Shallowest/Deepest Areas	Special attention is needed for these areas to verify all spikes are removed.
Check for steps in data	Change plan view to the mean depth colour data to verify no steps are present in the data.
Statistics Control	Final statistics exports per block/area to track and save the final specifications.



**Table 20: MBES target picking**

Step 5	MBES target picking
Target picking	Targets picked manually in Qimera from the grid

The MBES data was initially brought into QPS processing software Qimera, to check that the coverage and density requirements were achieved before any further steps were taken. It was confirmed that a post-processed navigation solution was not necessary, as the dynamic PPP applied online provided the vertical and horizontal accuracy necessary for the survey. THU and TVU values were checked and confirmed to be within the specifications defined for the dataset. The DTU21MSL vertical model applied in Qinsy online was confirmed to properly reduce the ellipsoidal heights to the project vertical datum. Subsequently, in Qimera, the bathymetry data for each data file is merged to create a dynamic surface, to review the standard deviation and sounding density results.

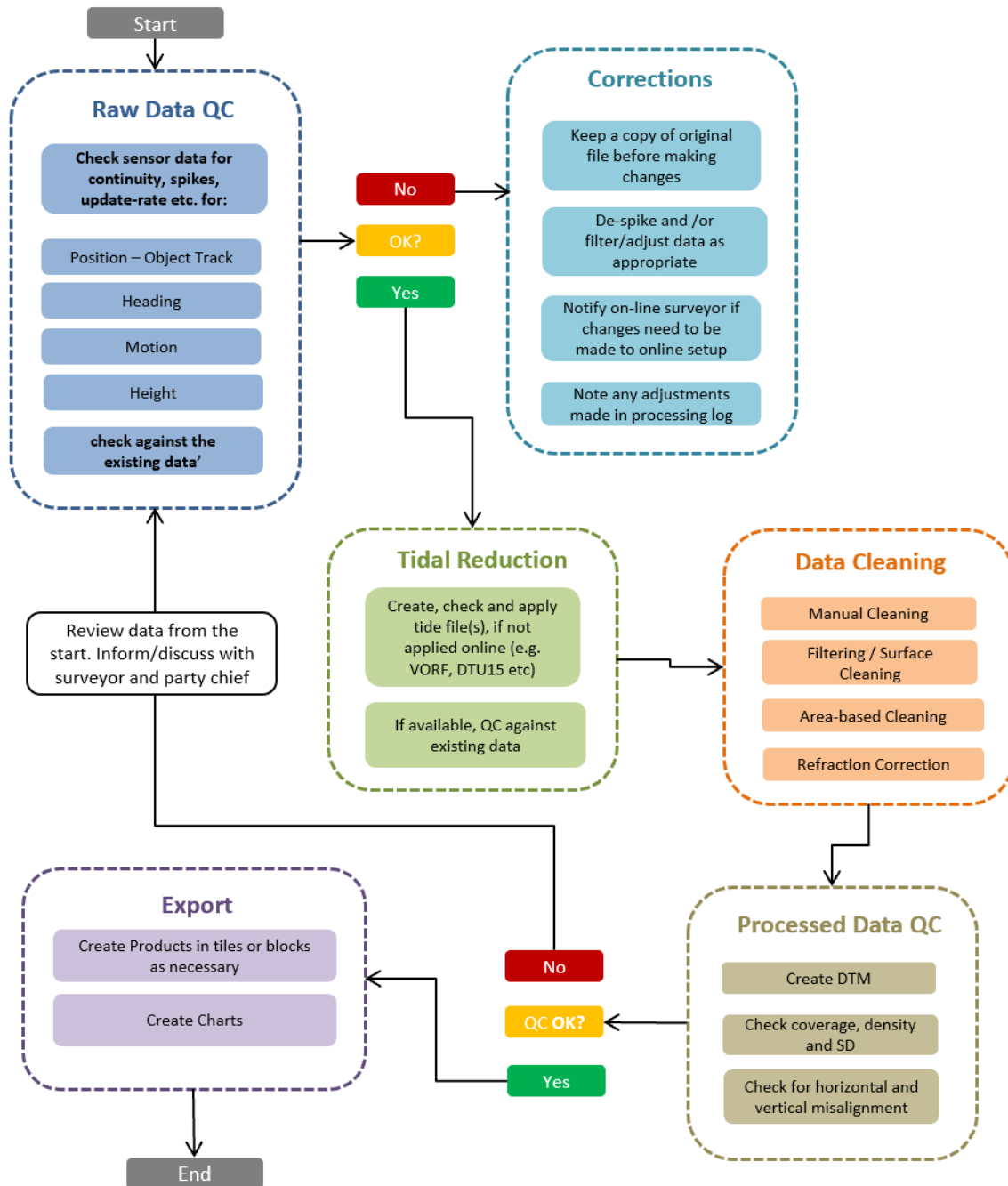
After this preliminary check and after confirmation that the data was within the project specifications, the process of removing outlying soundings, refraction and SVP corrections, as well as the refined cleaning routine, was performed.

The last step of processing was carried out in Autoclean, as it has been proven that, if no further processing was needed in the data coming from QINSy (post processing, computation recalculation, misalignments adjustments...), the Beamworx software manages high amounts of MBES data more quickly, which made the cleaning process more efficient and faster. In addition, it allows a more detailed statistical analysis to be performed at the end of the processing process.

Finally, MBES target picking was carried out after processing using the automatic tool in BeamWorx Autoclean software. Targets were detected based on a reference grid, which automatically measures the targets in Length x Width x Height. The detection process is fully automated and based on input parameters. These parameters could change per area depending on data quality, target numbers, size, and seabed complexity, but always in accordance with the specification of the project relative to minimum size and their interpretation as per TSG requirement. Detection and accuracy are greatly dependent on data quality. Artefacts such as thermocline, vertical alignment and complex morphology could impact the detectability of potential targets.

After running the detection process, a manual QC was conducted and any amendment were applied if needed e.g. false positives are removed, false negatives are added, and target dimensions were adjusted manually if required. The automated routine combined with a manual QC gave this output a reliable result.

Finally, a target correlation was done with the SSS and MAG contacts, and a final QC was done to ensure consistency on the target classification across the sites.



**Figure 7: General MBES data processing workflow**

### 7.1.3 Backscatter methodology

The backscatter data were processed and exported, using QPS Fledermaus GeoCoder Toolbox (FMGT) software.

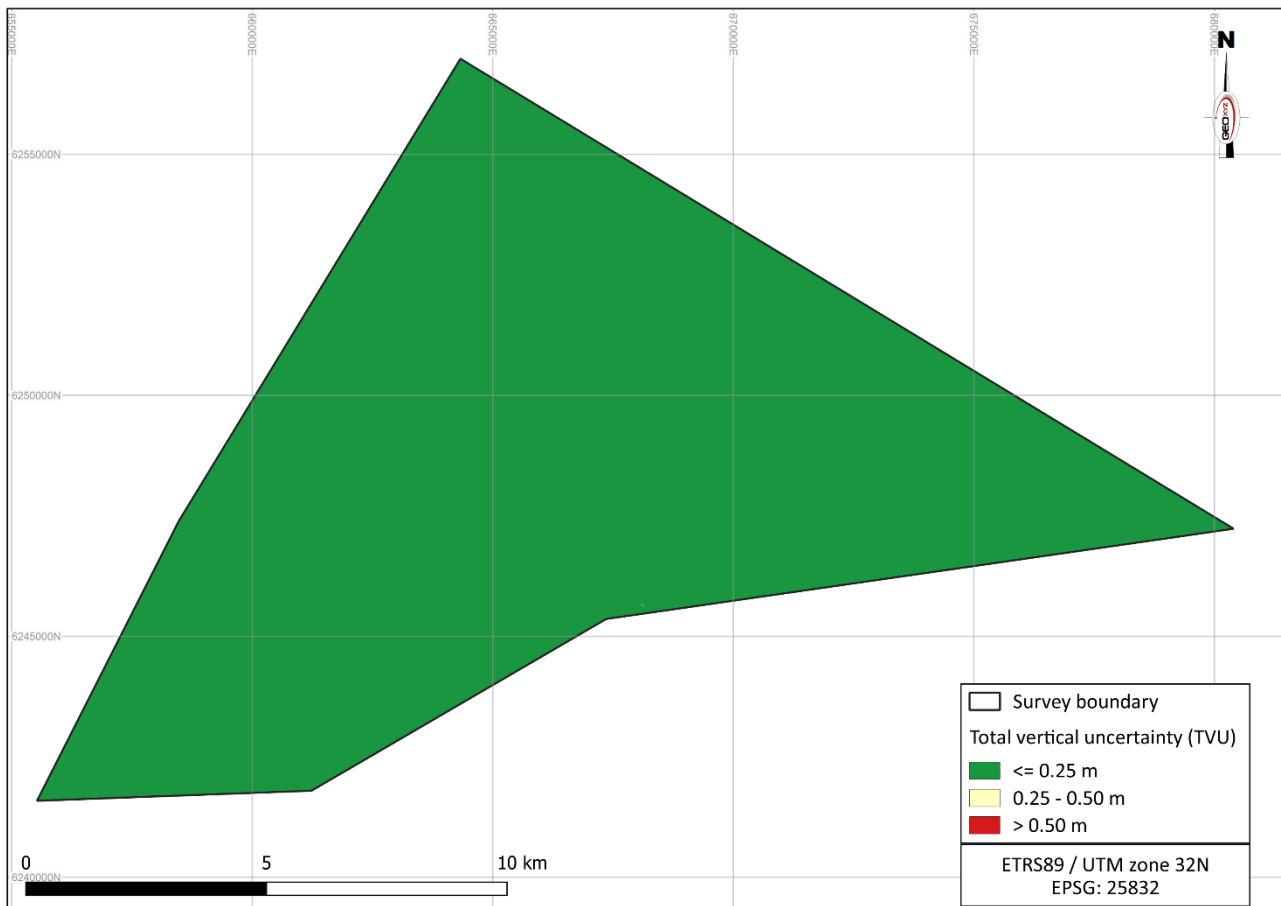
Backscatter processing was carried out on the fully cleaned and processed MBES data files, from previous steps in the Qimera software. Combined GSF (both heads exported in the same file) were exported and then imported in FMGT along with a MBES reference surface.

The gain was modified to normalize the intensity over the survey area. It was also optimized to enhance changes in seabed sediment composition and morphological features on the seafloor.

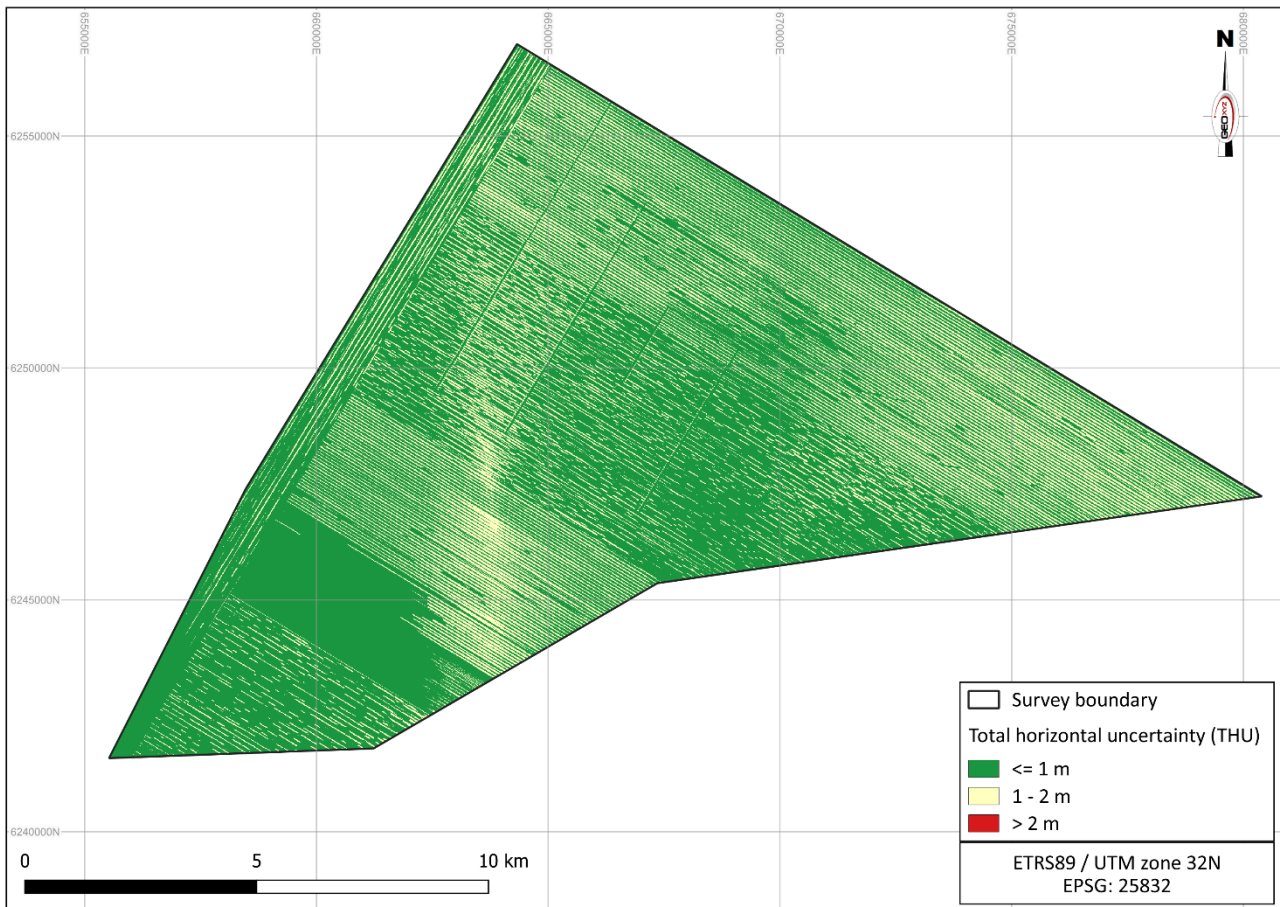
Data from both vessels (GOIV and GOV) were processed in the same FMGT block projects to optimize the blending of overlapping data from the two vessels.

#### 7.1.4 Data quality assessment

Overall, the data is of good quality and meets the project requirements. IHO Standards for Hydrographic Surveys define a maximum THU value of 2 m for a First Order Survey, and 100 % of the THU values for Hesselø South are below this limit. In case of TVU, the maximum limit is defined by a relation between the uncertainty that varies with the depth and the uncertainty not dependent of the depth. For Hesselø South, a theoretical mean TVU max calculated for the site is 0.60 m, being all TVU values below this theoretical limit. The TVU and THU values must be understood as an interval of  $\pm$  the stated value. The TVU and THU coverage maps are displayed in Figure 8 and Figure 9, respectively.



**Figure 8: TVU coverage map**



**Figure 9: THU coverage map**

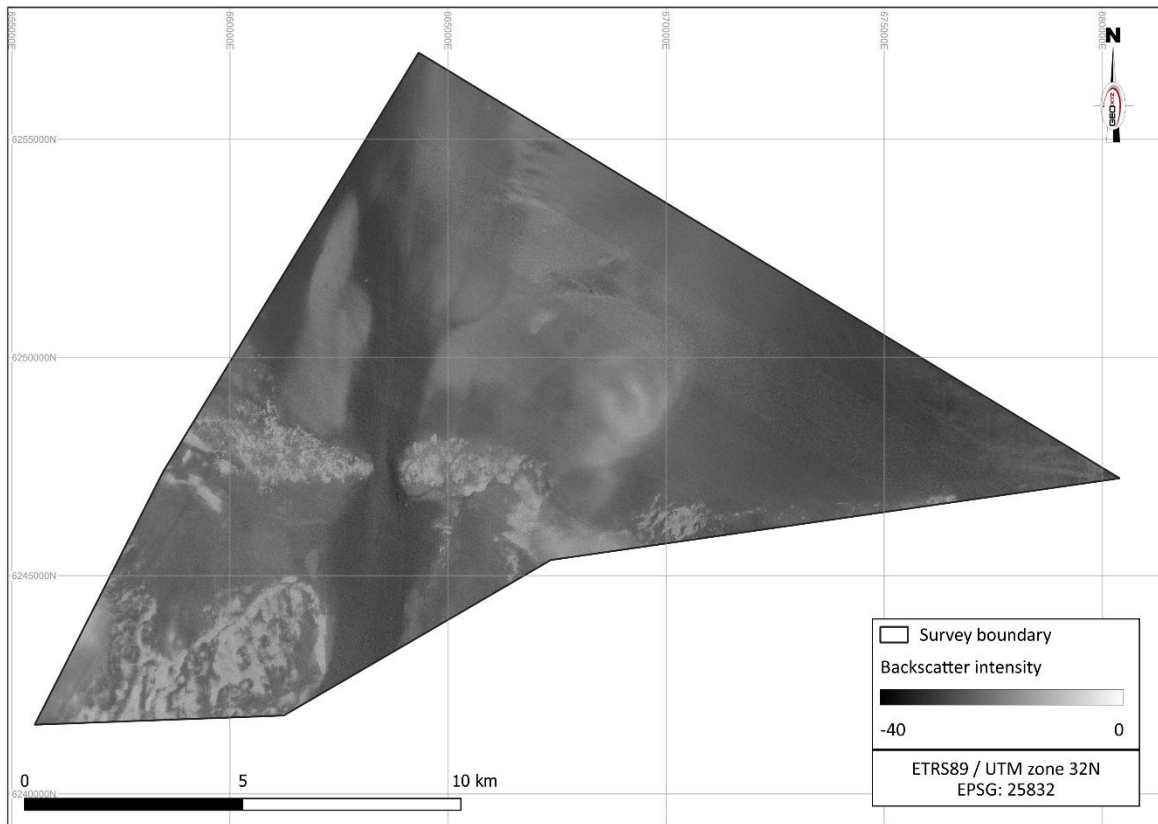
The quality of the final processed backscatter was assessed in GIS software (QGIS and Global Mapper) after combining all processed blocks in one gridded surface as 1 m resolution backscatter mosaic (Figure 10).

The processing of the backscatter was done to try to achieve a homogeneous colour scale between blocks. The colour scale was normalised between blocks. This step is necessary, as it is not possible, to process the entire survey area into a single mosaic due to the size of the dataset and the resolution specifications.

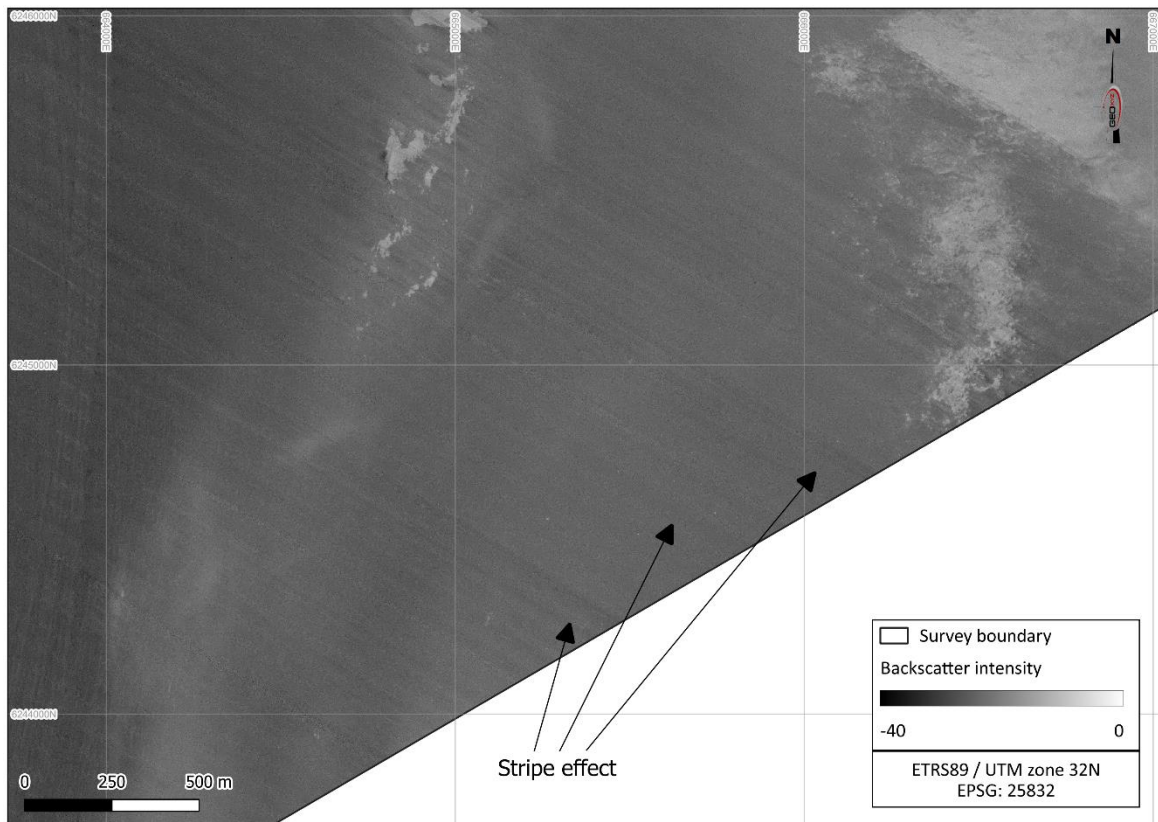
The backscatter Mosaic assessment indicated that the boundaries between different sediment types were differentiated and therefore the results were fit for purpose.

Some artefacts are present and mostly manifest as stripes aligned with the survey line direction (Figure 11). These artefacts also appear to be exacerbated during periods of poor weather. The MBES acquisition setup was preferential to the backscatter one.

Despite the presence of these artefacts, the backscatter data is of sufficient quality to derive sediment boundaries and assist to the interpretation as additional help to the SSS dataset.



**Figure 10: Backscatter data across the Hesselø South survey area**



**Figure 11: Example of stripe effect on the backscatter mosaic in Hesselø South**

## 7.2 SIDE SCAN SONAR

### 7.2.1 Data acquisition

The SSS system settings and client specifications are listed in Table 21 and Table 22, respectively.

**Table 21: SSS system settings**

Edgetech 4200 300/600 kHz	
Survey speed	Average 4 knots
Positioning	HiPAP 351 USBL
Mean fish altitude	Between 4.5 - 5 m
Trigger	High Frequency = Master
TVG / Gain	Recording RAW (*.jsf)
Range	HF = 70 m / LF = 70 m
Mode	High Definition Mode

**Table 22: SSS specifications**

Item	Client Specification	Achieved by survey
Resolution sufficient for detecting seabed feature/object	0.5 m (height, width, and length)	< 0.5 m (height, width, and length)
Towing altitude	8 - 12 % of range (optimised for data quality)	10 % of the range
Positional accuracy	± 2 m (using vessel course-over-ground and USBL)	± 2 m (using vessel course-over-ground and USBL)
Operating mode	High Definition Mode	High Definition Mode
Range	70 m	70 m
Coverage	200 %*	200 % except under nadir: coverage 100 %

\* SSS coverage adjusted to 100 % for nadirs, due to thermocline/pycnocline effects. Also, coverage in some places was accepted to be only 100 %.

During the geophysical survey operations, a dual SSS configuration was employed to increase coverage and help mitigate the potential effects of pycnocline interference. This comprised each SSS being towed on separate winches, with a longitudinal offset (nominally of approximately 20 m). A depressor was employed on one of the SSS fish, to ensure both fish flew at similar, consistent altitudes within the water column.

### 7.2.2 SSS data processing

Side Scan Sonar (SSS) data were processed and interpreted using Chesapeake SonarWiz software. The SSS processing steps are outlined in Table 23 to Table 29. Figure 11 outlines the SSS processing workflow used for the project.

**Table 23: Importing SSS data into SonarWiz**

Step 1	Importing data: overview of the acquired lines
Set Up Project	<p>The raw sonar files (*.jsf) had corrected navigation applied, using the SonarWiz NavInjectorPro utility, before being imported into Chesapeake SonarWiz software. The navigation data was de-spiked and exported from QINSy validator, to provide a smoothed position, with a bearing to towpoint heading solution. The processed sonar files (*.jsf) were imported into the SonarWiz project with the appropriate file type specific settings, as those were determined during the mobilization and calibration tests.</p> <p>A smoothing filter of 100 pings was applied during import. Once the parameters were agreed and checked with the Employer's Offshore Supervisor, they were used for the remainder of the dataset.</p>
Bottom track	Using the automatic bottom tracking feature, SSS data were bottom tracked, line by line, and then, if needed, bottom track was manually adjusted.

**Table 24: Navigation correction in SonarWiz**

Step 2	Navigation correction
Check position	The SSS data were checked for positional accuracy against the MBES data, by locating clearly distinguishable features and contacts in both datasets and comparing their positions. If needed, the navigation data were re-processed and re-exported from Qinsy as new navigation files (x, y, heading) and injected into the SSS data, using the SonarWiz NavInjectorPro utility. After that, positional accuracy was checked again.
Navigation	<p>The towfish heading source was set to the fish heading to tow point. Using the SonarWiz ZEdit utility, navigation spikes were corrected and the positional accuracy was checked.</p> <p>The towfish heading was QC'd for small data jumps or artifact "vortex" effects.</p>

**Table 25: SSS signal processing**

Step 3	Signal processing
EGN (Empirical Gain Normalization)	An EGN (Empirical Gain Normalization) table was calculated and applied to the data, creating a normalised gain, both along track and across track.
TVG (Time Variable Gain)	If the EGN table applied to the data did not have the desired effect, an Auto TVG was used.

**Table 26: SSS infill assessment**

Step 4	SSS infill assessment
Manual check for gaps	Manual check for data gaps, overlap and data loss during QC/QA.
Check for pycnocline interference	Quality control check for pycnocline interference towards swath edges. Affected areas were marked for infill and re-run if required.
SonarWiz coverage	Checked for 200 % coverage (100 % nadir coverage for pycnocline- thermocline affected data), using SonarWiz Coverage report.

**Table 27: SSS contact picking**

Step 5	SSS target picking
Target picking	Must include:

Step 5	SSS target picking
	<p>H-L-W measurements</p> <p>Description of the target</p> <p>Confidence level</p> <p>The interpretation of contacts was performed in SonarWiz digitizing mode, in accordance with the specifications. Contacts were digitized alongside MBES data and confidence level was updated accordingly. Wrecks and cables were correlated to relevant databases.</p>
Criteria of object detection	<p>Minimum of 0.5 m (height, width or length)</p> <p>Object is identified as deviation from natural seabed forms</p> <p>The object is verified in wing line side scan image</p> <p>Position is verified with MBES data</p> <p>Man-made objects or very clear objects (even if only detected on one line only)</p> <p>Contact classification criteria defined with the Reporting Coordinator and sent to the Data Coordinator onshore.</p>
Image picture	Colour grey inverted
Confidence level (Low, Medium, High)	<p>Every contact has a confidence level attributed to it based on its detection in:</p> <ul style="list-style-type: none"> <li>• 1 SSS line -&gt; Low,</li> <li>• 2 or more SSS lines -&gt; Medium</li> <li>• 1 or more SSS lines and MBES data -&gt; High</li> </ul>
Boulder fields	<p>Boulder field areas were outlined in SonarWiz map view whereas waterfall view was also used where needed. The boulder zone defining criteria are:</p> <ul style="list-style-type: none"> <li>• &lt; 40 boulders: Not a boulder zone</li> <li>• 40 – 80 boulders: Boulder zone type 1: Intermediate boulder density</li> <li>• &gt; 80 boulders: Boulder zone type 2: High boulder density</li> <li>• No minimum size requirement, all covered boulders count towards the minimum boulder amount to determine boulder zones</li> </ul> <p>The digitized polygons have been edited in QGIS and re-imported in SonarWiz. No manual target picking was performed within the boulder field polygons and a machine learning automatic picking algorithm was used instead. The results were confirmed to be representative and correct.</p> <p>Man-made objects have been manually picked within the boulder field areas</p>

SSS contact picking was performed using two different methodologies related to the presence or not of boulder fields in the area.

Outside boulder fields:

Contacts were manually picked in the waterfall display in the Sonarwiz project, and measured for length (largest dimension of object), width (perpendicular to length) and height of the target.

Picking targets was in accordance with the specification of the project relative to minimum size and their interpretation as per TSG requirement. All contacts from 0.5 m were picked. Once all SSS targets were picked, they were correlated with MBES and MAG contacts.

Several QC steps are performed during the manual target picking and interpretation, and a final QC by the Lead Geo is done to ensure consistency on the target classification across the sites.

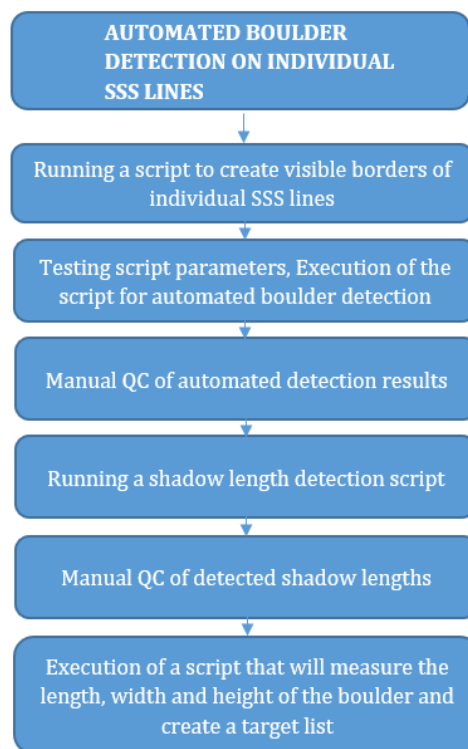
Inside boulder fields:



Automatic boulder picking was performed using an algorithm to analyse contacts from raster analysis. This methodology runs different scripts that detect and isolate the crucial components of reflections and shadows from the SSS data, which are fundamental for the representation, identification and measurement of boulders/targets.

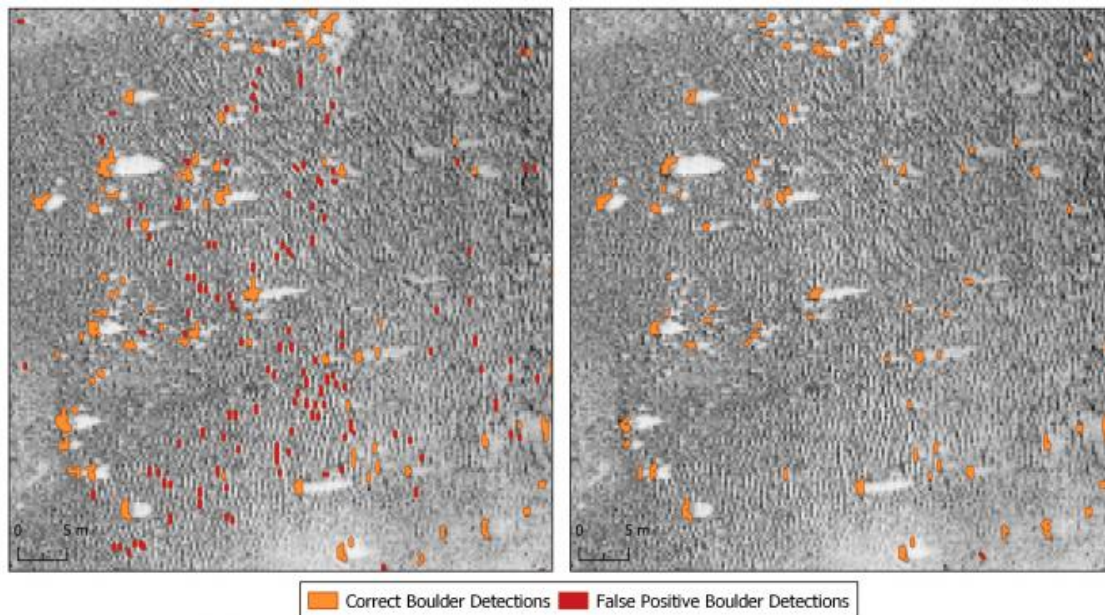
Inside the mapped boulder fields, picking targets was in accordance with the specification of the project relative to minimum size and their interpretation as per TSG requirement. All contacts from 2 m and all MMO/debris were picked.

The detection process (Figure 12) was performed on each individual SSS line, and for each target the automated detection yielded a polygon that outlines the reflection and a line that outlines the shadow. When requested to identify the same target from several SSS lines, a specifically developed tool compared target position and dimension on different lines and created average values for one representative target. This task was especially challenging inside high-density boulder fields where target reflection varied between the lines and shadows overlaps between contacts.



**Figure 12: Automated boulder detection progress**

A QC process was manually performed by a processor to check whether the detection results correspond to the real target by size and location, making adjustments if necessary to avoid false positive target detections (Figure 13). Manual quality control enabled the processor to ensure accurate and reliable detection results, adjust the results where needed, and improve the overall quality of the detection process.



**Figure 13: Automatic correct boulder detection vs false positive boulder detection**

Once the algorithm was run and the QC was finished, a SSS boulder shapefile was exported and correlated with the MBES and MAG contacts. A final QC by the Lead Geo was done to assure the correct definition of contact.

The accuracy of this tool's detection varies between 90 % and 95 %, depending on the morphology of the seabed and the data quality.

**Table 28: SSS mosaic creation**

Step 6	SSS mosaic creation (HF and LF)
Adjust SSS line drawing order	SSS lines drawing order was adjusted to optimize the exported seabed image
Line grouping	Lines were grouped in: Approved, Rejected, Trials or Other
EGN and gain check	Final QC of EGN and gains was performed. If required, new EGNs and gains were recalculated and reapplied.
Inter file gap check	Data was checked for small inter-file gaps. SonarWiz inter-file gap tool was used when required.
Range check	Range was adjusted for optimized quality without compromising the 200 % data coverage.
Mosaic export	SSS mosaics were exported using the standardised project tile size and arrangement.

**Table 29: SSS seabed classification**

Step 7	Seabed classification
Seabed features	Seabed features have been created and QC'd using the exported SSS LF mosaics. SSS HF mosaics and the MBES exports were also taken into account.
Seabed Geology	The SSS LF and HF mosaics, as well as the MBES data and the SBP contours were used in order to outline the sediment differences, as those are represented by the

<b>Step 7</b>	<b>Seabed classification</b>
	reflectivity changes mainly on the SSS mosaics. Grab samples were the most useful for editing and confirming the outlined sediment boundaries

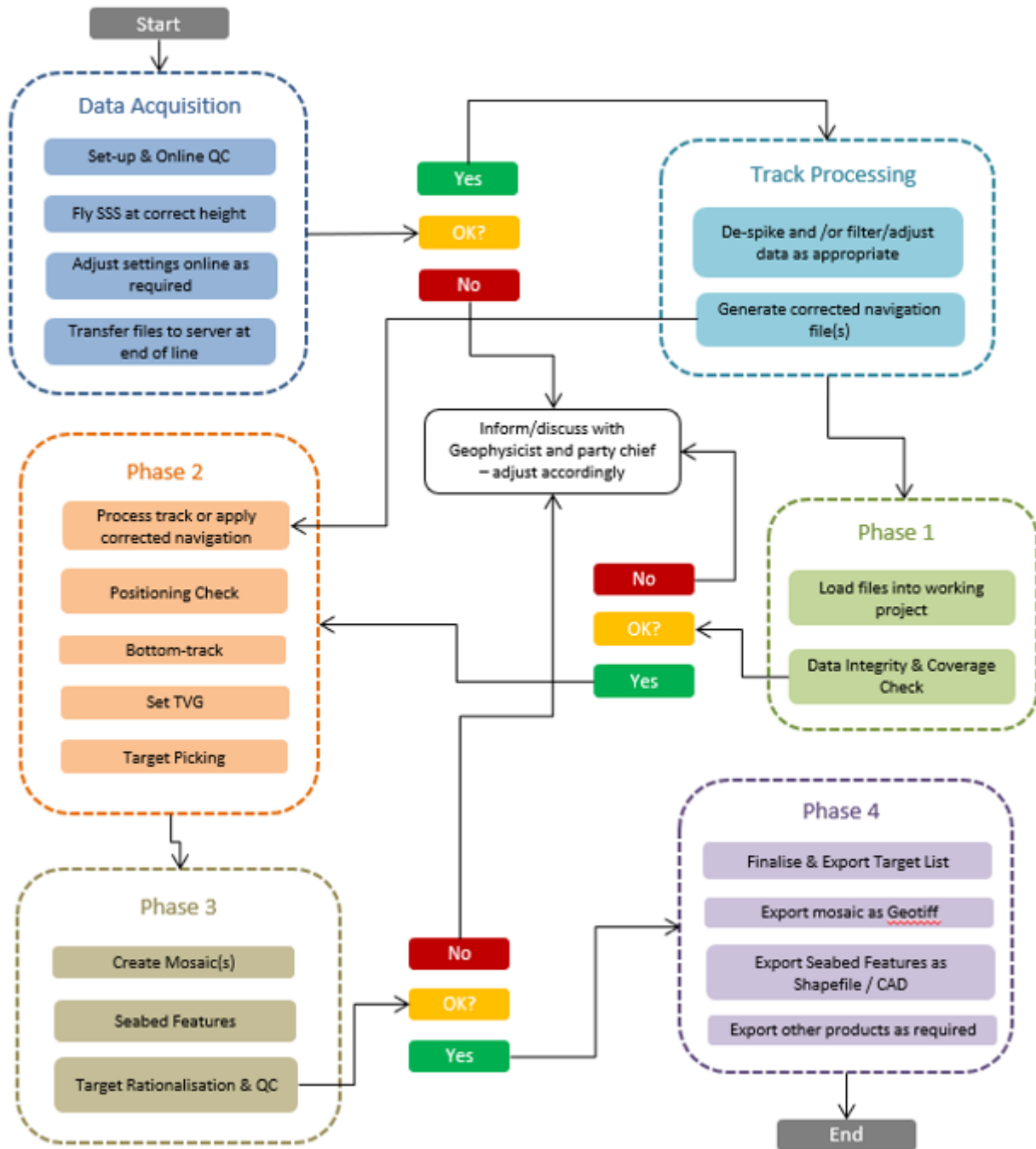


Figure 14: SSS data processing workflow

### 7.2.3 Data quality assessment

Hesselø South was affected by pycnocline and generally 200 % coverage was achieved across the site, resulting in no infill being required (Figure 15). In various places within the survey blocks, SSS coverage was reduced from 200 % to 100 % due to severe thermocline and pycnocline effects (Figure 17).

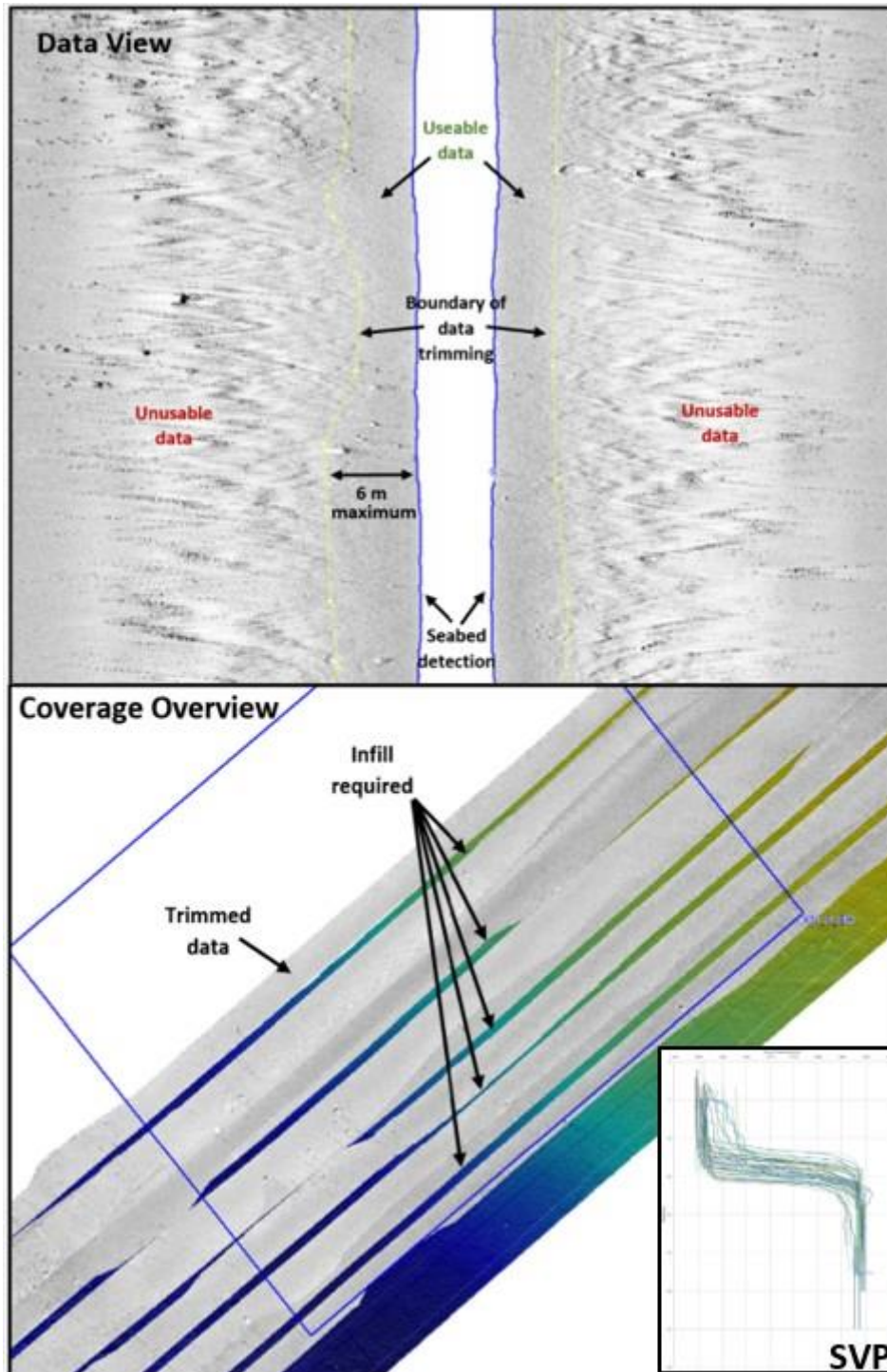


Figure 15: Pycnocline influence on the SSS data in the Data View (top), Coverage Overview (bottom), and the SVP chart (insert)

The pycnocline resulted in marginal/bad data in the outer range of the SSS lines. The affected parts have been removed during processing and good quality data has been used for mosaic exports and target picking (Figure 17).

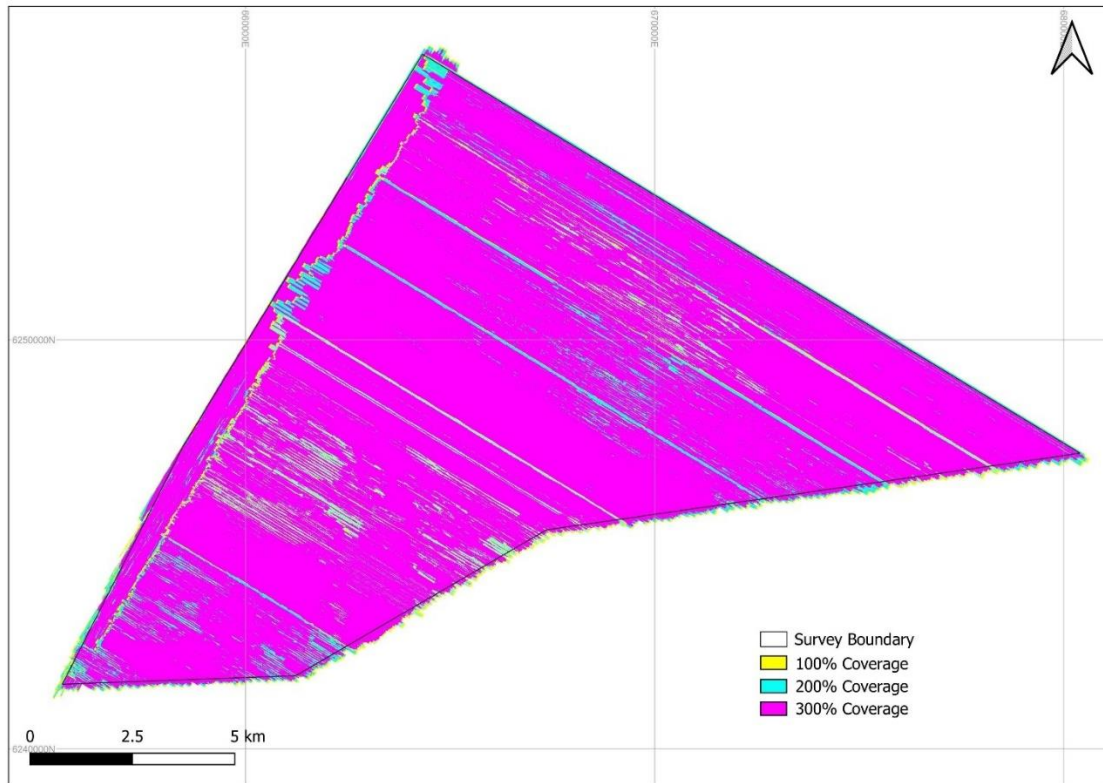
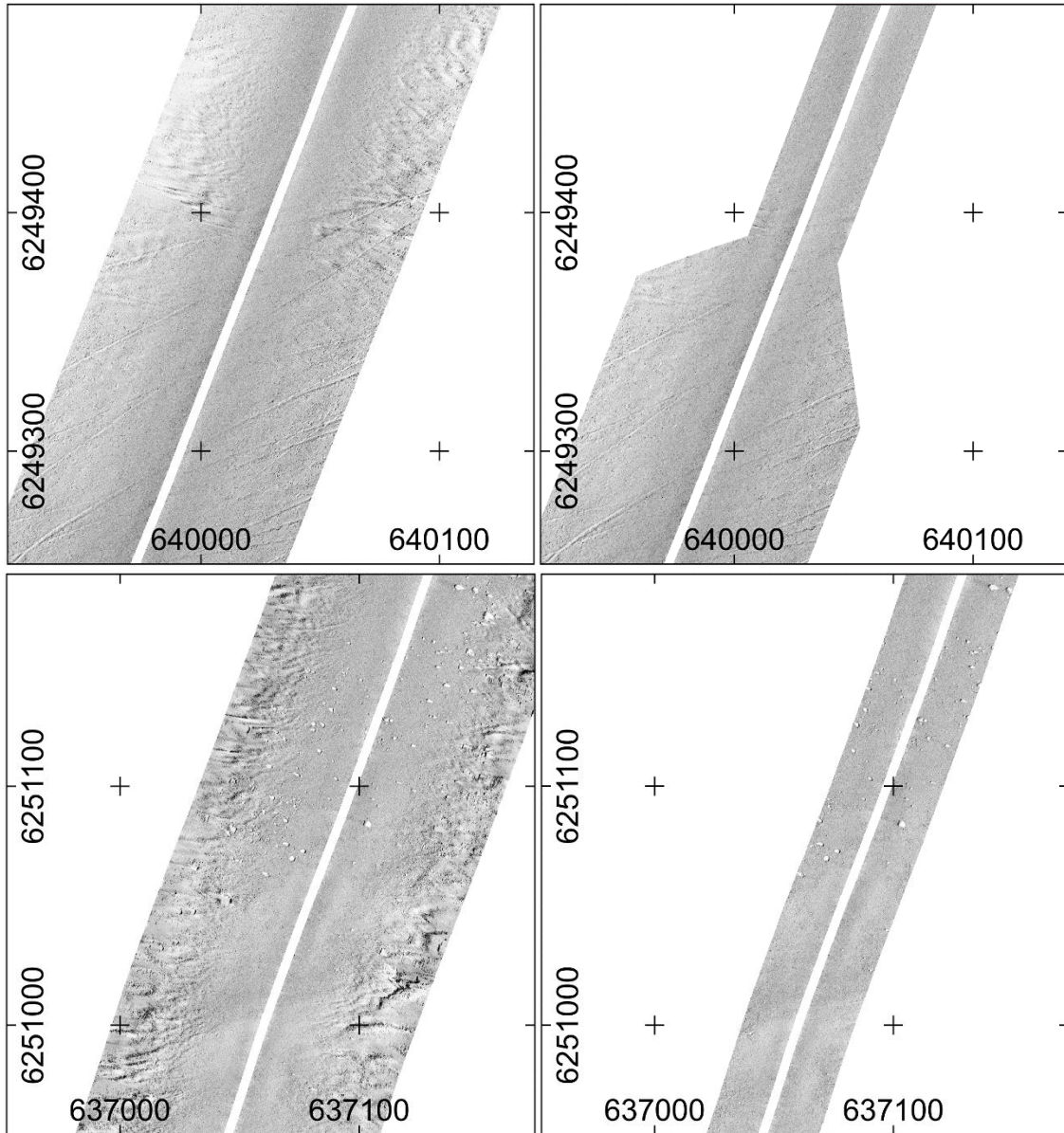
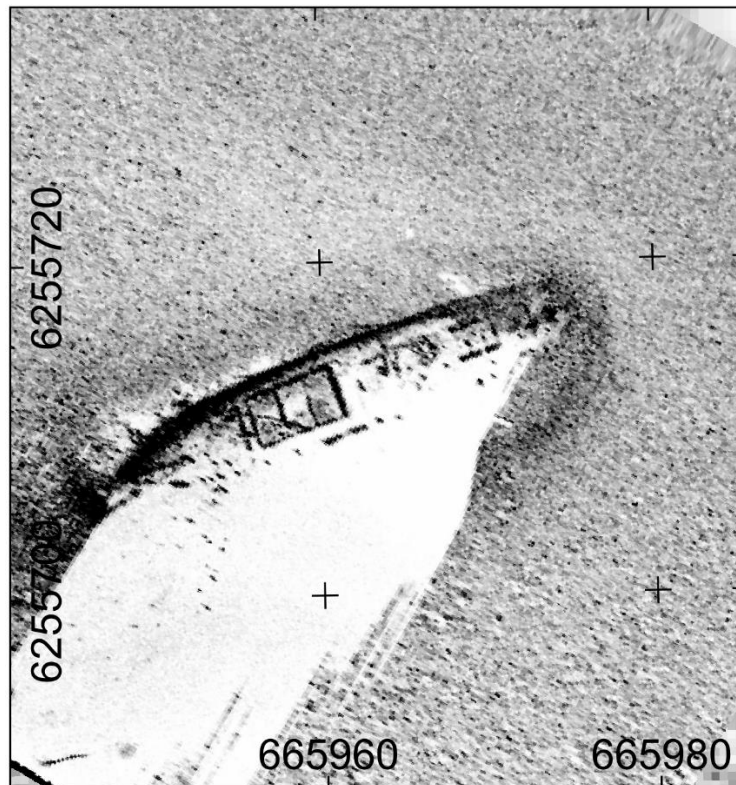


Figure 16: SSS coverage map



**Figure 17: Pycnocline effect on the outer range of the SSS data (left) and trimmed-cleaned SSS data after Far field transparency function in SonarWiz (right)**

Overall, the SSS data quality was monitored throughout the survey and was of high quality, achieving Client specifications (Table 22). An example of good SSS data quality is presented in Figure 18. Shipwreck's details are clearly presented with good image definition.



**Figure 18: SSS data example HS\_B02\_SSS\_GO6\_0523 (MMO ID 107)**

## 7.3 MAGNETOMETER

### 7.3.1 Data acquisition

The MAG system settings and client specifications are listed in Table 30 and Table 31, respectively.

**Table 30: MAG system settings**

Geometrics G882	
Survey speed	Average 4 knots
Positioning	Hipap 351 USBL
Fish altitude	2 to 3 m
Frequency	10 Hz

**Table 31: MAG client specifications**

Item	Client Specification
Seabed altitude	≤ 6 m*
Measurement sensitivity	0.01 nT
Sampling frequency	1-20 Hz (selectable)
Noise level	≤ 2 nT

The magnetometer was towed behind the SSS in a “piggyback” configuration. The magnetometer data was collected together with all analogue data as a single pass.

### 7.3.2 Magnetometer data processing

The magnetometer data were processed using GeoSoft Oasis Montaj. The magnetometer processing steps used for the project are outlined in Table 32 to Table 38.

**Table 32: Magnetometer navigation processing**

Step 1	Magnetometer navigation processing
Backup of "CMP_Easting" and "CMP_Northing"	The raw easting and northing for the common mid-point (CMP), ( <i>CMP_Easting</i> and <i>CMP_Northing</i> ) of the Eiva Scan Fish were copied; all subsequent navigation processing were performed upon these copies.
De-spiking	Data windowed for survey site Non-linear filter applied, with a fiducial width of 5 (and tolerance of 1.5 m). The filter was used to remove small spikes present in the data.
Interpolation	Interpolation of the gaps created by removing the navigation spikes. This was done using a linear interpolation, for gaps over six fiducials (one more than the de-spike length).
Back up of smoothed navigation	The smoothed/interpolated/de-spiked data were backed up
Projection	Project projection is set
Distance	Calculates the total distance along the track for each fiducial.
Distance Separation	The distance between each fiducial is calculated. This was done by applying a convolution filter to the distance. The settings were -1, 1, 0. The results were written to the <i>Dist_QC</i> channel. This helped to monitor the frequency (10 Hz) of the magnetometer, it helped to spot any "freezes" in the data acquisition. It was compared to the magnetometer signal. Any large jumps in distance separation could have caused a spurious anomaly or missed data.
Comparison	The raw navigation, de-spiked navigation, smoothed navigation, the distance separation and magnetometer signal had their profile plotted together within Oasis Montaj. This allowed the quality control (QC) of the navigation and its processing. The database view plots these profiles against each other.

**Table 33: Magnetometer altitude processing**

Step 2	Magnetometer altitude processing
De-spiking	The raw altitude of each magnetometer was de-spiked. The filter stripped out any data spike that is above 10 m (or the value of the altitude cut-off defined during the EVT). This was done within Oasis Montaj using channel tools and channel mathematics.
Interpolation	The interpolation restored the gaps created by removing the altitude spikes. This was done using a linear interpolation, for gaps over ten fiducials (approximately 2 m).
Smoothing filters	A set of filter (low pass and B-spline) was applied to the de-spiked/interpolated altitudes to produce a smooth, more realistic values for altitude.
Alt cut-off	Clipped any data above 4 m and below 1.5 m
Clip X and Y with Alt masked	Clipped the position according to the altitude cut-off



Step 2	Magnetometer altitude processing
Copy Mask of interpolated altitudes to Easting and Northings	Not done at this step
Comparison	The raw altitudes, de-spiked, smoothed altitudes, averaged altitudes and smoothed average altitudes, the distance separation and magnetometer signal had their profile plotted together within Oasis Montaj. This allowed QC of the altitude and the processing.

**Table 34: Magnetometer data QC**

Step 3	Magnetometer data QC
De-spiking	A de-spiking filter was applied to the total magnetic TMF values.
Non-linear filtering	A non-linear filter was applied to attenuate any noise present in the data.
B-spline smoothing	A "B Spline" filter was applied to the non-linear filter. This helped to make the signal to appear more realistic (smooth).
Removal of data with poor magnetic signal	Any data with a magnetic signal strength below 200 was removed.
Copy Mask of interpolated TMF values and poor magnetic signal to Easting and Northings	The stripped magnetic data is used to mask the eastings and northings. The data gaps that are present in the interpolated TMI values were reintroduced by using these TMI values to mask the eastings and northings. This is done because original gaps may have been reduced due by the previous smoothing filters.
Comparison	All the processing steps for the TMI are plotted along with the magnetometer signal for QC.

**Table 35: Magnetometer background calculation**

Step 4	Magnetometer background calculation
Background	To obtain the background magnetometer signal, a series of non-linear filters were applied. These were as per GeoXYZ's procedures. An additional geological filter was produced by using a variation of filter parameters to attenuate magnetic anomalies.
B-Spline	A "B Spline" filter was applied to the final non-linear filters to smooth the result.
Compare	The final data were compared with the raw data to identify over or under filtering of the data.

**Table 36: Magnetometer residual field calculation**

Step 5	Magnetometer residual field calculation
Residual (Anomalies)	Filtered magnetometer data minus the background signal (anomaly and geology).
Residual (Geology)	An additional geological residual field was also calculated using an additional non-linear filter set.
Gridding	Data were gridded using Minimum Curvature with a Cell Size of 0.5 m and a blanking distance of 6 m. Coverage assessment for infills were based in dynamic coverage analysis.

**Table 37: Magnetometer dynamic range calculation**

Step 6	Magnetometer dynamic range calculation
Detection ranges	Detection ranges were calculated from a pre-survey equipment evaluation test (EVT)

Step 6	Magnetometer dynamic range calculation
Coverage plot	Coverage plots were created through use of proportional symbols within Oasis Montaj rather than blanking data to various distances. Dynamic coverage calculation: $C0 = 2 * (\sqrt{X.X^2 - (C1 + 1.5)^2})$ C0 = Dynamic Coverage X.X = Detection range depending on altimeter values. C1 = altitude 2 = the burial depth
Final grid blanking distance	Caution was required when selecting the final blanking distance, to ensure that the edge of survey results were not exaggerated.

**Table 38: Magnetometer target picking**

Step 7	Magnetometer target picking
Analytic Signal	AS grids were produced using a 0.5 m cell size, blanking distance set at 6 m.
Target picking	Anomalies greater than 5 nT peak to peak were picked. The background removal was checked to be optimal for target picking and the pick-to-pick measures are correct. Residual field was checked against total field to help determine anomalies.
De-duplication of targets	Compare targets with Altitude and Residual and TMI profiles. Targets were de-duplicated as required.
Target List	Magnetometer target list was compiled, as per client requirements

The general magnetometer processing workflow used in the project is outlined in Figure 19.

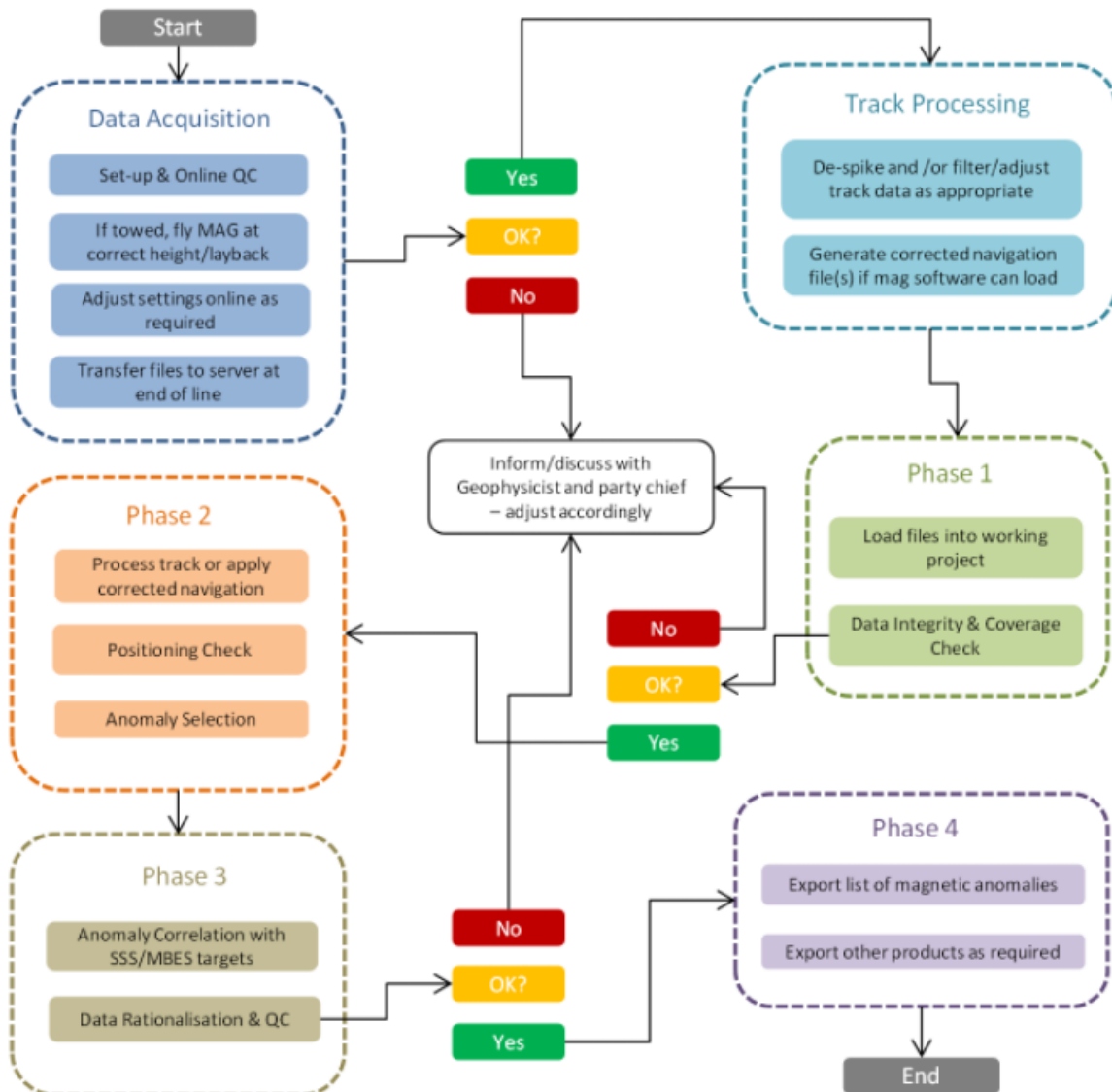
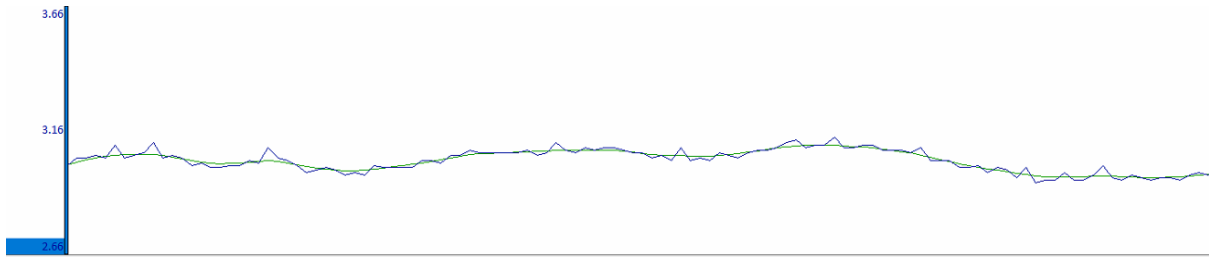


Figure 19: Magnetometer processing workflow

### 7.3.3 Data quality assessment

In general, the MAG dataset meets the project requirements and presents good quality data. Spikes occur within the data of the total magnetic field. Spikes are overall more frequent for the altitude channel. A comparison between raw and filtered and smoothed altitude values is presented in Figure 20.



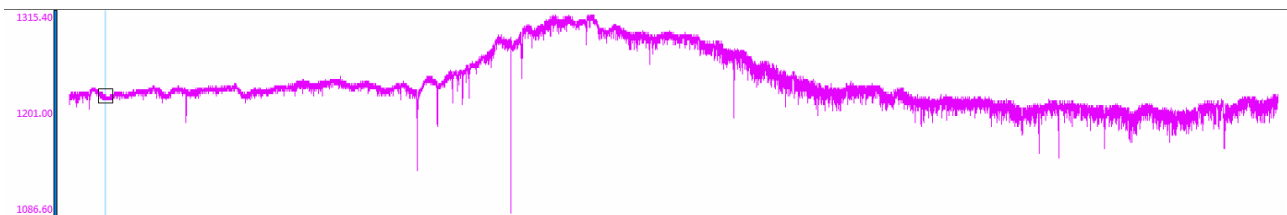
**Figure 20: Data example showing comparison between raw and filtered altitude values**

A non-linear filter was used for de-spiking and smoothing was achieved using the B-Spline filter. Further processing then continued on the filtered data.

Easting and northing coordinates were de-spiked and smoothed as well, however, only few jumps or spikes were present in navigation. Where gaps were present due to navigation drop out, interpolation to 20 m was performed. Infill or replayed lines were included in the data to solve any jumps in navigation.

Based on final Easting and Northing coordinates residual was generated as well. The Residual was generated from the measured total magnetic field and calculated background. The background field was calculated using a series of non-linear filters. Based on this calculation, anomalies were highlighted.

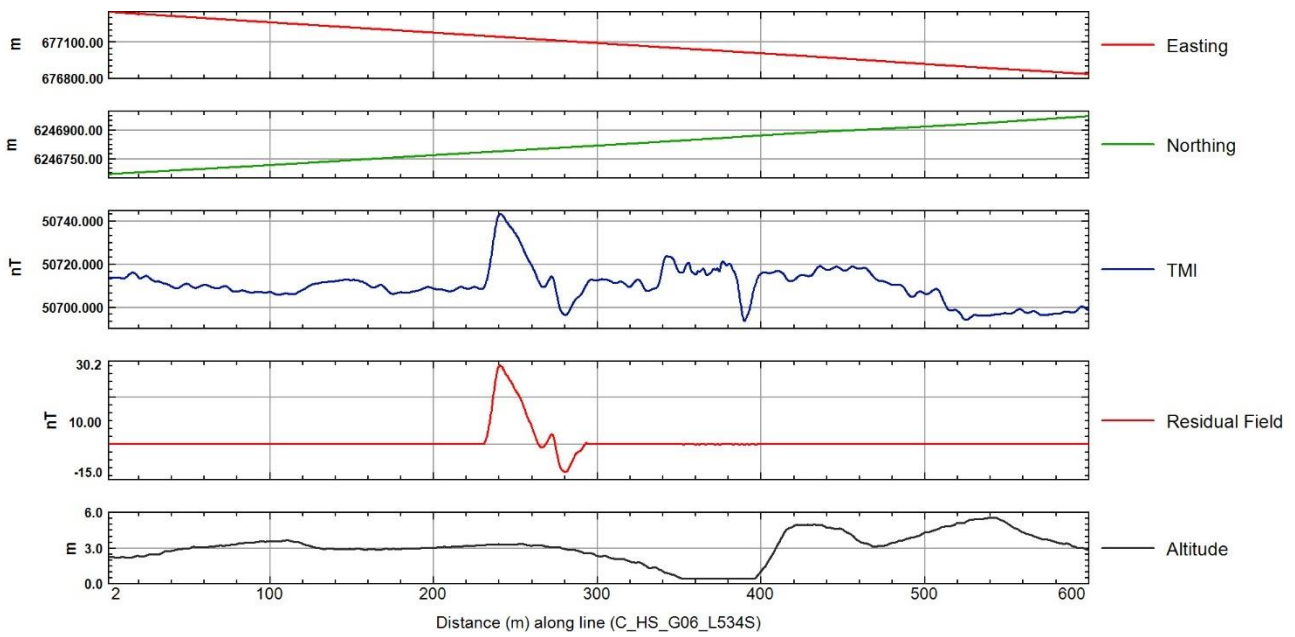
Signal strength values were mostly above 1000. Short drop out in signal strength values were present, yet, these were under acceptable values.



**Figure 21: Data example of a signal strength profile (line 1542\_- \_5376\_C\_KG\_GO5\_1623V\_- \_MAG)**

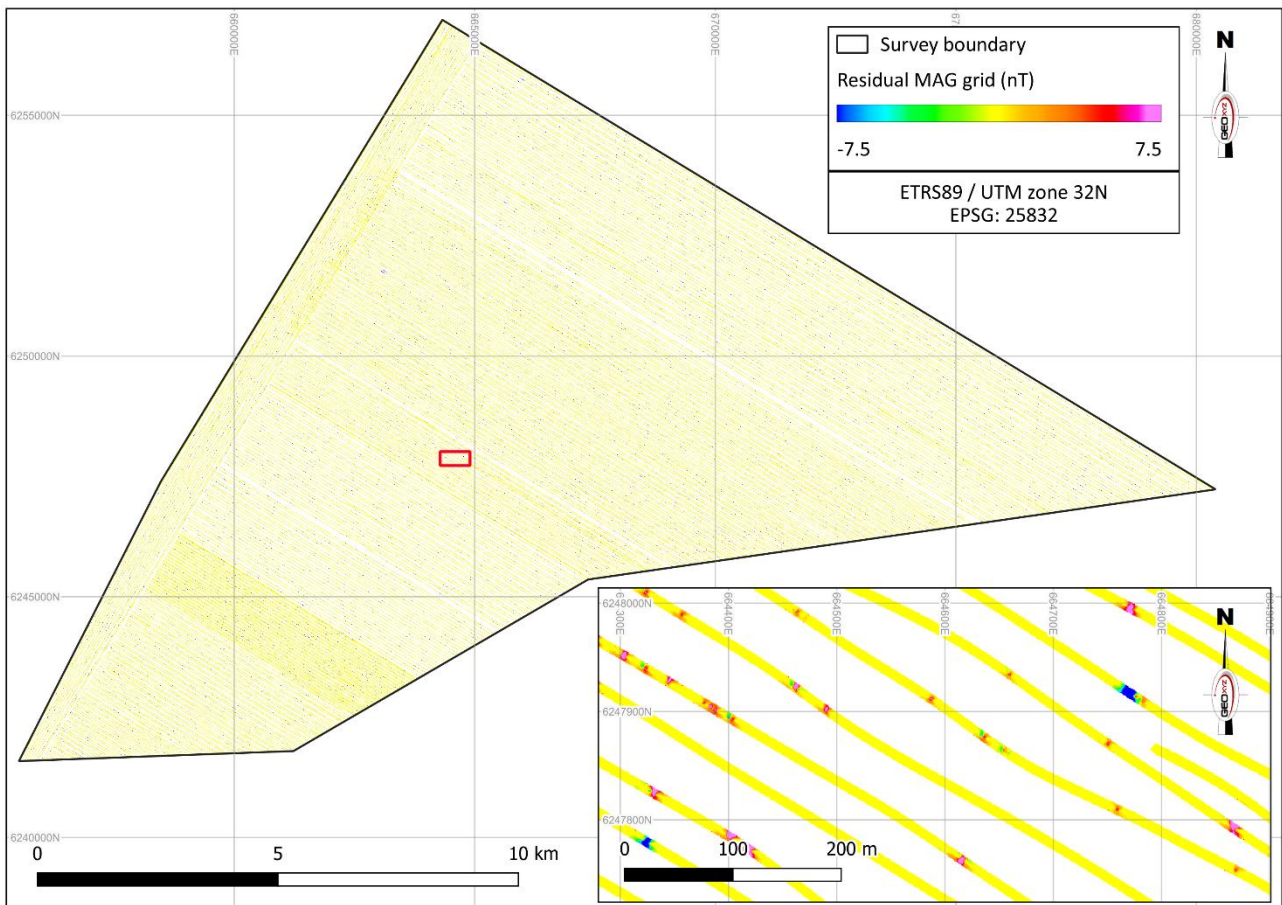
#### 7.3.4 Magnetometer dataset profile example

An example profile for the MAG dataset crossing a wreck (Target HS\_B03\_MAG\_GO6\_0019) is presented in Figure 22 below.



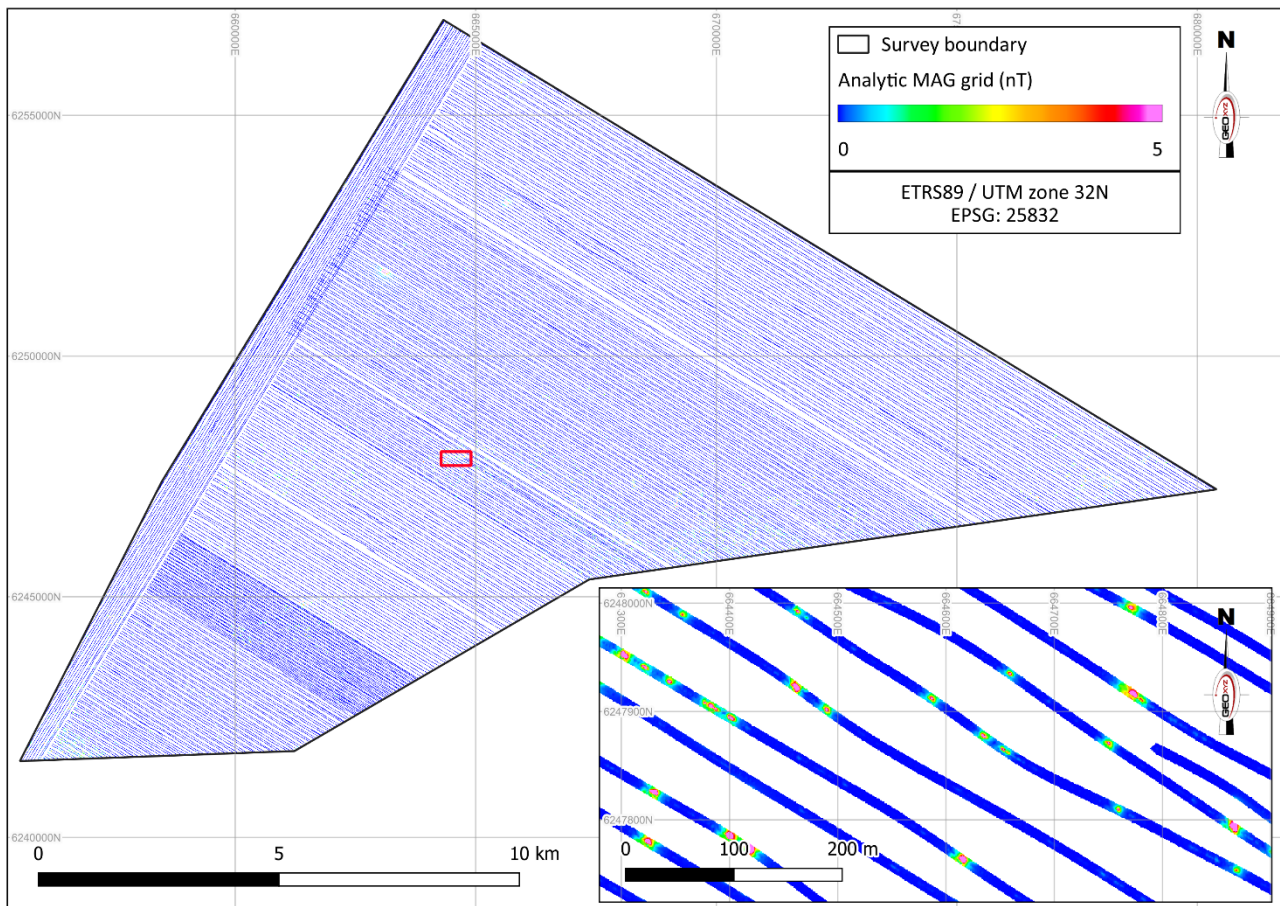
**Figure 22: MAG profile example, line C\_HS\_G06\_L534S)**

### 7.3.5 Magnetic residual anomaly grid



**Figure 23: MAG residual anomaly grid across the survey area**

### 7.3.6 Magnetic analytic anomaly grid



**Figure 24: MAG analytic anomaly grid across the survey site**

## 7.4 SUB-BOTTOM PROFILER

### 7.4.1 Data acquisition

Both vessels were mobilised with the Innomar SES-2000 Medium. The SBP system was recorded with the Innomar software and data tidally corrected using reduced GNSS height data recorded during acquisition. The SBP client specifications are listed in Table 39. SBP lines were recorded along every sailed line and were used to identify subsurface reflectors. The SBP was mounted on the vessels and interfaced to heave compensating unit(s) located close to the position of the high frequency system transducer.

**Table 39: SBP client specifications**

Item	Client Specification
Penetration	10 m
Vertical resolution	0.3 m
System	Innomar SES 2000 or similar

### 7.4.2 Data processing

Sub-bottom profiler (SBP) data were acquired using an Innomar SES 2000 Standard System and recorded using SESWIN recording software. SBP data processing and data QC was performed using Innomar ISE, Innomar SES Convert and Stema Silas software.

The main SBP processing steps used for the QC are outlined in Table 40.

**Table 40: SBP data import and data QC**

Steps	SBP data import and QC
Import of SEGYS	Import SEGY Tide file applied
Data Quality	Lines checked for: No empty pings Correct bottom detection No motion influence No noise in the data No artefacts in data Good reflector visibility Good penetration (5 m)
Position check	Lines checked for: Data coverage Verification of the absolute height by importing the MBES grid (no manual offset is accepted, after tide/heave correction applied online)

### 7.4.3 Data quality assessment

In terms of data quality/utility, the general standard is very good. In general, good imaging of the shallow geology is produced. The data are uniform across the different vessels used in acquisition. The vertical resolution allows separation of surfaces ~0.15 m apart.

The high resolution and narrow beam angle make the sensor worse for boulder detection as the qualities of the instrument all results in reduced diffractions. The SBP data do show evidence for boulders at the seabed where there is till at or close to outcrop. However, sub seabed evidence is ambiguous but there is probably boulders present.

In order to assess the frequency of sub seabed boulder distribution (up to a depth of 10 m BSB), a stratigraphic approach was adapted based on careful calibration of the likelihood of boulders in each unit (the Holocene, the post-glacial, and till units). The Holocene unit only shows very rare indications of boulders and was factored as 1. The post-glacial unit, which shows slightly more numerous indications was factored as 3. Finally, till shows much more numerous boulder indications and was factored as 10. Eventually, the thickness of each unit in metres was multiplied by the boulder factor to obtain the likelihood of boulders.

The depth grids show some very minor artefacts (<0.2 m) related to busts between adjacent lines. These artefacts are primarily caused by the high density of survey lines and slight variations in horizon picking between these lines.

## 7.5 2D UHR SEISMICS

### 7.5.1 Data acquisition

The Client minimum survey specifications are listed in Table 41.

**Table 41: Client 2D UHR specifications**

Item	Client Specification
Fundamental frequency	Between 1 and 3 kHz
Vertical resolution	0.3 m to 40 m depth; 0.5 m to 100 m depth
Minimum Penetration	100 m
Fire rate	2 pulses/second
Feather angle	<12° during 95 % of the shots
Variable energy levels	Between 100 and 1000 Joules
System	A suitable multi-channel and multi-element hydrophone streamer with depth control plus depth measurement for continuous monitoring and recording of streamer depth

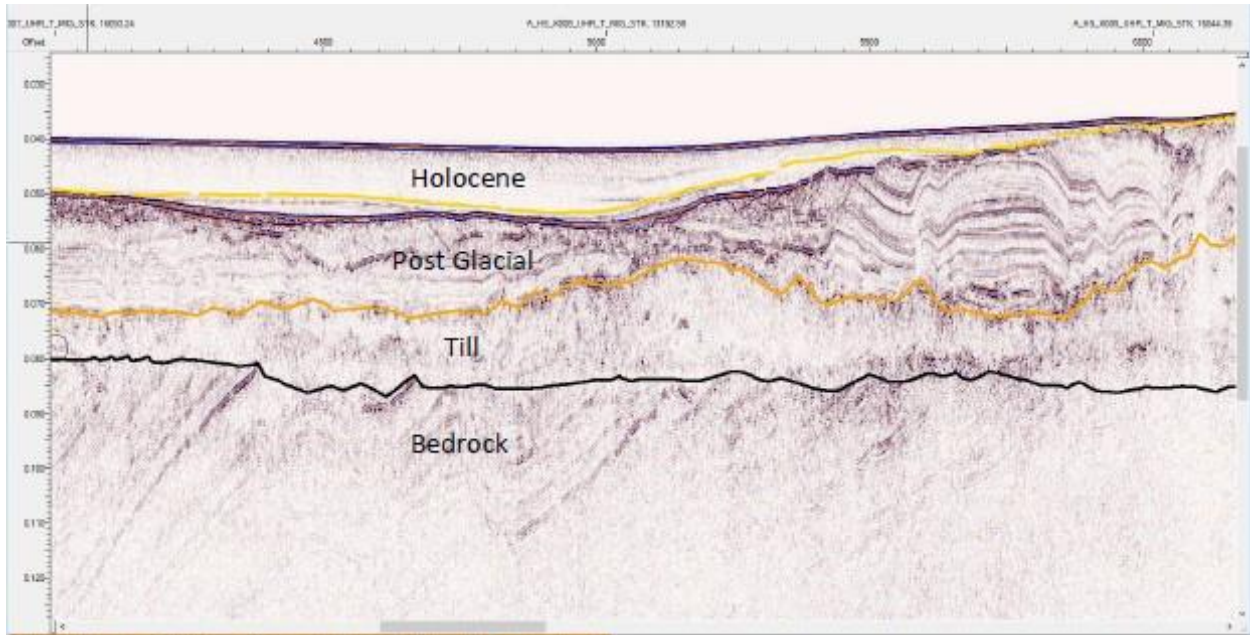
### 7.5.2 Data processing

A horizontal tow configuration (with the head and tail at 1 m water depth) was employed. This configuration was tested during the verification phase at the start of the project and adjusted to determine the optimal consideration to vertical resolution and weather dependency of survey operations. Sparker and streamer components were towed inline to optimise launch and recovery activities and line turns. The processing workflow applied to the datasets for Hesselø South is outlined in detail within APPENDIX A.

### 7.5.3 Data quality assessment

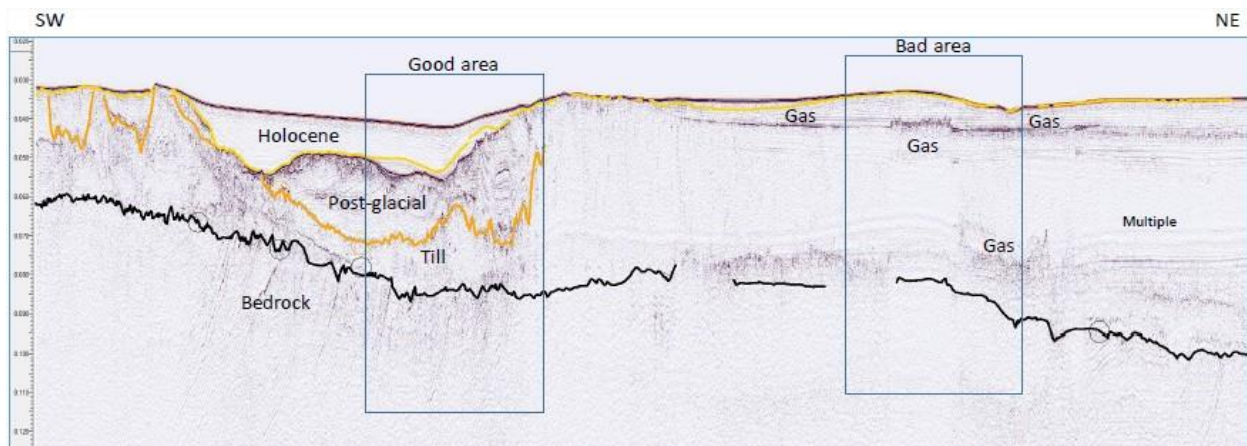
In terms of data quality/utility, the general standard is very good and there is very limited variation in UHR and SBP data quality. There is minor variation in signal phase in some of the lines and occasional missed shots. These faults have a negligible effect on interpretation. Figure 25 presents an example showing good data quality on the site. In the latter, penetration is about 100 m below seabed (BSB), despite the bedrock being situated at 35 m BSB, and unit characters can clearly be differentiated.





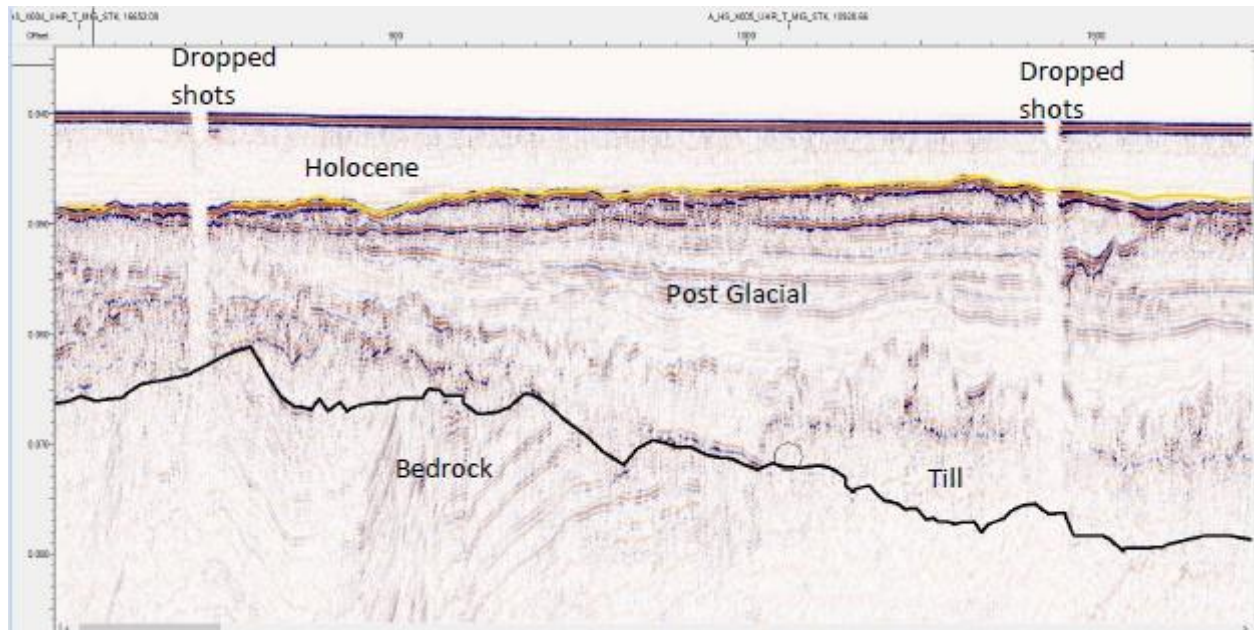
**Figure 25: Example of UHR data of high quality and good utility in Hesselø South site**

There is significant variation in UHR data utility. Gas blanks out the seismic signal and sets up reverberations over quite extensive areas. This made it difficult or impossible to map surfaces below the level of the gas. The latter is not due to an error in processing or acquisition, but is due to the physical properties of gas and the geophysical limitations of a pressure wave. Figure 26 presents an example of good quality data (as presented in Figure 25) and less quality data on the same line, showing that the usefulness of the UHR data depends on the distribution of gas rather than variation in processing or acquisition.



**Figure 26: UHR data example showing useful data (good area) and low quality data (bad area) due to the presence of gas**

The only data fault in the UHR dataset are occasional small gaps due to dropped shots (Figure 27). However, these have no consequences in making maps/grids.



**Figure 27: UHR data example showing dropped shots**

The data allow separate mapping of reflections approximately 0.5 m apart. The data were depth converted using stacking velocities and a time grid of the top bedrock. The interpretation was depth converted using a velocity of 1600 m/s to Unit III, 1800 m/s was applied to Unit III.

## 7.6 SEABED SAMPLING

The geotechnical ground-truthing phase of the survey was conducted, in order to provide initial surface sediment classifications and establish baseline physico-chemical parameters at specific locations across the site.

A total of fifty-five sampling stations were proposed by the onboard senior Marine Environmental Scientist and grab samples were collected at each of these stations. Samples were successfully acquired at fifty-three of the proposed fifty-five stations. Samples could not be acquired at stations HS\_030 and HS\_031, due to coarse sediment conditions. Similar conditions resulted in only the PC1 sample being acquired at station HS\_055. Samples acquired at stations HS\_026, 032, 033, 038, 052 and 055 were obtained from grabs with recovery volumes of <40 %; however, these were deemed to be of sufficient volume and of representative sediment type, to justify retainment for analysis. A full suite of physico-chemical samples (PC1 and PC2) were obtained at all of the other stations.

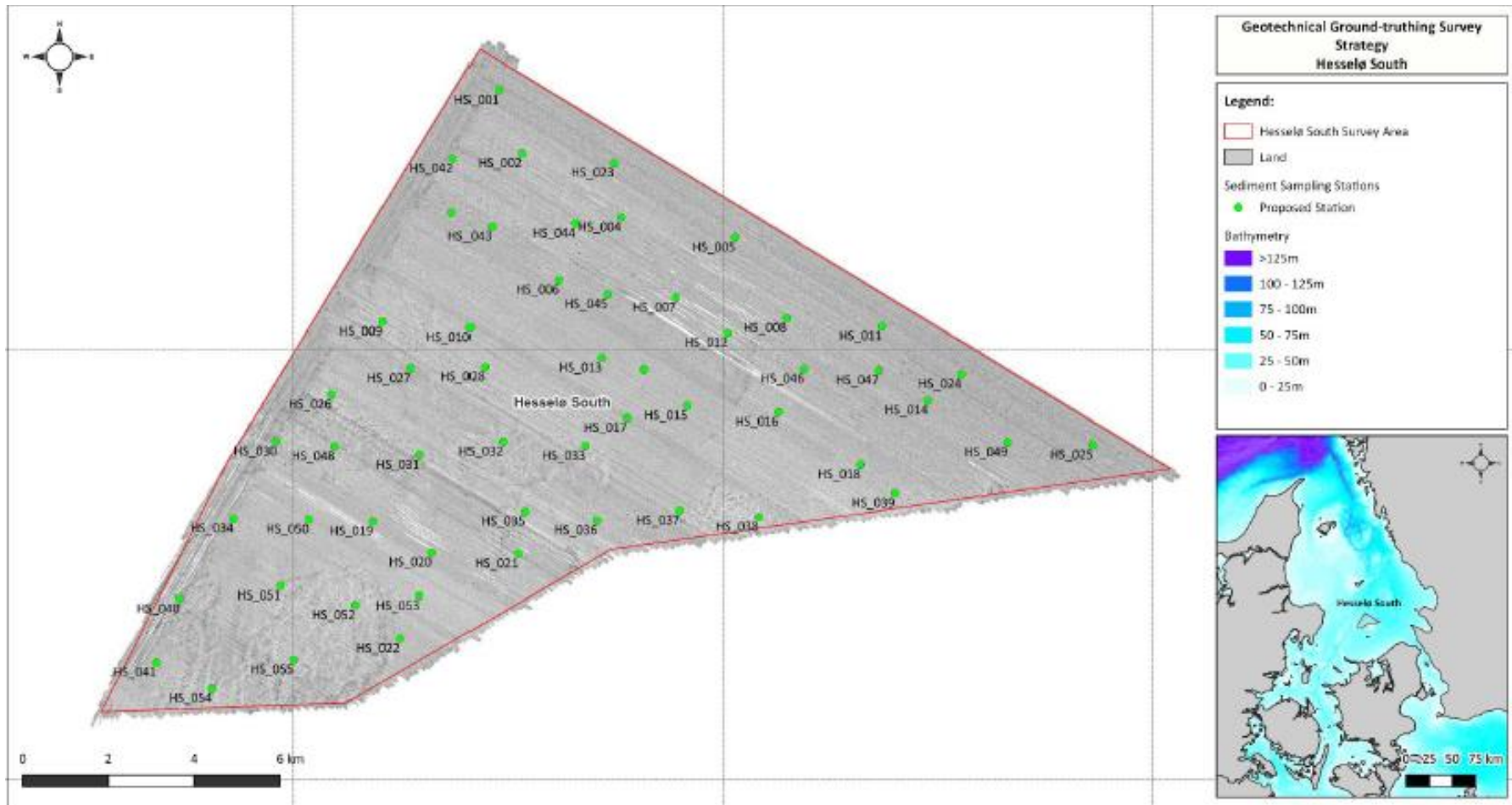
One full suite of physico-chemical samples were acquired at each of the stations, using a 0.1 m<sup>2</sup> dual van Veen grab sampler or a 0.1 m<sup>2</sup> mini Hamon grab.

A basic suite of Physico-Chemical (PC) samples, comprising a single primary (PC1) and single secondary (PC2) were acquired at each location. Particle Size Analysis (PSA), Total Organic Matter (TOM) and Carbonate Content (CC) components were sub-sampled *ex-situ* once sent to the benthic laboratory. PSA1, TOM1 and CC1 were subsampled from the primary (PC) sample and PSA2, TOM2 and CC" were extracted from the secondary (PC2) sample, as required.

Any conspicuous benthic macrofauna and species of potential conservation value were noted.



Figure 28 below indicates the proposed grab sampling positions across the Hesselø South site. The full results of the geotechnical ground-truthing at the Hesselø South site can be found in APPENDIX B of this report.



**Figure 28: Proposed surficial geotechnical ground-truthing sampling locations within the Hesselø South area**

## 8 RESULTS AND INTERPRETATION

### 8.1 CLASSIFICATION CRITERIA

#### 8.1.1 Slope classification criteria

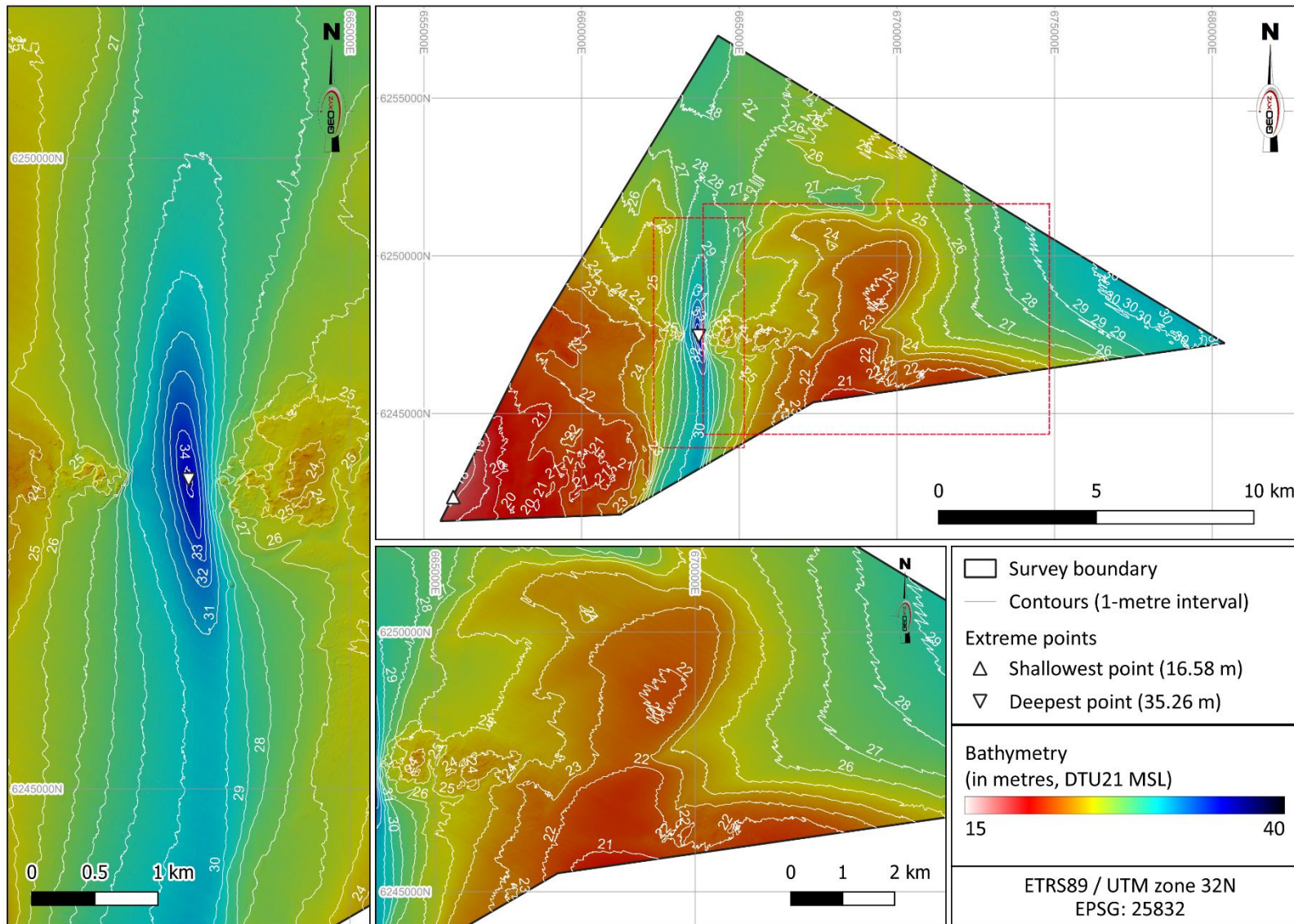
Seabed gradient has been classified as per Table 42 below.

**Table 42: Slope classification**

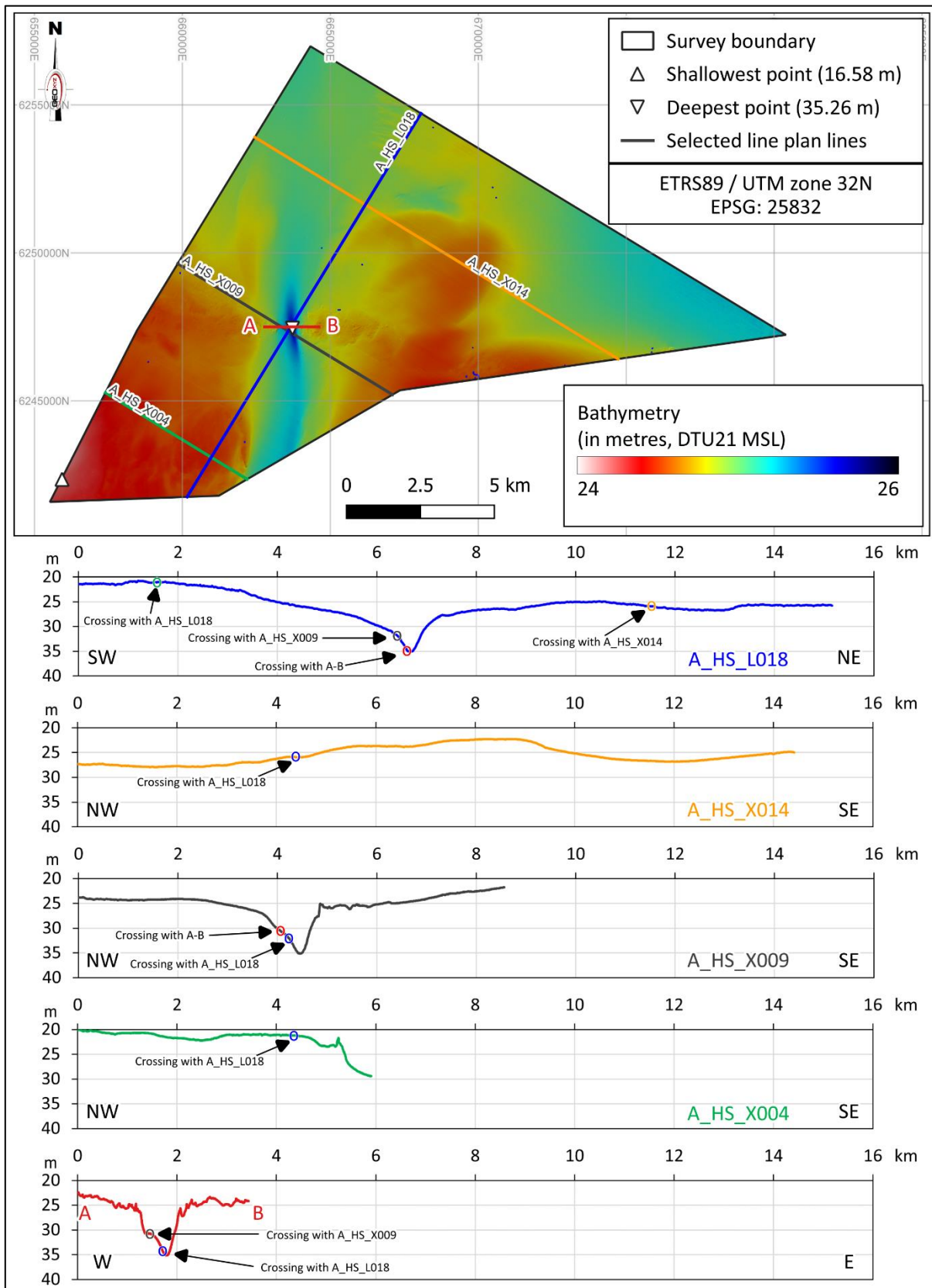
Classification	Slope
Very Gentle	< 1°
Gentle	1° - 5°
Moderate	5° - 10°
Steep	10° - 15°
Very Steep	> 15°

### 8.2 BATHYMETRY

Seabed levels across the Hesselø South site range from a minimum of 16.6 m MSL, near the south-western corner of the site at 655932 mE, 6242349 mN, to a maximum of 35.3 m MSL, in the central western section, near 663720 mE, 6247452 mN. Overview of bathymetry within the Hesselø South survey is shown in Figure 29, whereas bathymetry profiles for several line plan segments and a channel feature are shown in Figure 30.



**Figure 29: Bathymetry across Hesselø South area**



**Figure 30: Bathymetry profiles based on selected line plan segments and a profile across the broad channel feature (A-B)**

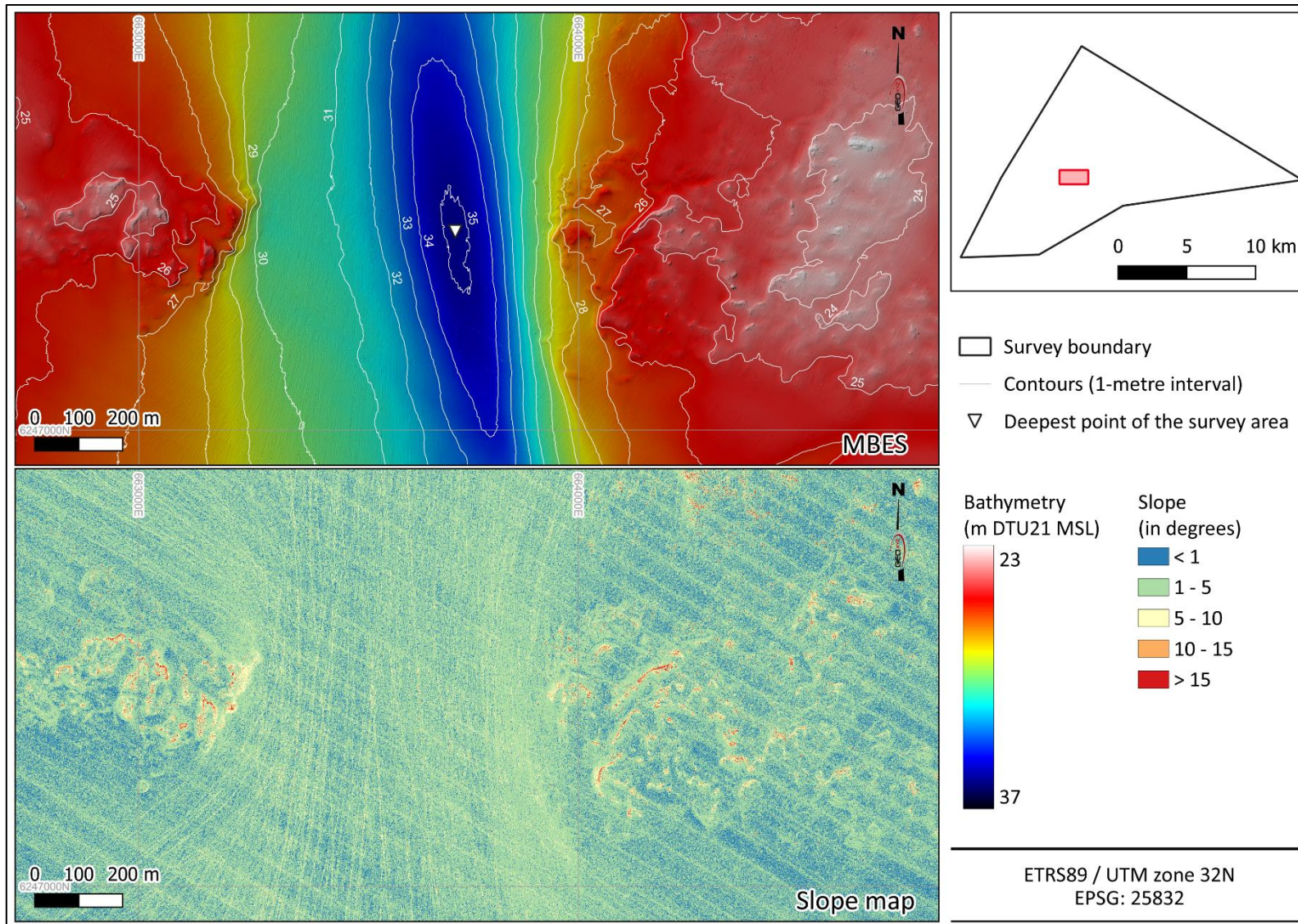
A broad channel feature crosses the western side of the site (left-most chartlet in Figure 29, visible on several profiles in Figure 30), approximately delineated by the 27.0 m MSL contours. This feature is between 750 m and 3000 m wide and runs approximately north-south. Seabed levels within the channel range from approximately 25.0 m MSL to a maximum of 35.3 m MSL, near 663720 mE, 6247452 mN, at its narrowest part.

To the east of the narrow channel feature, seabed levels undulate very gently between approximately 21.0 m MSL and 30.0 m MSL. Levels initially shoal very gently eastwards, towards a broad (2000 – 3000 m wide), NNE-SSW orientated, low ridge feature, centred at approximately 669450 mE, 6248850 mN and which stands approximately 3.0 m above the surrounding seabed (bottom chartlet in Figure 29, visible in the second profile in Figure 30). To the east of the low ridge feature, seabed levels deepen again very gently towards the east and north-east, reaching a maximum of 30.1 m MSL at the extreme eastern corner of the site, near 680400 mE, 6247230 mN.

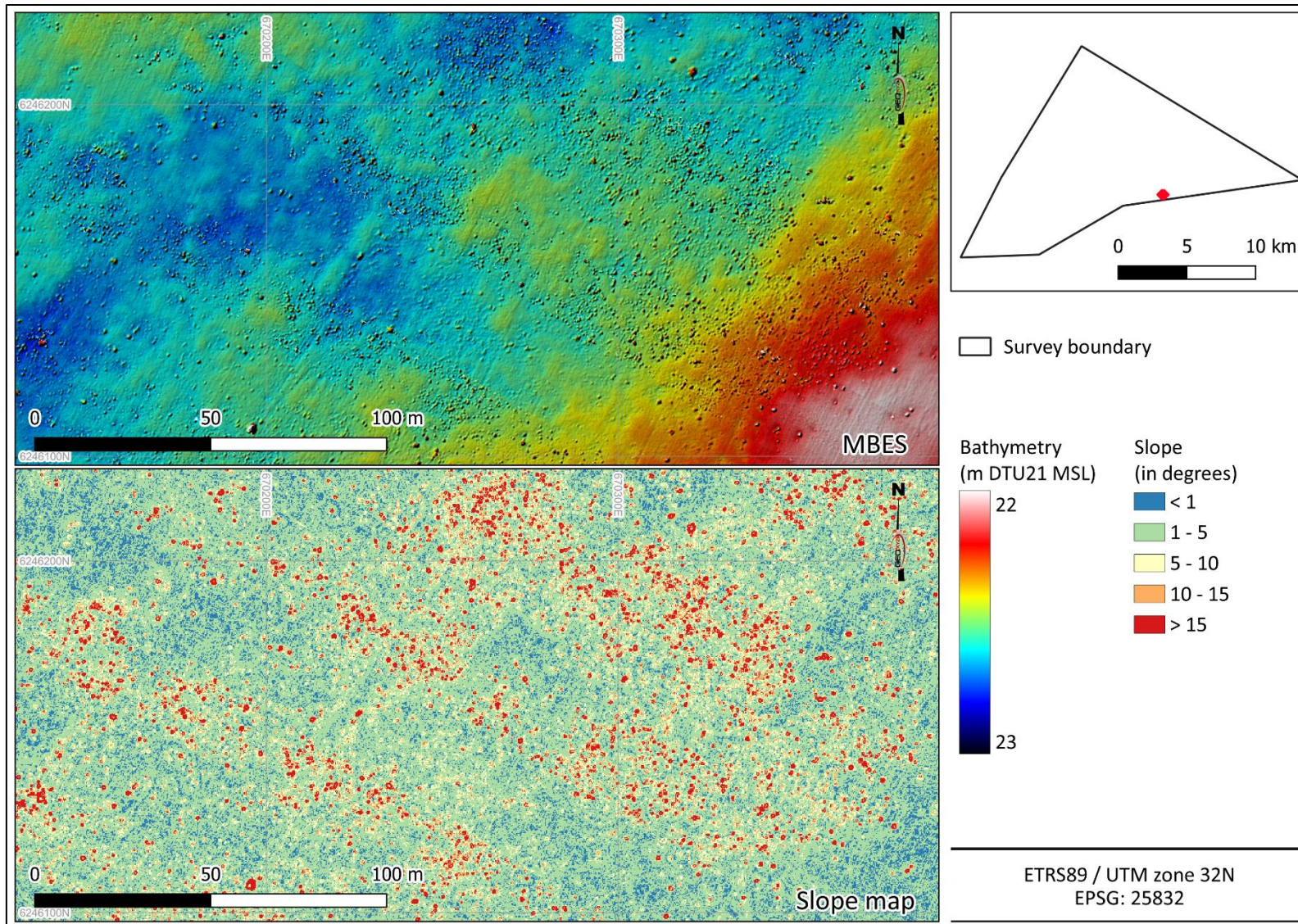
To the west of this broad channel feature, seabed levels deepen very gradually towards the east, or east-northeast, at a slope gradient of  $<0.1^\circ$ . The seabed slopes on the western side of the channel dip eastwards at gradients of  $0.2^\circ$  -  $1.4^\circ$ . Similarly, the seabed slopes on the eastern side of the channel range from  $2.2^\circ$  -  $3.2^\circ$  (Figure 30 and Figure 31).

The highest slope values (very steep slopes;  $>15^\circ$ ) are found in seabed features such as boulders (Figure 32) and wrecks (Figure 33), as well as on the sides of ridges and smaller elevated features (an example is shown in Figure 34).

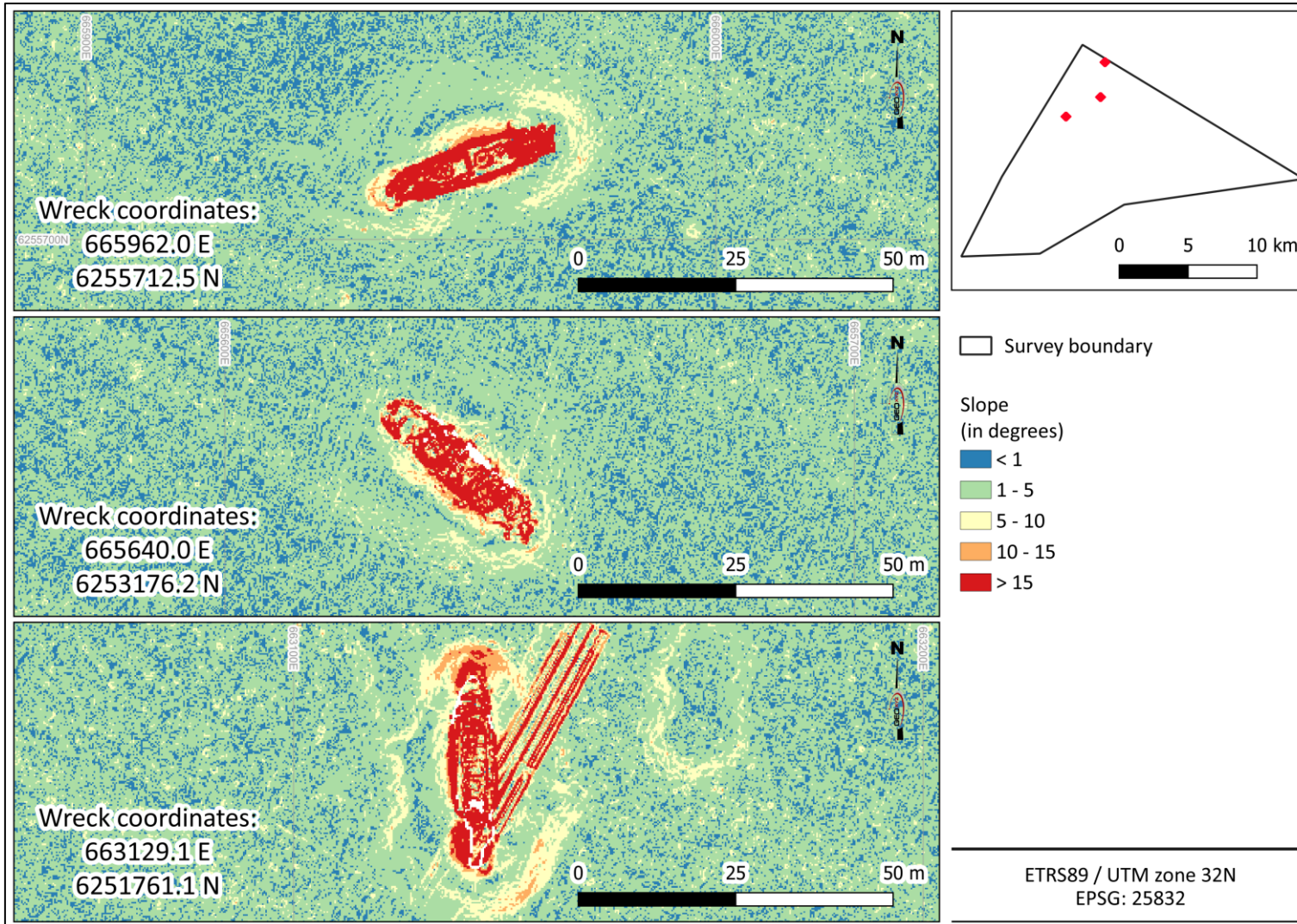




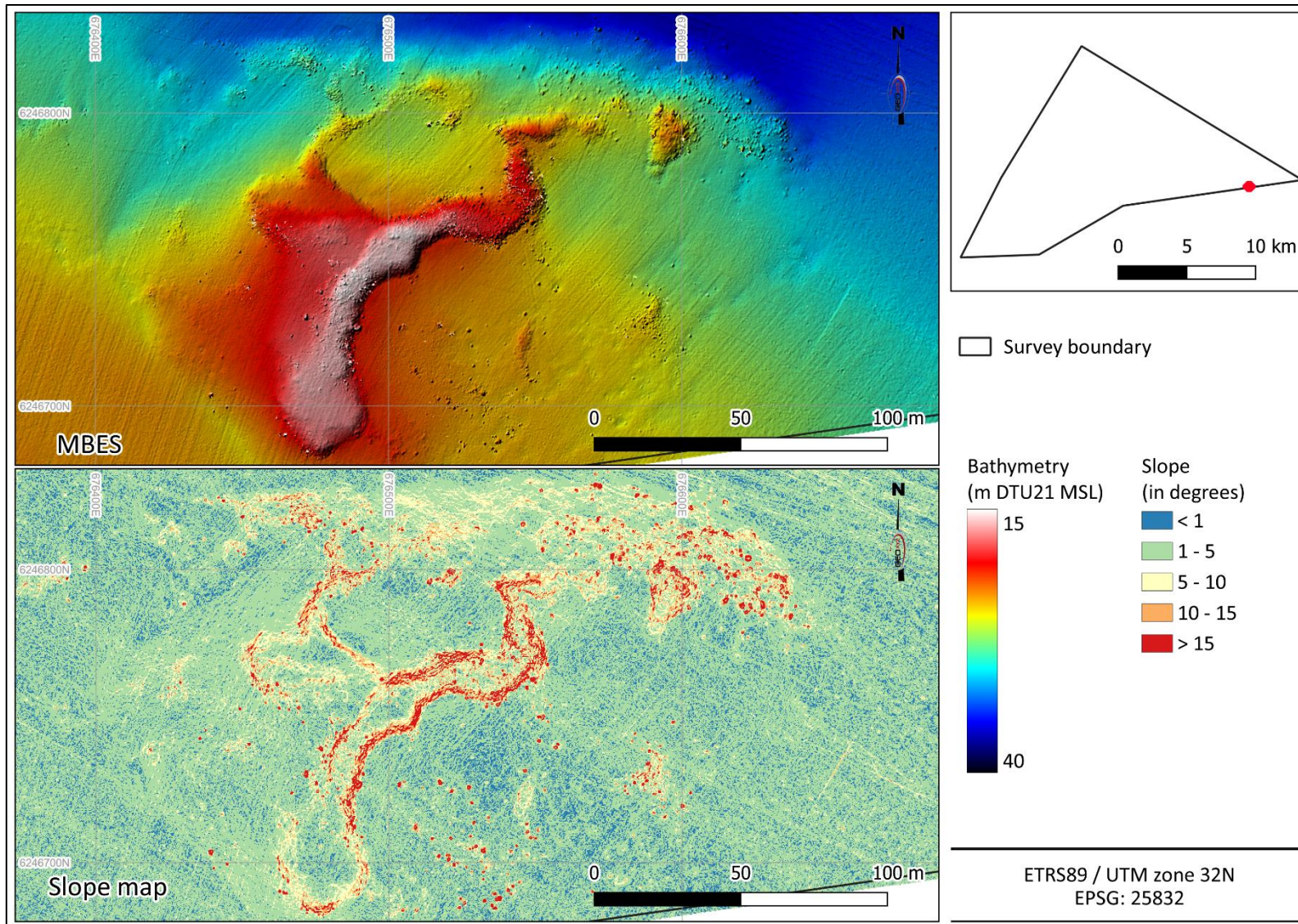
**Figure 31: Bathymetry and slope map of the broad channel in the western central part of the survey area**



**Figure 32: Bathymetry and slope map of a boulder field in the southern part of the survey area**



**Figure 33: Slope map of the three wrecks found within the survey area**

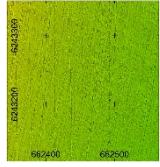
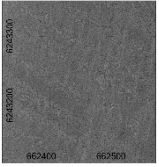
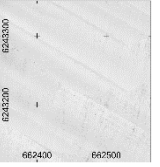
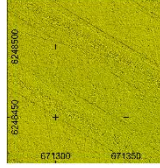
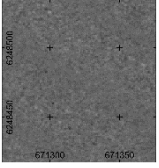
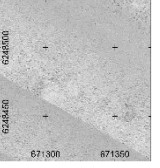
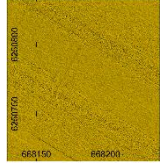
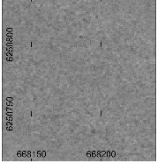
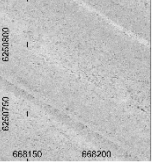
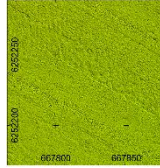
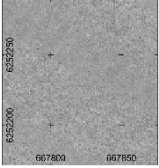
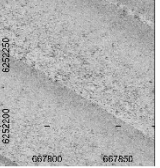
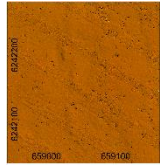
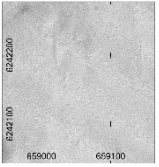
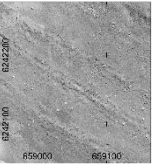


**Figure 34: Slope map of a smaller elevated feature in the southeastern part of the survey area**

### 8.3 SEABED SURFACE CLASSIFICATION: GEOLOGY

The seabed geology for Hesselø South site was evaluated from the interpretation of the low and high frequency SSS data, the backscatter imagery and the MBES dataset. Data analysis and classification was performed using the seabed acoustic characteristics, such as reflectivity and backscatter strength, as well as the seafloor relief and the overall pattern. During the interpretation of the SSS data, higher reflectivity areas – higher intensity sonar returns (darker grey to black colors) have been related to relatively coarse-grained sediments and lower reflectivity areas – lower intensity sonar returns have been related to relatively fine-grained sediments (Table 43). GEUS terminology was used to define the identified seafloor sediment in the survey area.

**Table 43: Acoustic characteristics of the sediment types within the Hesselø South site**

Geological interpretation	Colour and code	Sediment interpretation	Acoustic description	MBES image	Backscatter image	LF SSS image
Mud and sandy mud	21	Predominately mud with minor to significant fractions of sand. May contain minor fractions of or gravel	Low reflectivity			
Muddy sand	13	Predominately sand with significant fractions of mud and muddy sand. May contain minor fractions of or gravel	Low to medium reflectivity			
Sand	12	Predominately sand. May contain minor fractions of mud and/or gravel	Medium reflectivity			
Gravel and coarse sand	11	Mixed sediment. Predominately gravel and sand. May contain mud.	Medium to High reflectivity. Patches of high reflectivity interspersed in areas of low to medium reflectivity			
Till/diamicton	41	Mixed sediment. Constituents range between mud and boulders.	Low to High reflectivity. Patches of high reflectivity interspersed in areas of low to medium reflectivity. Usually, positive relief in MBES data			

Bathymetric data aided the interpretation mainly in outlining of possible outcrops and the boulder field delineation.

The resultant seabed surface geology has been correlated to the soil description of the surficial grab samples and the onshore laboratory results. For the grab sample analysis, the definition of the particle sizes followed the Wentworth scale (Figure 35).

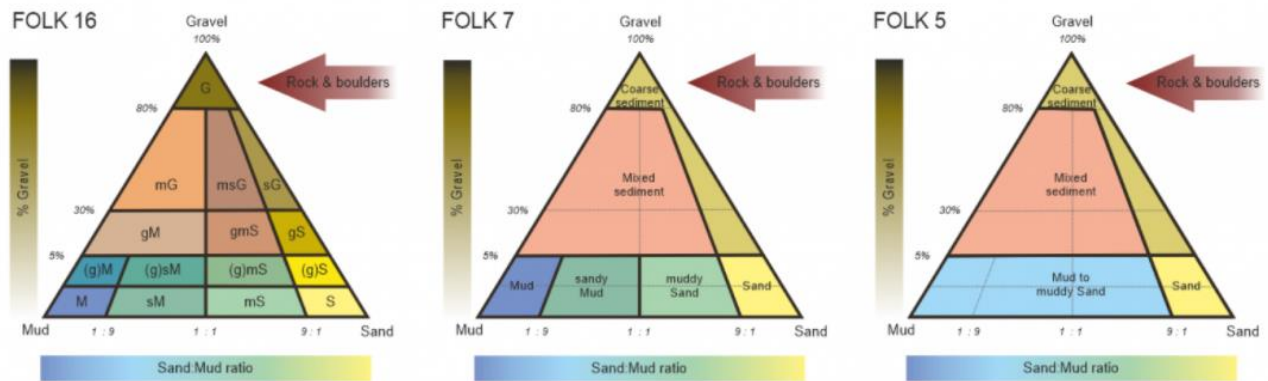
Major Grade	Phi ( $\Phi$ ) limits		Wentworth size class
	Lower	Upper	
gravel	<-8	-8	boulder
	-8	-6	cobble
	-6	-2	pebble
	-2	-1	granule
sand	-1	0	very coarse sand
	0	1	coarse sand
	1	2	medium sand
	2	3	fine sand
	3	4	very fine sand
mud	4	5	coarse silt
	5	6	medium silt
	6	7	fine silt
	7	8	very fine silt
	8	>8	clay

Scale by Wentworth (1922) classifying sediment particles according to the diameter expressed in units of N (phi, the negative log 2 of the diameter in millimeters).

**Figure 35: Wentworth Scale – classifying sediment particles**

For the needs of correlation, the results were further processed and reclassified, according to the Folk 7 classification system (Figure 36). For Sand, Muddy sand, and Mud and muddy sand seafloor sediment classes there is a direct correlation to the Folk 7 classification. Gravel and coarse sand, and Till/diamicton sediment classes have been correlated to Mixed sediment grab samples and, for their separation, reflectivity, relief and sub-surficial geology have been considered.

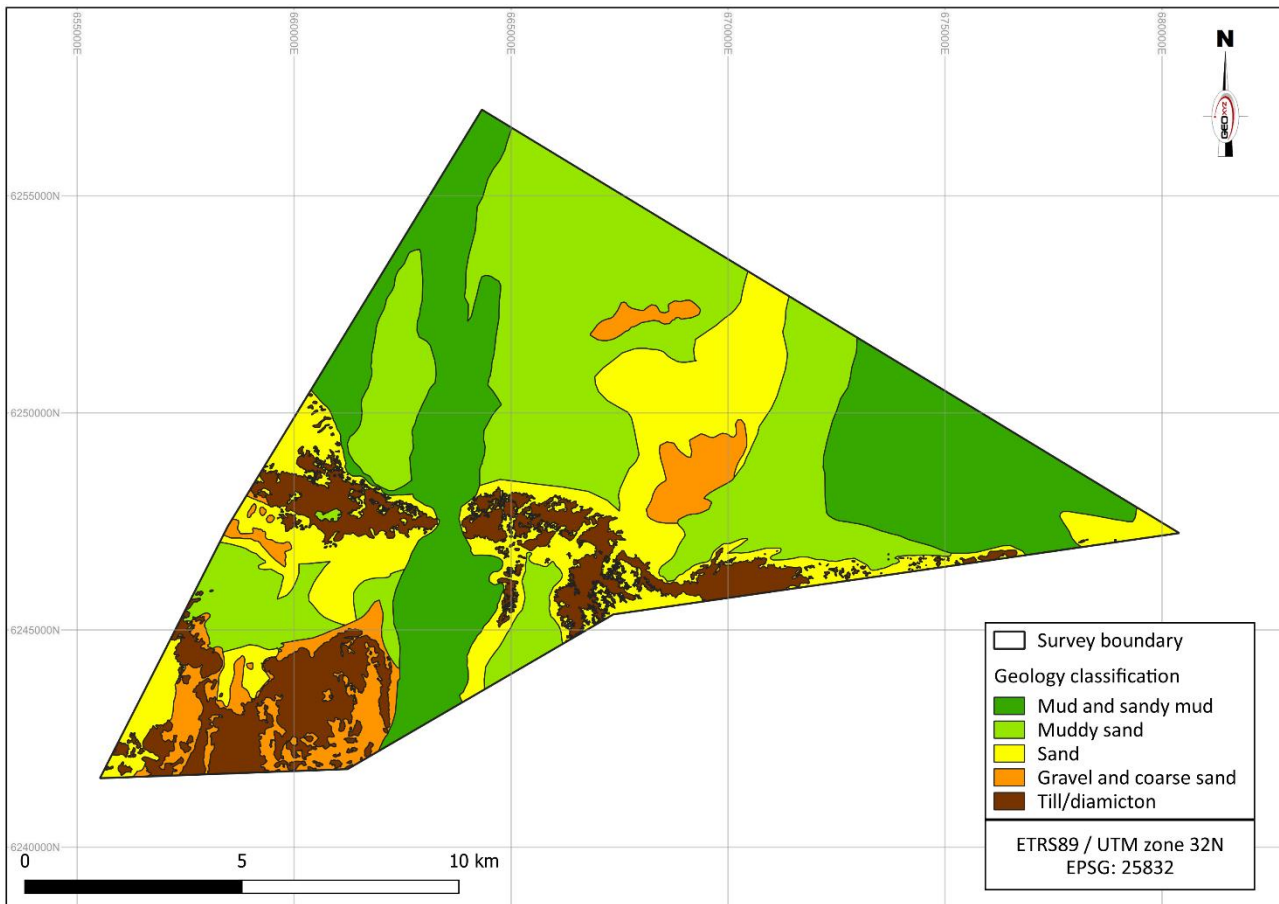
**EMODnet Folk substrate classification**



FOLK, 16 classes	FOLK, 7 classes	FOLK, 5 classes
Rock & Boulders	Rock & Boulders	Rock & Boulders
Gravel - G sandy Gravel - sG gravelly Sand - gS	Coarse sediment	Coarse sediment (Gravel >= 80% or (Gravel >= 5% and Sand >=90%))
muddy Gravel - mG muddy sandy Gravel - msG gravelly Mud - gM gravelly muddy Sand - gmS	Mixed sediment	Mixed sediment (Mud 95-10%; Sand < 90%; Gravel >= 5%)
(gravelly) Mud - (g)M Mud - M	Mud (Mud >= 90%; Sand < 10%; Gravel < 5%)	Mud to muddy Sand (Mud 100-10%; Sand < 90%; Gravel < 5%)
(gravelly) sandy Mud - (g)sM sandy Mud - sM	sandy Mud (Mud 50-90%; Sand 10-50%; Gravel < 5%)	
(gravelly) muddy Sand - (g)mS muddy Sand - mS	muddy Sand (Mud 10-50%; Sand 50-90%; Gravel < 5%)	
(gravelly) Sand - (g)S Sand	Sand (Mud < 10%; Sand >= 90%; Gravel < 5%)	Sand

**Figure 36: EMODNET Folk substrate classification**

Finally, seafloor sediment classification has been integrated to the sub-seabed geology data. The seabed substrate across the Hesselø South area consists predominantly of muddy sand (Figure 37).



**Figure 37: Seabed surface geology classification**

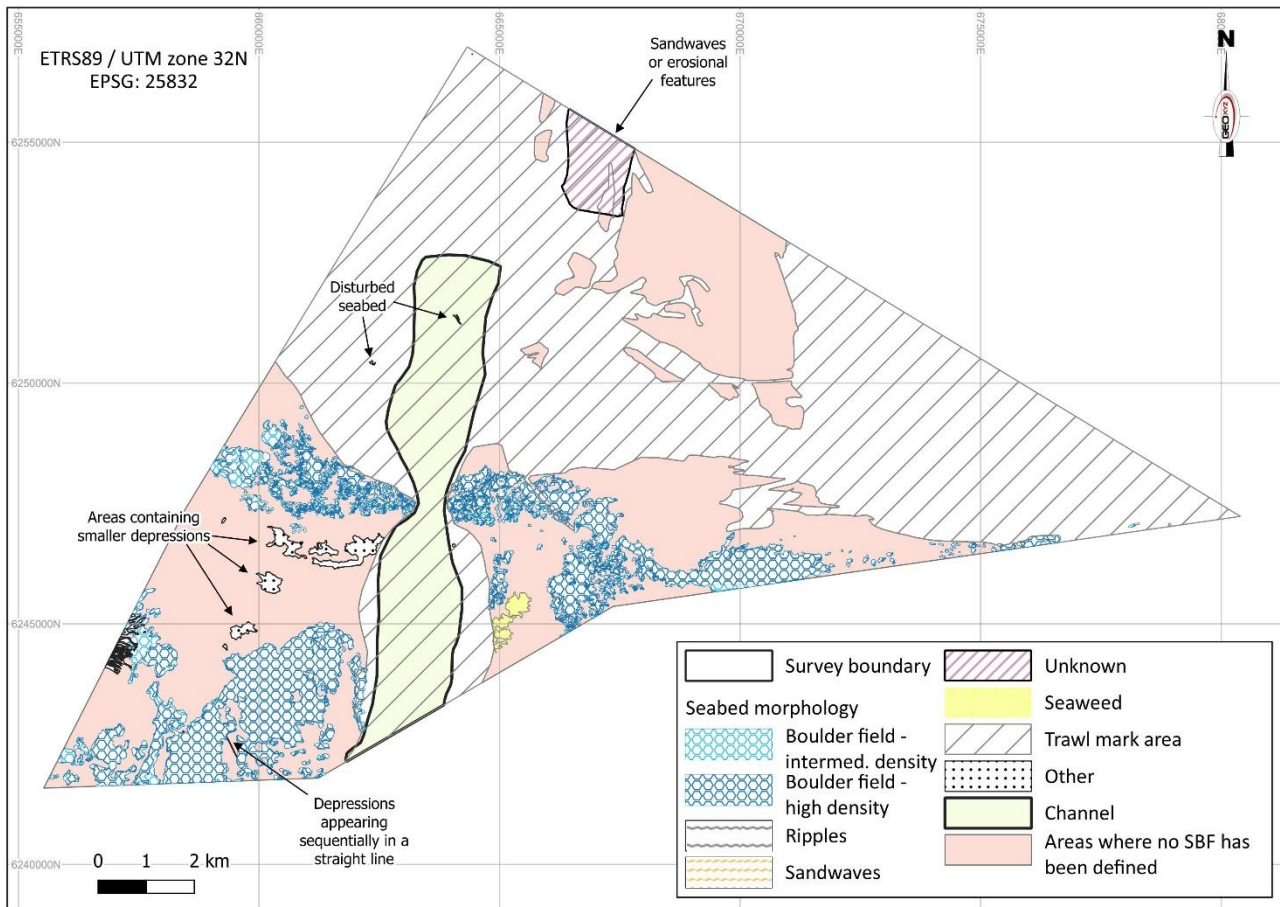
The seabed sediments within the broad, N-S channel feature in the western half of the site and across the deeper, eastern section of the site, comprise mainly mud and sandy muds (silts/clays and sandy silts/clays). Across the northern section, the seabed sediments generally comprise extensive areas of sands and muddy sands (silty/clayey sands), with occasional coarser patches of gravel and coarse sands.

The southern section of the site is more complex, comprising raised areas of outcropping Till/diamicton, surrounded by extensive areas of sands and/or gravel and coarse sand. One of these raised areas of Till forms an irregular ridge feature, which runs from west to east across the central part of the area. Finally, the south-western section of the site comprises a large area of outcropping Till/diamicton, surrounded by sands and/or gravel and coarse sands.

#### 8.4 SEABED SURFACE CLASSIFICATION: MORPHOLOGY

Seafloor morphology and seabed feature descriptions were based on the interpretation of SSS, BKS and MBES datasets whereas the results from the SBP have been considered. Various morphological seabed features of different dimensions were identified across the Hesselø South site. Some of them are the result of variable geological environment as well as past and present hydrodynamic conditions within the regime of sea level fluctuations (e.g. Areas of boulders, Ripples, etc.) whereas others have anthropogenic origin (e.g. Trawl marks, Disturbed seabed). An overview of the seabed features is presented in Figure 38 below.




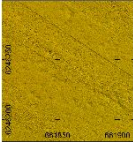
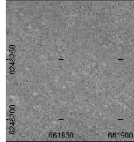
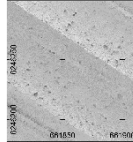
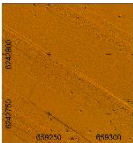
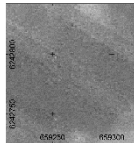
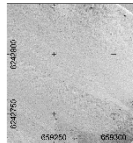
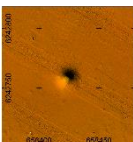
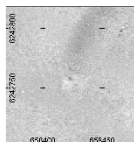
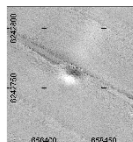
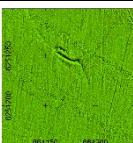
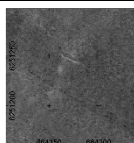
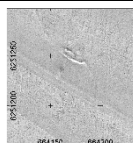
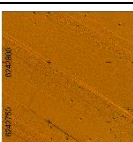
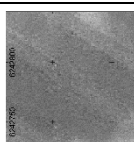
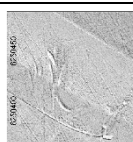
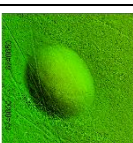
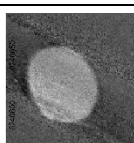
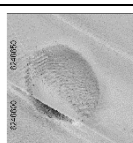


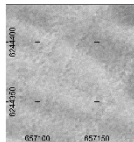

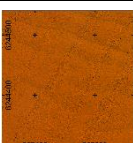
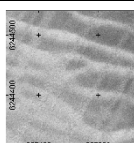
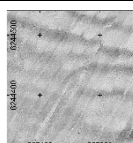

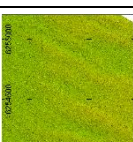
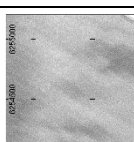
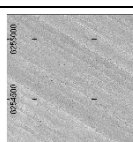



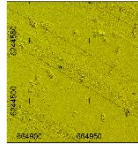
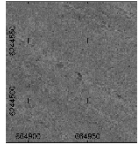
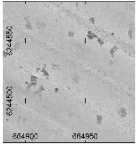

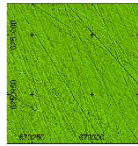
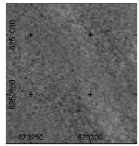
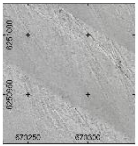
**Figure 38: Seabed surface morphology classification**

The acoustic characteristics of the interpreted seabed features across the Hesselø South area are summarized in Table 44.

**Table 44: Morphological interpretation**

Seabed Feature	Symbology	Description	MBES image	Backscatter image	SSS image
Boulder Field – intermediate density (Class 1)		High reflectivity contacts of intermediate density (40 to 80 boulders in a 100x100 box), visible in MBES			
Boulder Field – high density (Class 2)		High reflectivity contacts of high density (more than 80 boulders in a 100x100 box), visible in MBES			
Channel		Low to medium reflectivity, easily distinguishable in BKS, visible in MBES			

Seabed Feature	Symbology	Description	MBES image	Backscatter image	SSS image
Other – Area of depressions		Medium to high reflectivity circular objects, visible in MBES			
Other – Linearly aligned depressions		Medium to high reflectivity circular objects, linearly aligned along a SW-NE line, visible in MBES.			
Other – Depression		Medium reflectivity object, visible in MBES			
Other – Disturbed Seabed		Low to medium reflectivity, visible in MBES			
		Low to medium reflectivity pattern visible in MBES			
		Medium to high reflectivity elliptical object, visible in MBES			
Ripples			Low to high reflectivity alternating areas. Not clear in MBES. Wavelength (0.5 – 2.0 m) is the primary classifier		
Sandwaves		Low to high reflectivity alternating areas. Visible in MBES. Wavelength (20 – 130 m) is the primary classifier. Sandwave crests have been also traced as linear features			
Unknown – Sandwaves or possible erosional features		Low reflectivity, distinguishable only in BKS and MBES			

Seabed Feature	Symbology	Description	MBES image	Backscatter image	SSS image
Biology – Seaweed		High reflectivity irregular patches, visible in MBES			
Trawl marks		Low to medium reflectivity linear features, visible in MBES			

Boulder fields are visible in the southwestern and central part of the site (Figure 38). The high-density boulder fields (Class 2) generally coincide with the areas of outcropping/subcropping till/diamicton, while the intermediate density boulder fields (Class 1) surround the Class 2 boulder fields.

Sandwaves and large ripples or megaripples were interpreted in the southwestern part of the survey area. These features have orientations between E-W, NW-SE and SW-NE and exhibit wavelengths between 20 m and 130 m, with heights between 0.1 and 1.0 m. Subordinate areas of ripples are present between the sandwaves. These features are similarly orientated, with wavelengths between 0.5 m and 2 m.

A channel feature is seen to cross the site, with a general N-S direction. In the northern tip, its limits are not clear, whereas it becomes more distinct within the central and southern sections of the site.

Extensive fishing activity, with numerous well-preserved trawl marks of different orientations, are outlined, mainly in the northern half part of the Hesselø South site, as well as within the channel feature.

Six areas containing numerous, roughly circular, small depressions, between 0.1 m and 0.4 m deep and up to 5.0 m across, occur in the central-eastern part of the site (Figure 38). These six areas vary between 60 m and 1500 m in width and length. Similar features are seen along a SW-NE line in the southeastern part of the site, possibly related to fishing, surveying or construction activities. An isolated depression, with an approximate radius of 6 to 8 m and 1.5 m depth, occurs in the southern part of the site (Figure 38). Disturbed seabed areas, possibly of anthropogenic origin (fishing, survey, construction activities) are also present.

An irregular, NW – SE orientated seabed mound, approximately 65 m long and up to 2.0 m high, is present in the central part of the site (Figure 38).

An area of unknown seabed features is present in the northern part of the site (Figure 38). These are visible in the MBES data but are not recognizable in the SSS dataset. They could be interpreted as possible sandwaves, but no other evidence of other bedforms such as ripples is present. Alternatively, they could be possible erosional features/ice sculpted areas and a seabed expression of the H05 erosional surface, in an area where Unit II – periglacial-glaciomarine sediments are covered by a thin layer of Unit I Holocene deposits (Figure 50). The interpretation of those features is uncertain.

#### 8.4.1 Boulder field identification criteria

The boulder field identification criteria for the survey are outlined in Technical Query TQ-009. Seabed objects, including boulders > 0.5 m in any direction were interpreted and classified. Areas with high boulder densities were provided as POL delineated from the SW projects and classified as per Table 45 below. Individual boulders within the boulder fields were picked using the automatic boulder picking algorithm. Debris objects larger than 0.5 m in any direction within the boulder fields were isolated from the auto-picked boulder fields and further investigated.

**Table 45: Boulder field classification**

Boulder density	Classification	Description
Intermediate	Class 1	Concentration of 40 – 80 boulders within an area of 100 x 100 m
High density	Class 2	Concentration of > 80 boulders within an area of 100 x 100 m

### 8.5 SEABED SURFACE CLASSIFICATION: MAN-MADE FEATURES

Seabed surface objects which are determined to be man-made objects (MMO) are outlined in Table 46. A total of 924 objects were identified through the interpretation of the MBES, SSS and magnetometer datasets.

**Table 46: Summary of man-made objects**

Feature type	Total amount	Comment
Wrecks	3	There are three wrecks found within the Hesselø South site.
Metallic	450	450 contacts have been found within a 5 m radius of a magnetic anomaly. These metallic objects can be found as a single object or a cluster of objects.
Ropes	8	Eight contacts are related to possible soft rope items.
Other contacts	464	464 sonar contacts are identified to be related to either a cluster of contacts or a single contact item.
Cable/pipeline	0	No cable nor pipeline infrastructure was identified.

453 sonar contacts were noted within a 10 m radius of magnetic anomalies (450 metallic contacts and three wrecks). Some of those contacts are observed as a cluster. The contacts which are close to a magnetic contact (5-10 m), could be ferrous objects.

#### 8.5.1 Archaeological findings

GEOxyz is not specialized in providing archaeological services. As such, the findings in this report are based on an interpretation of data which is a matter of opinion on which professionals may differ.

#### 8.5.2 Wrecks

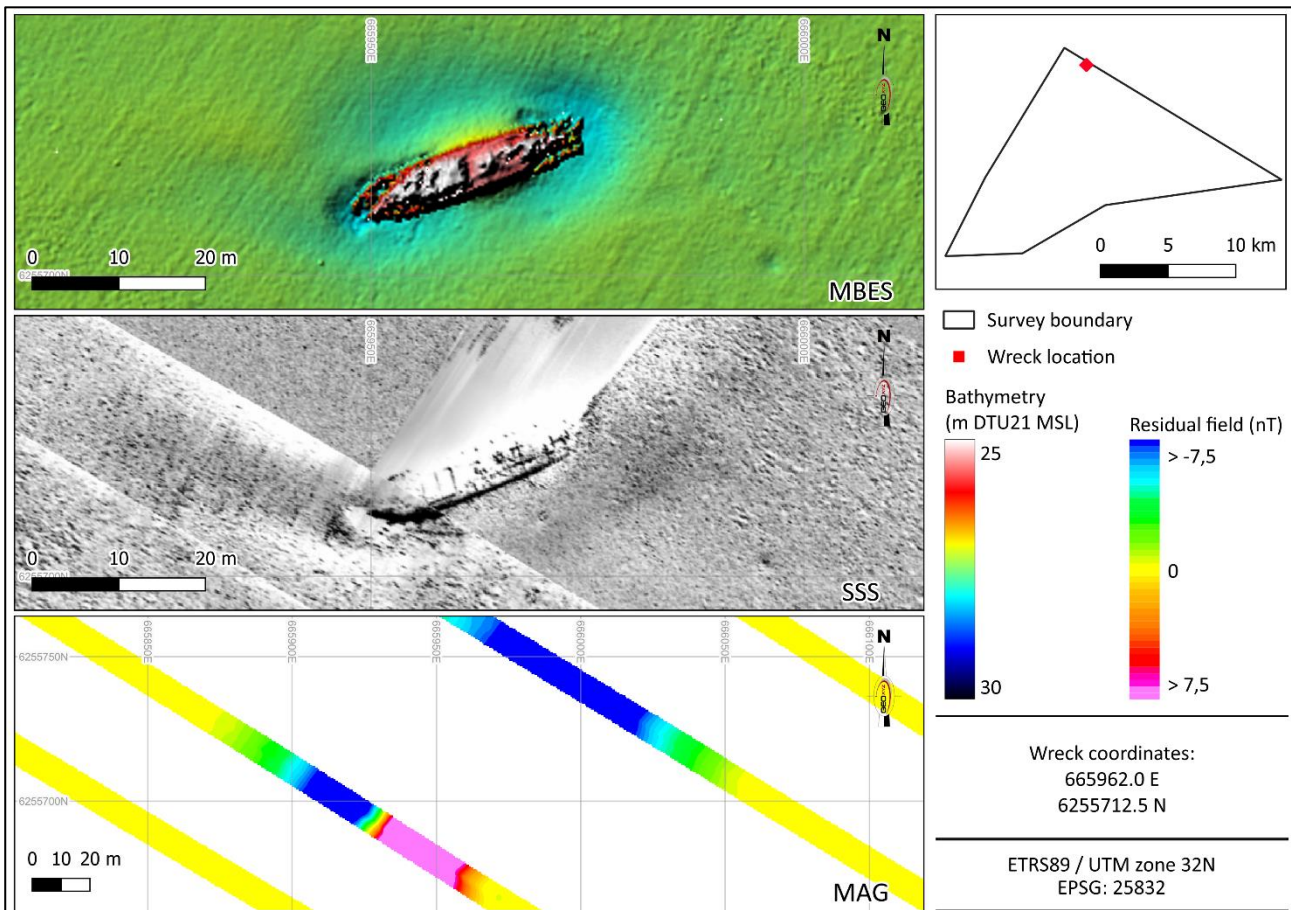
A total of three wrecks were identified across the Hesselø South area. A summary of the wrecks is presented in Table 47. All shipwrecks have been identified as unknown shipwrecks. They appear resting on the seabed and they are well preserved.

**Table 47: Wrecks within Hesselø South survey area**

Wreck No	MMO ID	Wreck Name	Easting (m)	Northing (m)	Length (m)	Width (m)	Max. Height (m)	Water Depth (m)	Comments
1	107	unknown	665960.6	6255711.9	29.0	6.0	5.0	24.0	Largely intact. Small magnetic signature
2	140	unknown	663128.7	6251761.4	31.5	8.0	7.0	28.0	Largely intact. Large magnetic signature.
3	116	unknown	665631.2	6253178.0	30.0	8.0	3.5	27.0	Broken up wreck. Very large magnetic signature

### Wreck 1

The feature is located in the northern part of the Hesselø South Block, in approximately 24 m WD (Figure 39).



**Figure 39: Overview of wreck 1**

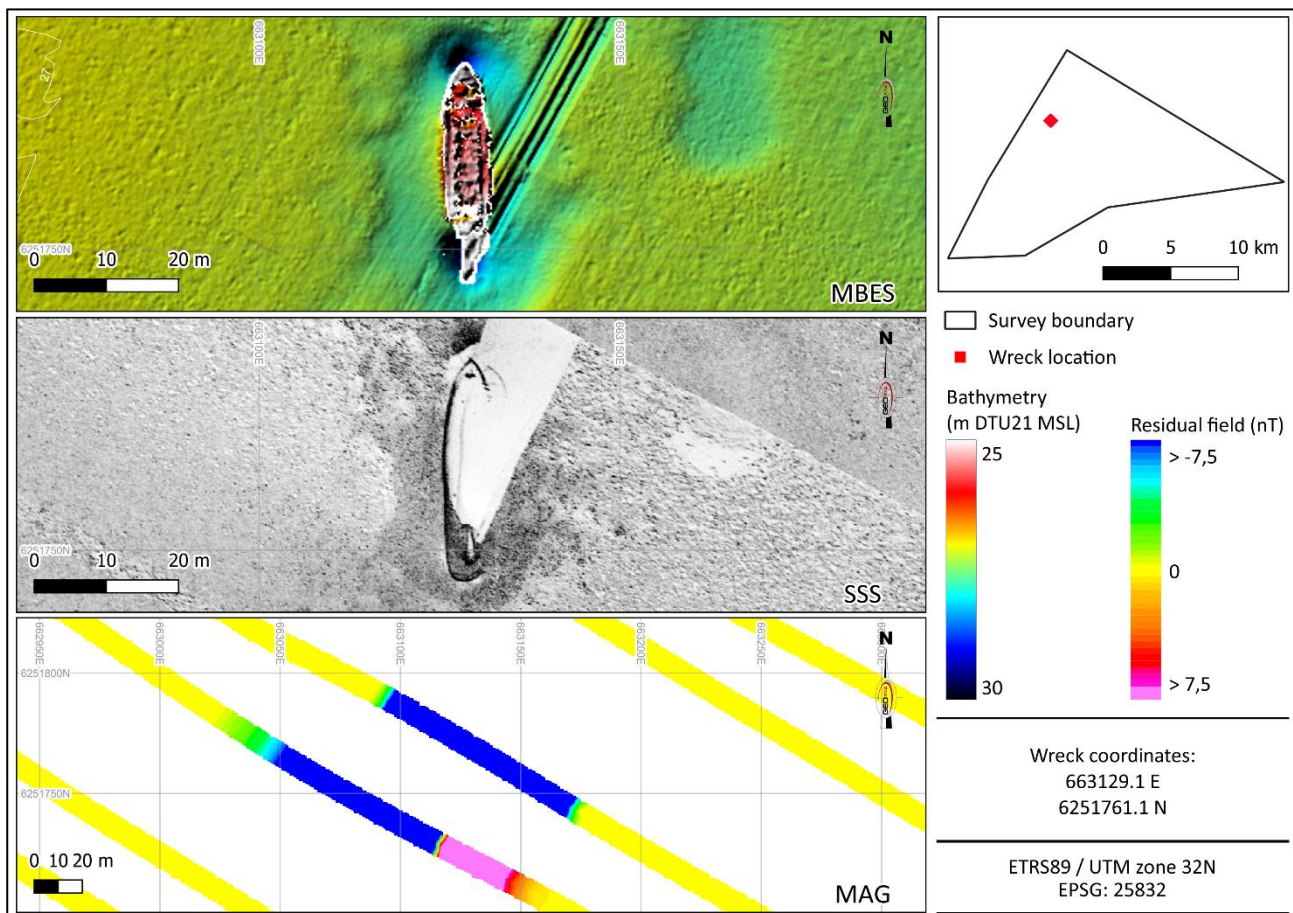
It was measured as 29 m x 6 m x 5 m (L x W x H), where 5 m is the approximately maximum height above the surrounding seabed. The long axis of the object is oriented WSW-ENE.

The feature was identified on the port side of line C\_HS\_G06\_L503S creating a shadow effect on part of the sonogram.

The feature was also spotted on the magnetometer data in Oasis Montaj processing software as an anomaly of 34 nT of amplitude on line C\_HS\_GO6\_L504S.

### **Wreck 2**

The feature is situated in the northern part of the Block, approximately in 28 m WD (Figure 40).



**Figure 40: Overview of wreck 2**

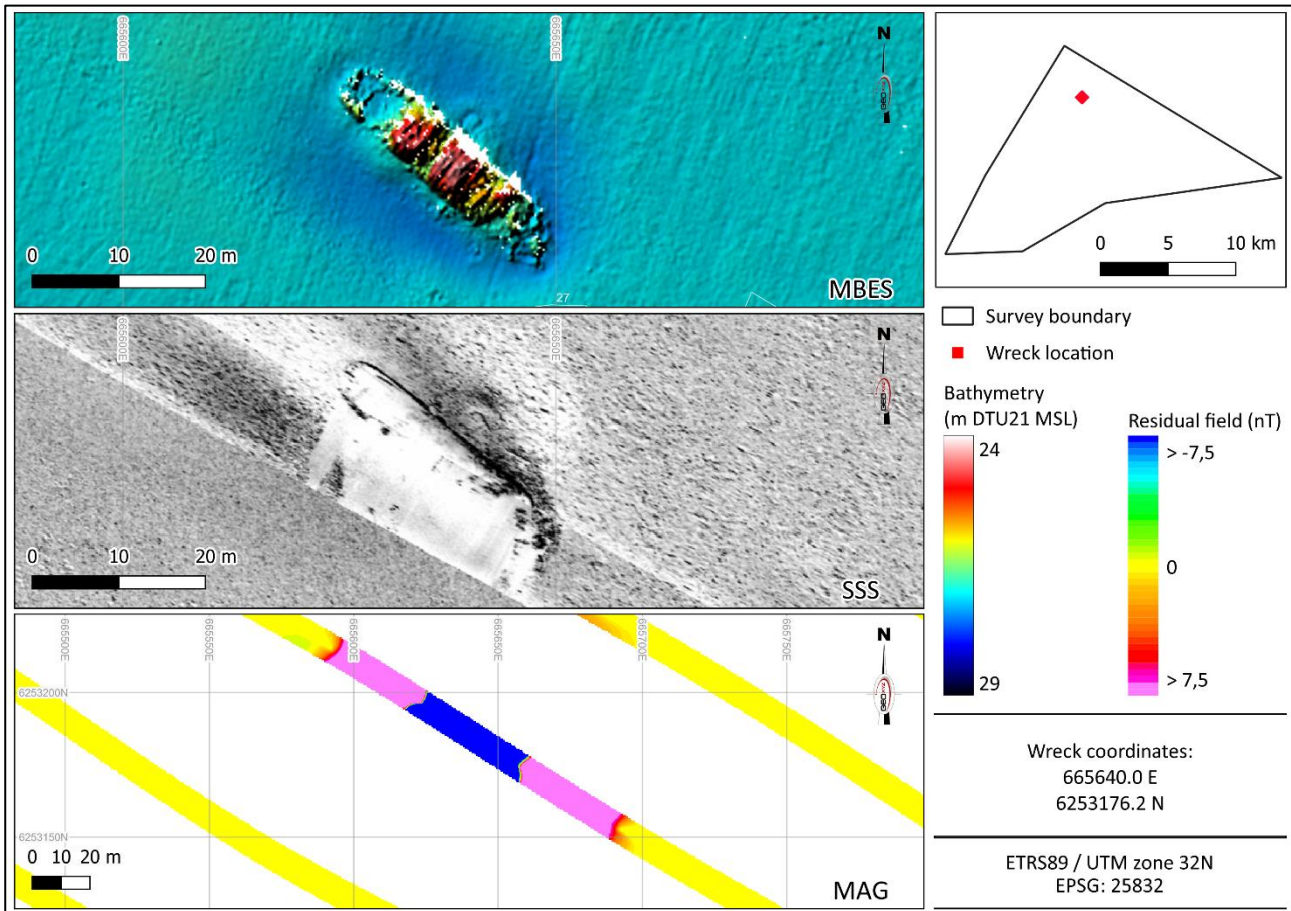
It was measured as 31.5 m x 8 m x 7 m (L x W x H), where 7 m is the approximately maximum height above the surrounding seabed. The long axis of the object is oriented N-S.

The feature was identified on the starboard side of lines C\_HS\_GO6\_L599S and C\_HS\_GO6\_L600S creating a shadow effect on part of the sonogram.

The feature was also seen on the magnetometer data in Oasis Montaj processing software on lines C\_HS\_GO6\_L599S and C\_HS\_GO6\_L600S as an anomaly of 3485.7 nT of amplitude on line C\_HS\_GO6\_L599S.

### **Wreck 3**

The feature is situated in the northern part of the Block, approximately in 27 m WD (Figure 41).



**Figure 41: Overview of wreck 3**

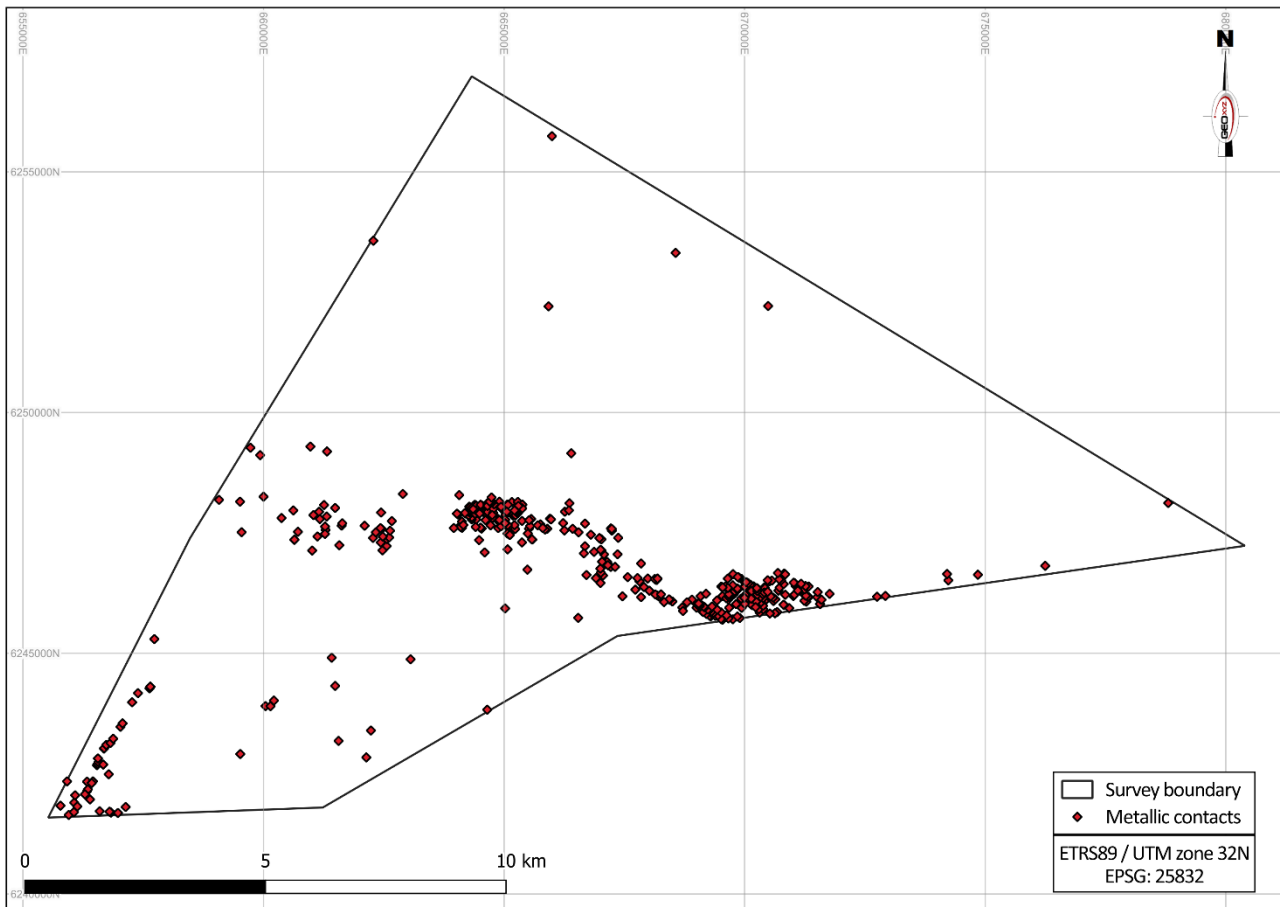
It was measured as 30 m x 8 m x 3.5 m (L x W x H), where 3.5 m is the approximately maximum height above the surrounding seabed. The long axis of the object is oriented NW-SE.

The feature was identified on the port side of line C\_HS\_GO6\_L543S and center of line C\_HS\_GO6\_L542S creating a shadow effect on part of the sonogram.

The feature was also seen on the magnetometer data in Oasis Montaj processing software on lines C\_HS\_GO6\_L543S and C\_HS\_GO6\_L542S as an anomaly of 56734 nT of amplitude on line C\_HS\_GO6\_L542S.

### 8.5.3 Metallic objects

Across the Hesselø South OWF site, there are a total of 450 sonar contacts labelled as “Metallic” (Figure 42). Along with the three wreck targets, these targets are sonar contacts recorded within a 10 m radius of magnetic anomalies.



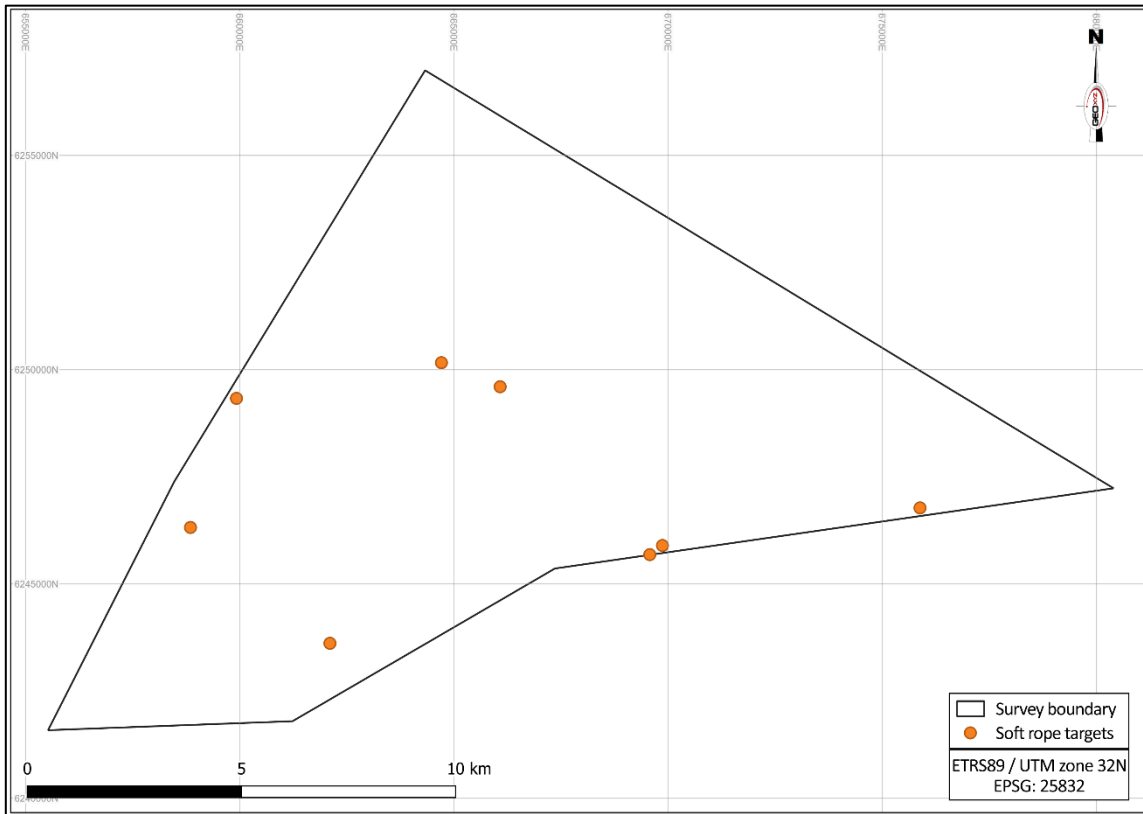
**Figure 42: Overview of metallic targets found within the survey site**

#### 8.5.4 Cables and ropes

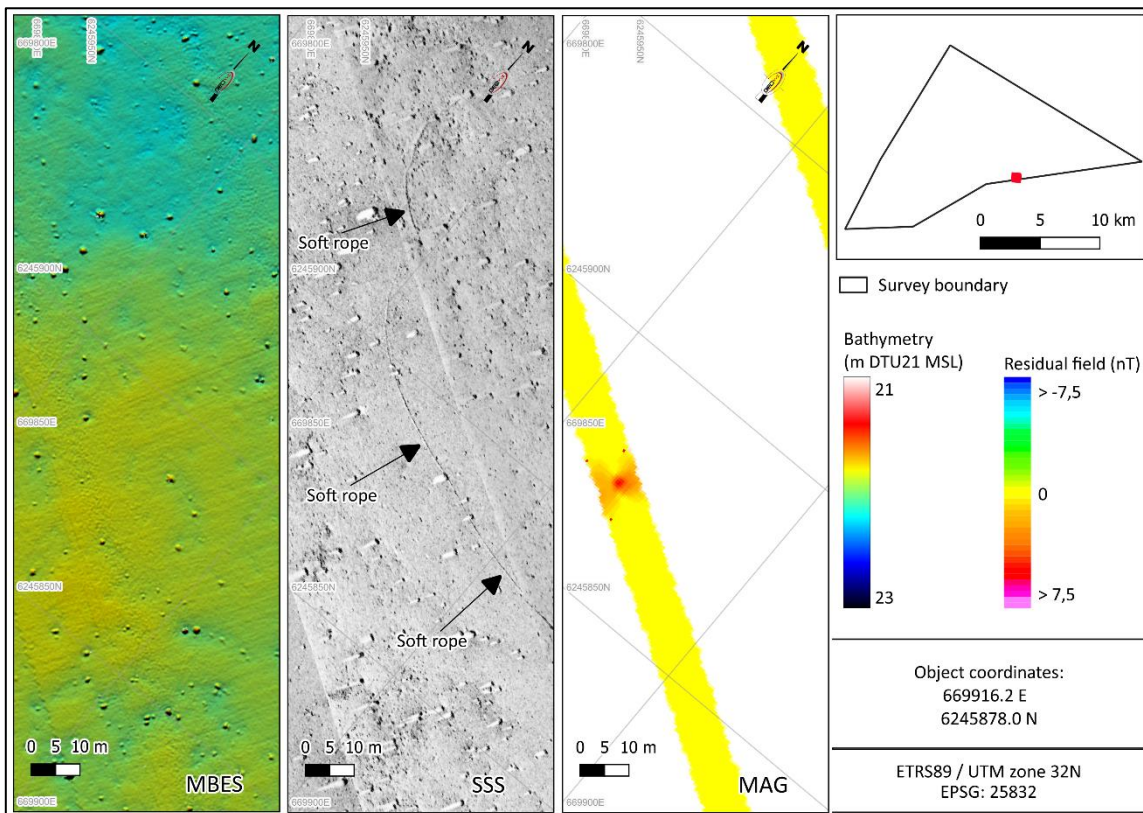
No infrastructure or communication-related cables were identified within the Hesselø South site.

A total of eight soft ropes were identified across the Hesselø South OWF site (Figure 43). They range from 3.0 to 36.0 metres in length. An example of a soft rope MMO in multiple sensors is shown in Figure 44.





**Figure 43: Overview of soft rope targets found within the survey site**



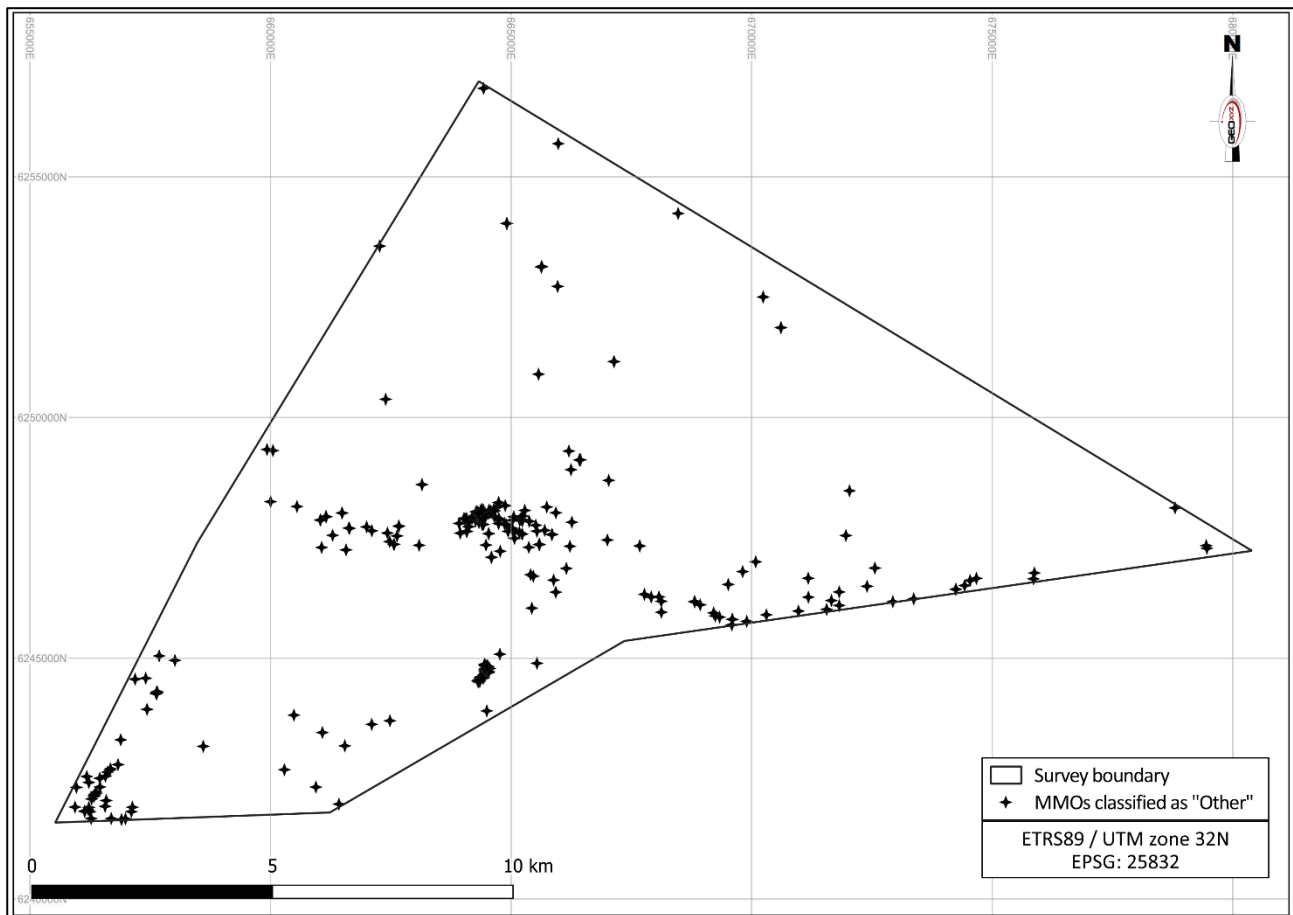
**Figure 44: Example of an MMO identified as soft rope (HS\_B05\_SSS\_GO6\_1587)**

### 8.5.5 Pipelines

No pipelines were identified within the Hesselø South OWF site.

### 8.5.6 Other man-made objects

A total of 464 man-made objects classified as “Other” were found within the Hesselø South site (Figure 45). All of these items within the site survey are classified as non-ferrous objects. One of the targets is associated with fishing activities (Section 8.5.7, Figure 46) whereas two targets were found near/adjacent to the wrecks.



**Figure 45: Overview of other man-made targets within the survey site**

### 8.5.7 Items related to fishing activity

Only one man-made object was described as possibly being related to fishing activities (Figure 46).

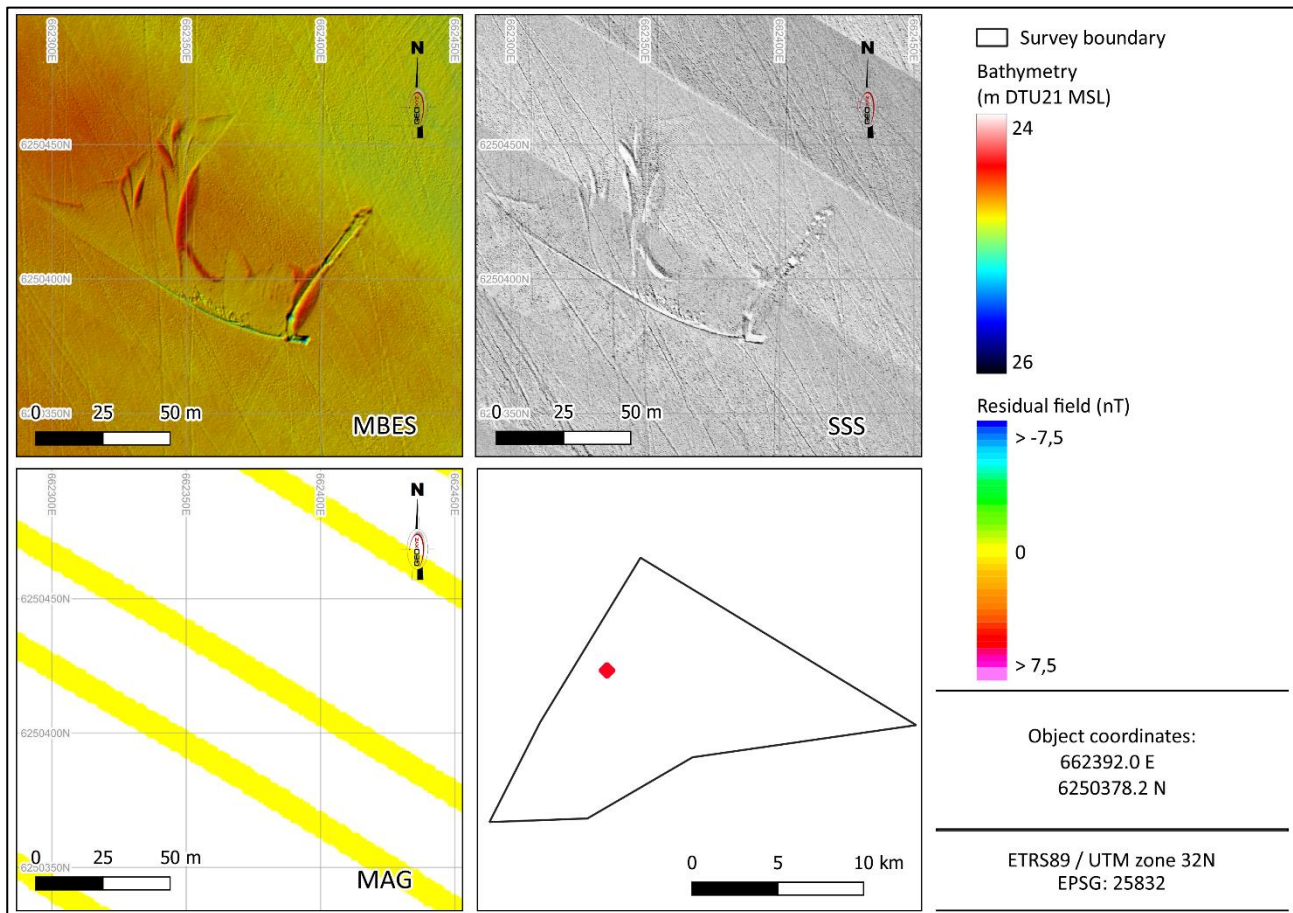


Figure 46: MMO related to fishing activities (HS\_B05\_SSS\_GO6\_1648)

### 8.5.8 Seabed disturbances

No areas of seabed disturbance were identified within the Hesselø South OWF site.

## 9 SUB-SURFACE GEOLOGY

### 9.1 REGIONAL GEOLOGICAL HISTORY

#### 9.1.1 Pre-Quaternary Geology

The Hesselø South site is located near the south-western boundary of the Baltic shield between the southern part of Sweden, the Kattegat and the northern part of Jutland. In the late Cretaceous – early Paleogene, the previous subsiding depocenter became inverted, primarily along pre-existing faults, due to a change in the regional stress orientation, dominated by compression associated with the Alpine Orogeny and the opening of the north Atlantic. The bedrock of the Hesselø South OWF is expected to consist of Jurassic to Lower Cretaceous mudstone or siltstone and Precambrian crystalline rocks may be found in the northern part.

#### 9.1.2 Quaternary Geology

During the Quaternary period, several glacial events have been identified in the northern Danish area. The different glacial events are separated by interglacial or interstadial marine or glaciolacustrine conditions. Till from the Last Weichselian glaciation is found south of Anholt, along with late glacial and Holocene deposits. The Scandinavian Ice Sheet reached its maximum extent in Denmark about 22 ka BP, followed by a stepwise retreat. Around 18 ka BP, the sea began to inundate northern Denmark, which led to rapid deglaciation. At ca. 17 ka BP, the ice margin had retreated to the Halland coastal moraines along the Swedish west coast.

In the Danish area, the ice cap steadily retreated, which caused the opening of the Kattegat depression and transgression of the area. A glaciomarine environment was established, where the glacier was in direct contact to the sea. Therefore, discharge of meltwater-borne sediments could be dispersed from the glacier to the sea and drop stones, rafted by calving icebergs, should be expected. Thick glaciomarine deposits, related to late glacial, are reported from the area.

The interplay between eustatic sea-level rise, caused by global melting of icecaps and glacio-isostatic rebound (regional reaction to the relief of the glacier burden), causes the sea-level to fluctuate in the late glacial and Holocene. In the early Holocene, the sea level dropped and may have caused the area to become terrestrial for a short time, before a new transgression, from which marine conditions continued through the rest of the Holocene.

#### 9.1.3 Late Glacial and Holocene

In the period after the deglaciation, the southern Kattegat area was characterised by high-stand sea-level conditions, followed by a continuous moderate regression, until the eustatic sea-level rise surpassed the glacio-isostatic rebound in the early Holocene.

Late Weichselian subaqueous sediments occur typically as basin infill in the area north of the anticlinorium, or in local depressions elsewhere.

In the early Holocene, the relative sea level began to rise, as the eustatic sea-level rise surpassed the isostatic uplift of the crust. Mörner (1969, 1983) made comprehensive pioneer studies of the relative sea-level changes in the Younger Dryas–Holocene Kattegat, while later studies have resulted in more detailed

palaeogeographic reconstructions, based on sequence stratigraphical studies (Bennike et al. 2000; Jensen et al. 2002; Bendixen et al. 2015, 2017).

The Hesselø South OWF area has been submerged most of the time after the last deglaciation, but in the lowstand period around 10.5 ka BP only partly, and lowstand sediments must be expected. Already in the initial phase of the Holocene transgression the Hesselø South OWF area was fully submerged, while the cable corridor area has a longer transgression history.

## 9.2 SOIL UNIT INTERPRETATION

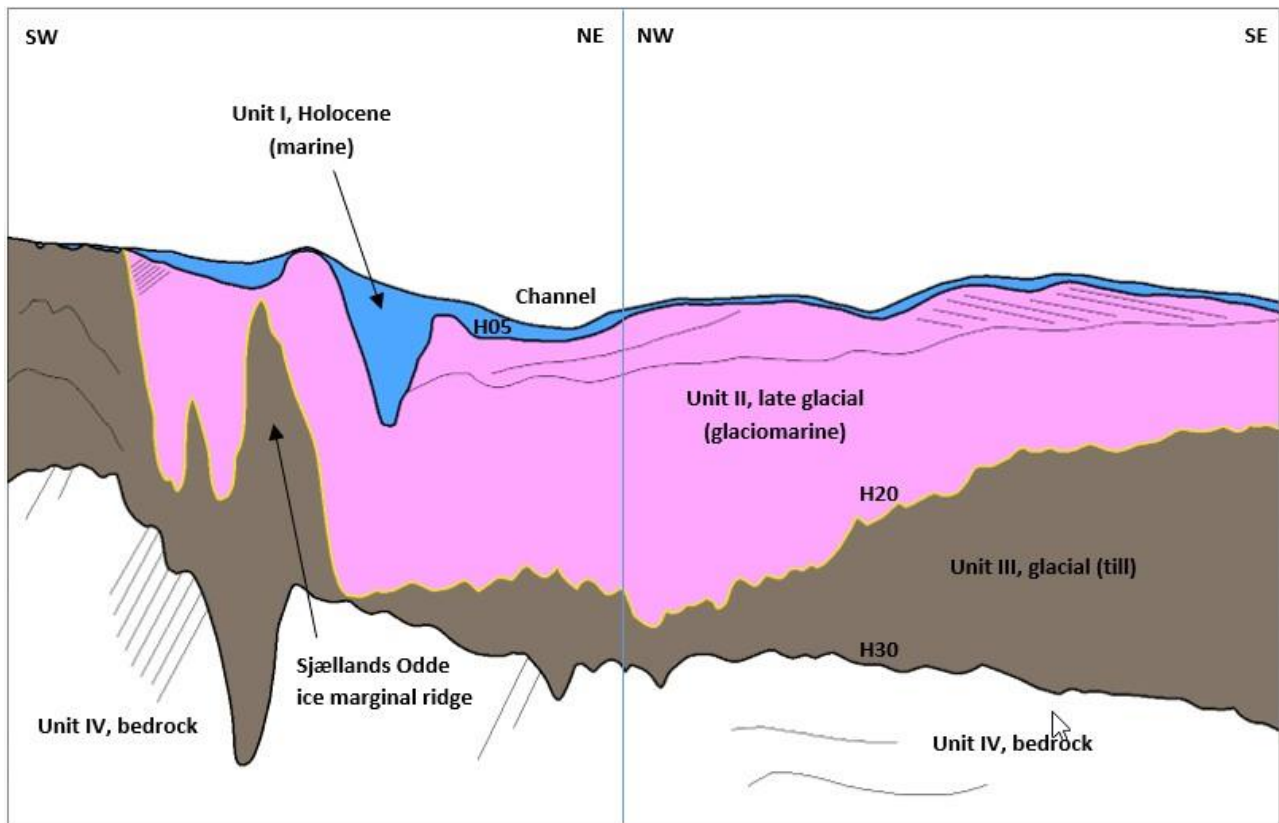
### 9.2.1 Shallow Geological Overview

The geological foundation zone extends to ~70 m below seabed. The rocks and sediments within this interval have been interpreted with reference to the supplied GEUS desk study. This desk study applies a stratigraphic model developed by Jensen et al (2002) in conjunction with archive seismic data and limited ground truth information. There is generally a good correspondence between shallow geology imaged in this project's sub-seabed data and the desk study. This project's unit names are equivalent with those in the desk study (for example Glacial deposits, GL, in this report are equivalent to glacial deposits, GL, within the desk study) this means that it will be easier for future workers to use these survey reports and the desk study together.

In overview the area has a glacial to post-glacial sequence of relatively recent sediments over much older bedrock. The recent sediments are generally 40-50 m thick, though locally these recent sediments are interpreted to be much thicker.

### 9.2.2 Stratigraphy and general arrangement of units

Figure 47 shows the arrangement of units within Hesselø South. Table 48 shows the basic characteristics of the stratigraphic units. Key surfaces are the top of Unit III (H20/H05/seabed) which is the top of potentially overconsolidated deposits and H30; the top of the bedrock.



**Figure 47: Geological schematic, general arrangement of units**

**Table 48: Shallow geological units**

Unit	Upper surface	Lower surface	Main Soil Description	Depositional Environment
I, H, Holocene	Seabed	H05	Silty, sandy CLAY with thin veneer of SAND at seabed	Post-glacial marine
II, LG, Late Glacial	Seabed/H05	H20	Variable, includes intervals of laminated CLAY, SAND-prone packages	Periglacial, glaciomarine
III, GL, Glacial	H5/H15	H30	Variable, CLAY-prone, locally overconsolidated	Glacial with localised ice contact
IV, BR, Bedrock	H20/H30	-	Various carbonates and clastics. Possible crystalline basement	

\*The Kingdom interpretation project included two intra Unit II unconformities, i.e., H15 and H18. These were originally mapped as potential unit bases but have retained in the interpretation project, they may have some value once calibrated by geotechnical data.

### 9.2.3 Quaternary Deglaciation History

The following stratigraphic units, largely derived from information in the GEUS desk study, have been linked to the changing paleoenvironments:

- In Denmark the Scandinavian Ice Sheet reached its maximum extent ~22 000 years BP followed by retreat with evidence for short-lived advances over the following four thousand years. The deposition of Unit III was associated with this ice sheet.
- Marine transgression began around 18 000 years BP, leading to rapid deglaciation and the establishment of glaciomarine conditions. An isostatic regression occurred shortly after 18 000 years

---

BP. This was followed by renewed marine transgression, related to the wasting of the Baltic Ice Stream. Over the course of this complex period, Unit II was deposited.

- After deglaciation, the area generally experienced high-stand conditions, though glacio-isostatic rebound outstripped background sea level rise around 10 000-11 000 years ago, driving a local regression. Unit I was deposited in this marine environment.

### **Unit I Holocene Deposits**

Unit I is a package of post-glacial silty, sandy CLAY which is less than 1.5 m thick over large parts of the site. The interval includes a thin veneer of sandier seabed sediments, though these are interpreted to be very thin and are seldom resolved in the SBP data (Figure 48 and Figure 49). The Holocene sediments are widely distributed over the study area (Figure 50). The Holocene is very thin or absent (unmapped) over an east-west trending glacial/glacio-marine ridge across the centre of the area and in the far south-west, where till is close to the seabed. Small pockets of Holocene may occur in these areas and a <0.2 m thick seabed veneer may be present.

The Holocene deposits are thickest over a north-south trending 1-2 km wide zone situated in the central southern part of the area. Here the deposits partially infill a channel which is still apparent at the seabed and are up to 18 m thick and commonly over 5 m thick. The sediments are best developed on the western side of the axis of the channel and subdue the complex morphology at the base of the Holocene. The channel appears to have its origin during the late glacial/glaciomarine period, it does not correspond with any feature at the top of the bedrock. Here, some of the bedded deposits included within Unit II (the Late Glacial division) may correspond with the earliest Holocene, the first ~2000 years prior to a short regression caused by glacio-isostatic rebound.

Acoustically the interval is almost featureless, with very low amplitude concordant internal reflections. Locally there are very subtle unconformities. These may represent sea level variations related to the interplay of isostatic rebound and background sea level rise.

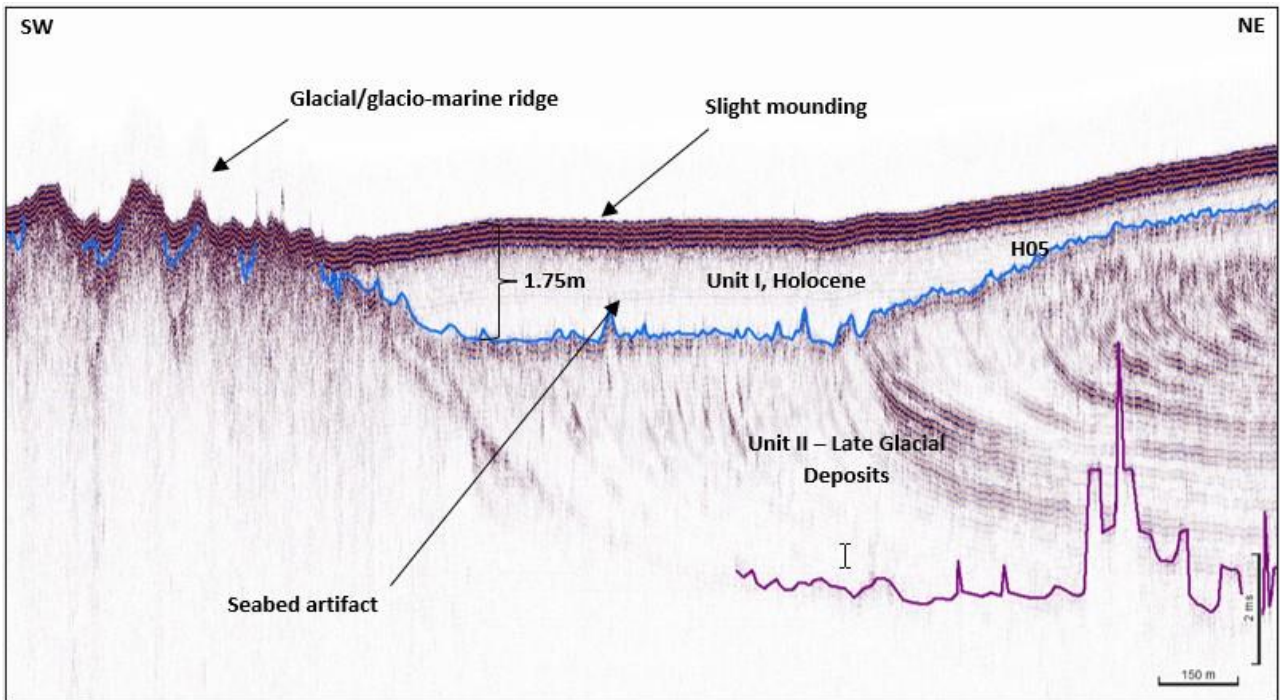


Figure 48: SBP data example, line L028 (location shown in Figure 50), Unit I ponded against glacial ridge

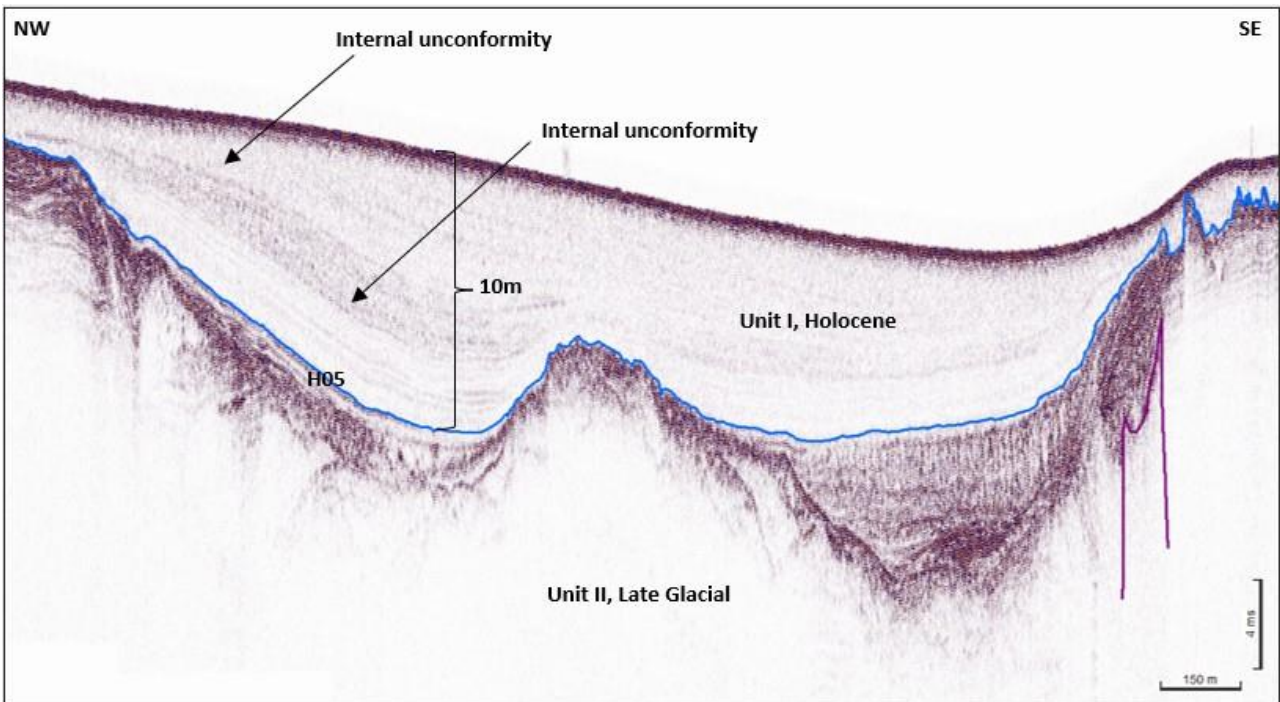


Figure 49: SBP data example, line X\_07 (location shown in Figure 50), Unit I within channel



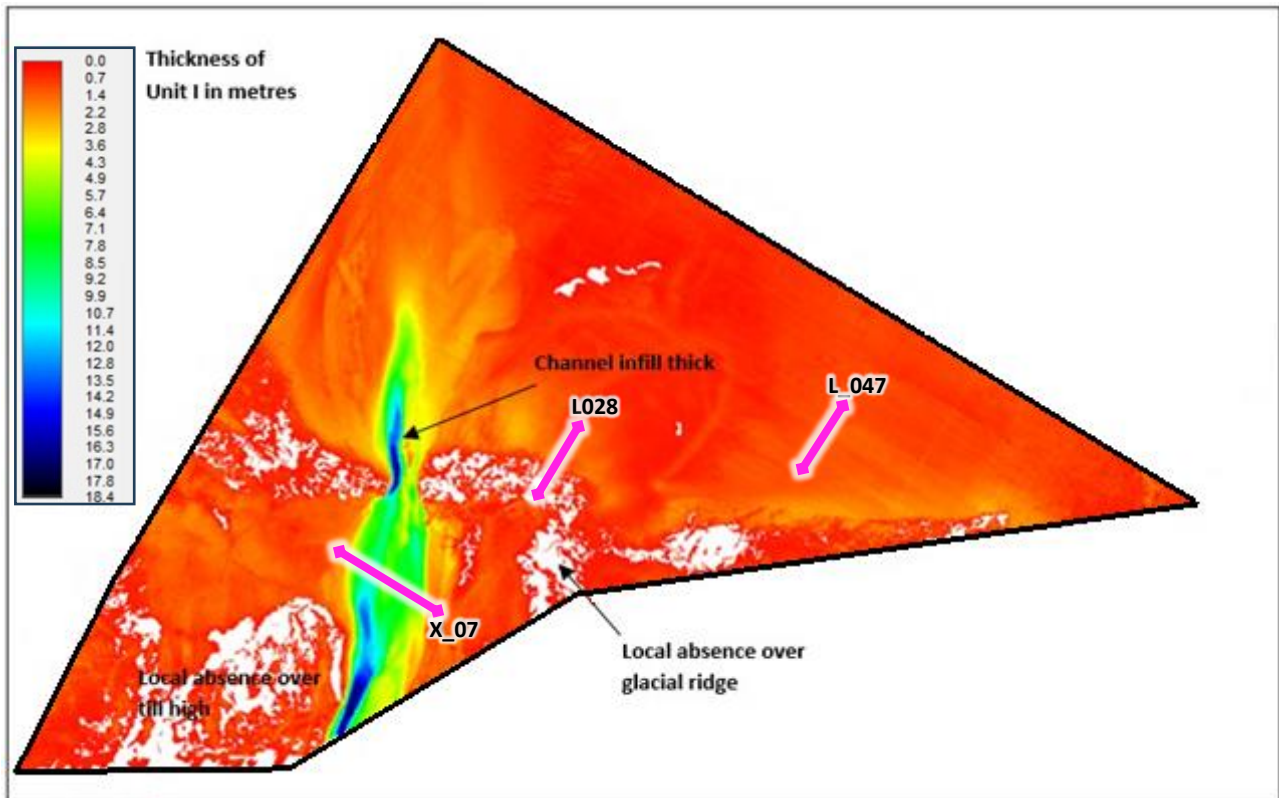


Figure 50: Thickness and distribution of Unit I Holocene deposits

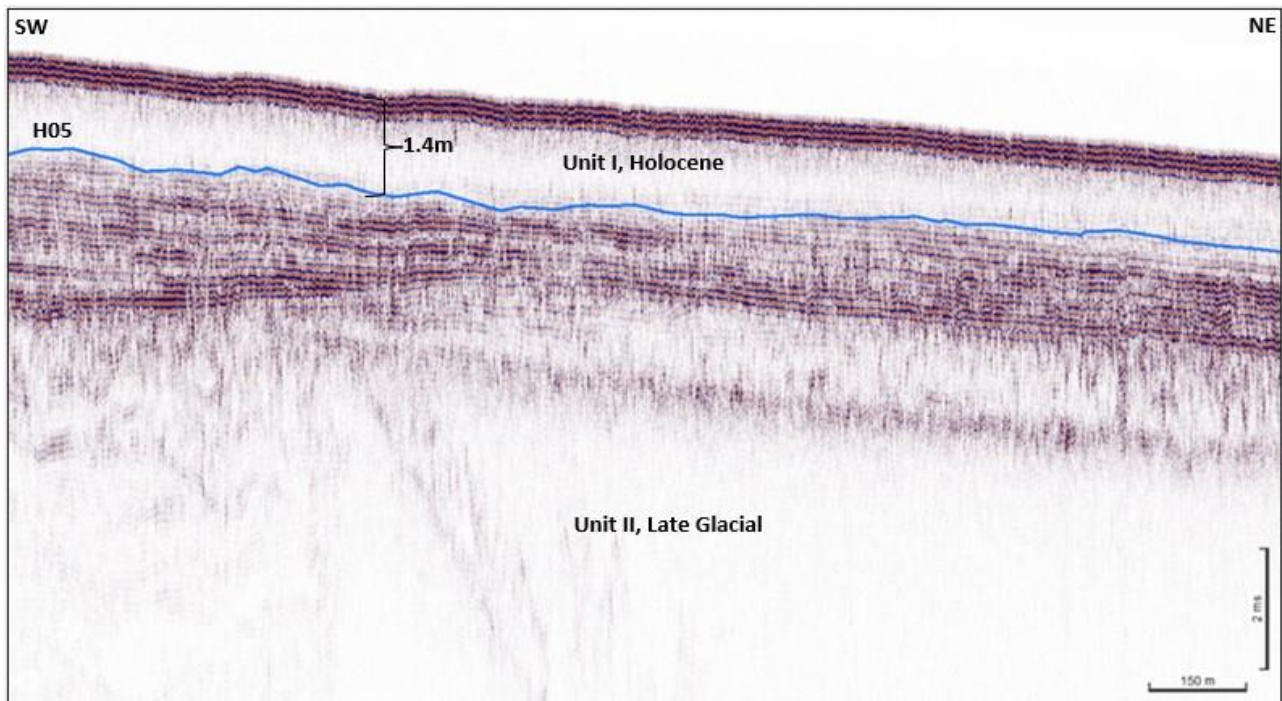


Figure 51: SBP data example, line L\_047 (location shown in Figure 50), Unit I, typical

---

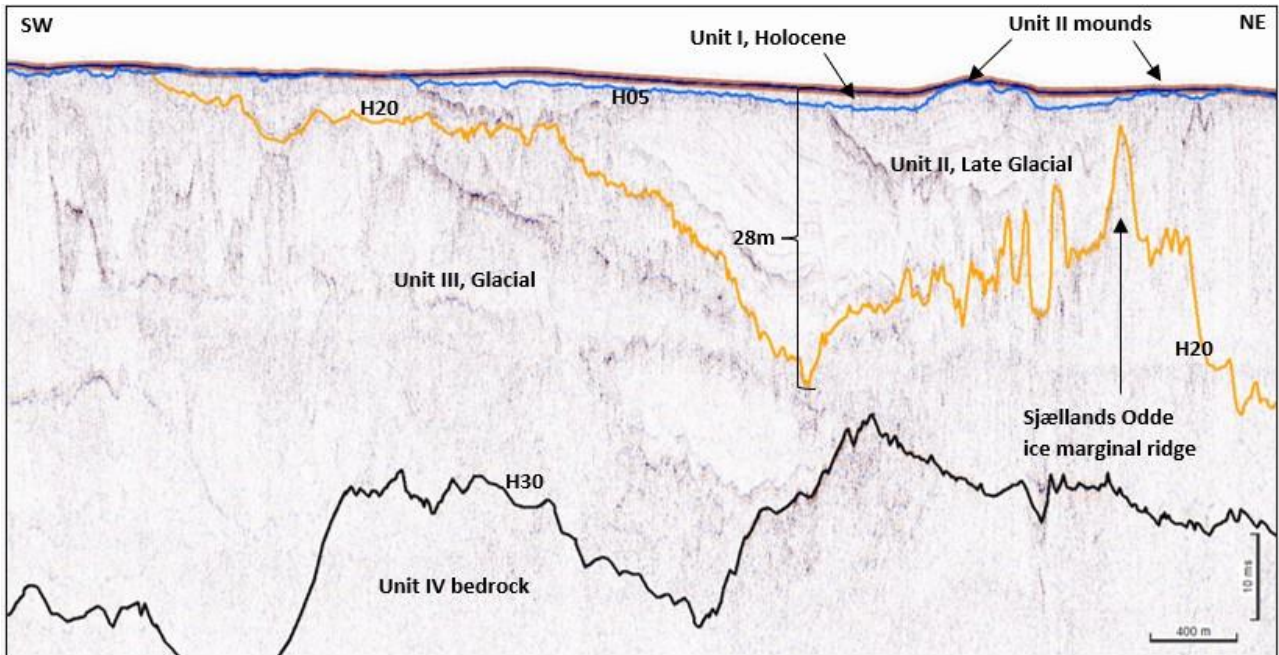
## **Unit II Late Glacial Deposits**

This interval is very complex (Figure 52 and Figure 53) due to the area's range of environmental conditions during the Late Weichselian and earliest Holocene. Some intervals show laminations indicative of clays and silts, others may represent sandy beach-type deposits. Locally there are potential signs of late ice contact. The interval is mapped with H20 at its base. This is generally at the top of deposits which show clear signs of ice contact, true glacial deposits. The relief at this surface strongly influences the thickness and distribution of the Late Glacial sediments.

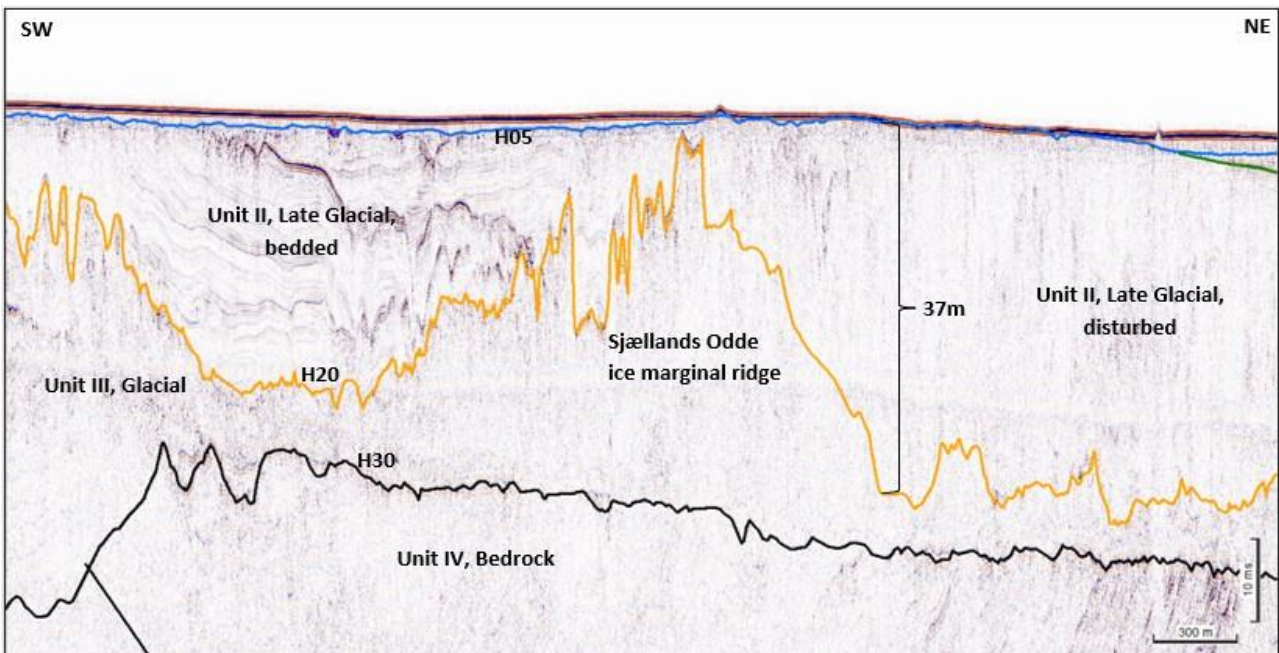
In the extreme south-west the Unit II glaciomarine sediments pinch out over a great thickening of the subcropping tills (Figure 54). Taken together, these two intervals form a delta-like complex of deposits sourced from the south (the landward direction), the lower deposits of Unit III show a greater, more direct, influence of ice, while the later Unit II deposits retain intervals of preserved bedded facies suggesting limited ice contact.

Further north the Unit II deposits thin over an east to west trending till (Unit III) ridge. (The GEUS desk study identifies this ridge as the Sjællands Odde ice marginal ridge.) North of the till ridge the glaciomarine deposits crop out and form a high. It is possible that the glaciomarine deposits to the north of the till ridge were pushed against the deeper till ridge during a later ice advance, perhaps by part of the Baltic Ice Stream. Unit II deposits in this area tend to have a more chaotic internal structure than those south of the till ridge.

The desk study divides the late glacial sequence into earlier and later parts. There is scope to further sub divide this sequence using the existing geophysical database, once geotechnical data are available to guide the work.



**Figure 52: UHR data example, line L\_006 (location in Figure 54), glacial/late glacial delta and till ridge**



**Figure 53: UHR data example, line L\_008 (location in Figure 54), late glacial character and till ridge**

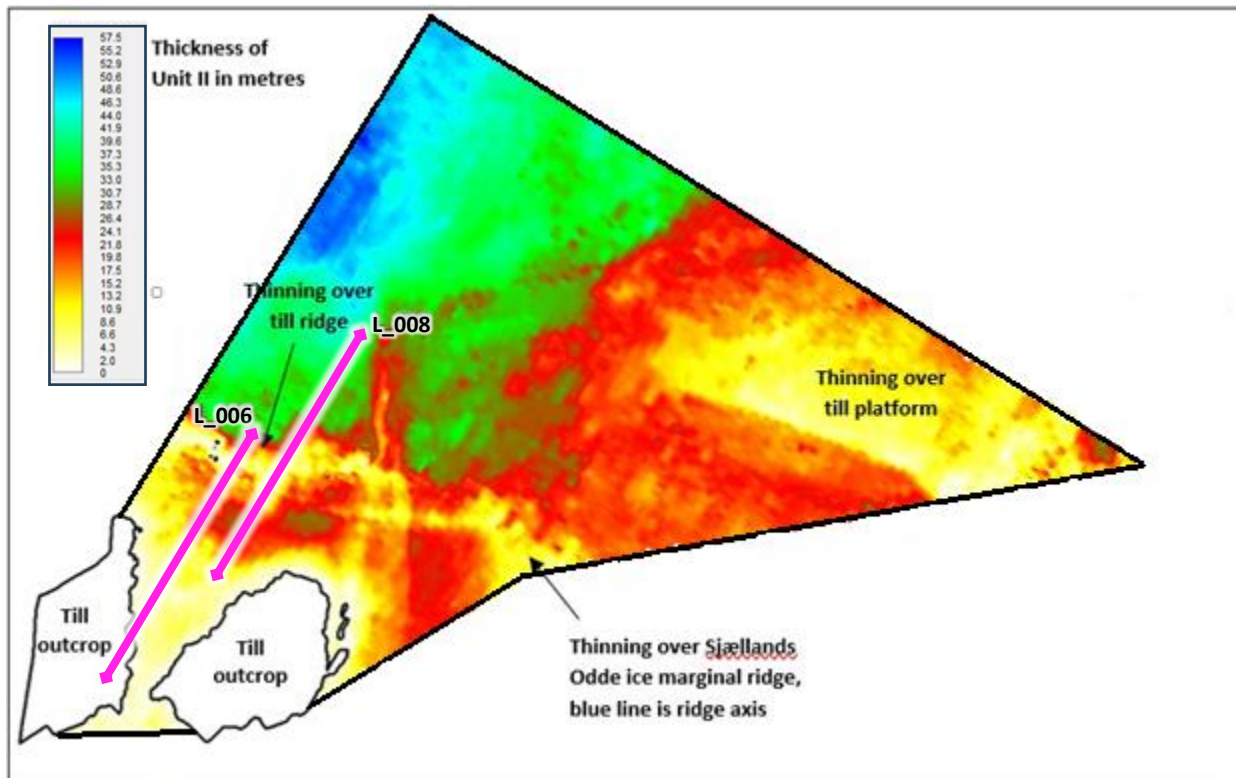


Figure 54: Thickness and distribution of Unit II late glacial deposits

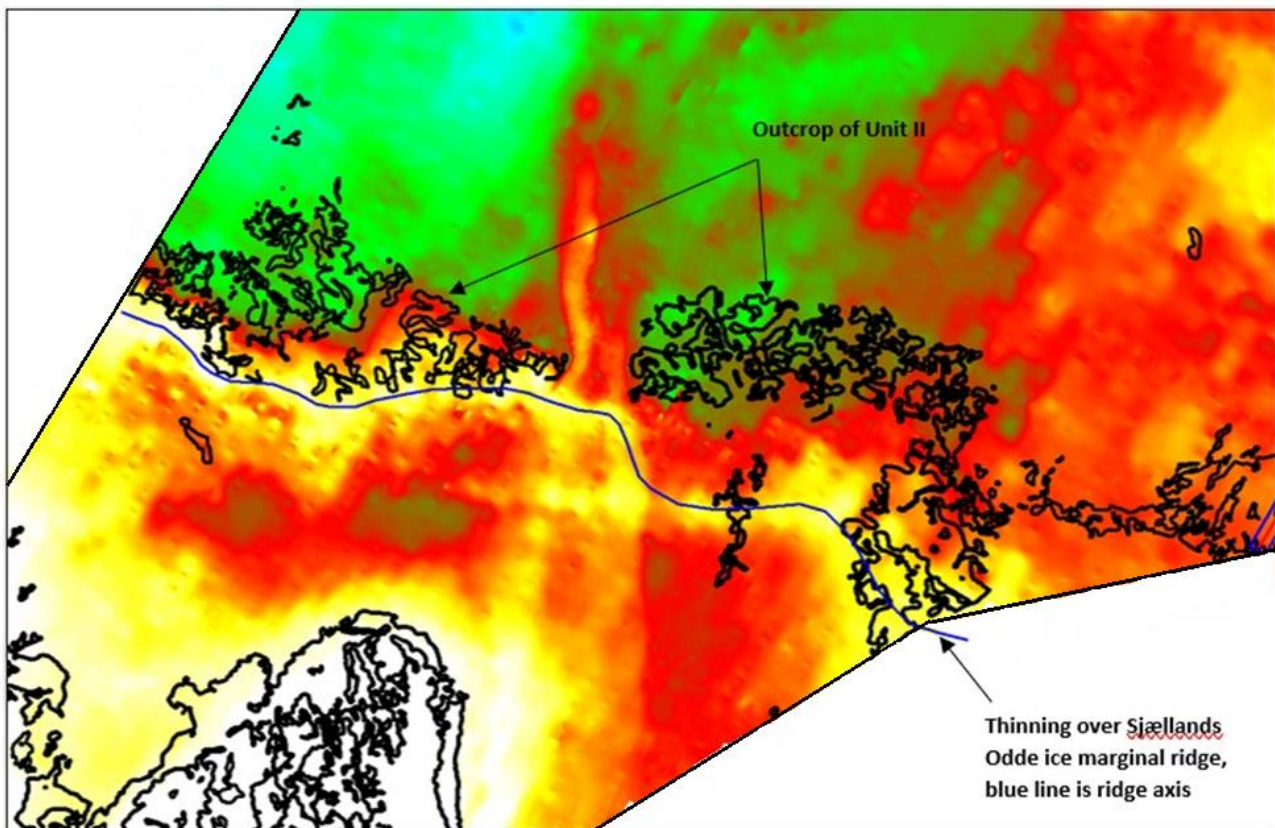


Figure 55: Interaction of till ridge, Unit II thickness and Unit I distribution/Unit II outcrop

---

### **Unit III Glacial Deposits**

Unit III deposits occur through most of the study area, only being absent over very small parts of the north of the site (Figure 56). Unit III is interpreted to be deposited in association with the last major ice advance over the area, approximately 22 000 years ago. The till forms a relatively thin blanket over central and northern areas where it is less than 10 m thick. The till is arranged in a thick platform to the east (Figure 57) and thickens considerably to the south where it is at or close to outcrop and comprises the entire post bedrock sequence (Figure 52). There is an east-west trending till ridge running across the site, just south of centre. This ridge generates an approximate 20 m thickness increase in Unit III and a similar reduction in the thickness of Unit II (Figure 53). The influence of the ridge on the character of Unit II is described in the previous section.

The desk study indicates that this till ridge is the Sjællands Odde ice marginal ridge. The till may be more heavily consolidated south of this ridge.

The upper part of Unit III is generally a glacial till which has been subjected to direct ice contact, though the unit contains other facies which may have been laid down in ice-marginal environments during oscillations of the ice front. The ice-contact facies may comprise a clay-prone diamicton which is likely to contain subordinate silt, sand, gravel, cobbles and boulders and will be overconsolidated. Consolidation levels may significantly vary over short distances. Seismically, the ice contact facies is structureless with a very irregular upper surface, which probably forms a series of ridges (Figure 57).

This sequence might be divided, perhaps separating the ice contact facies from the ice-marginal glaciomarine packages. It should be noted that even the glaciomarine intervals will have undergone some level of overconsolidation during the area's last ice advance.

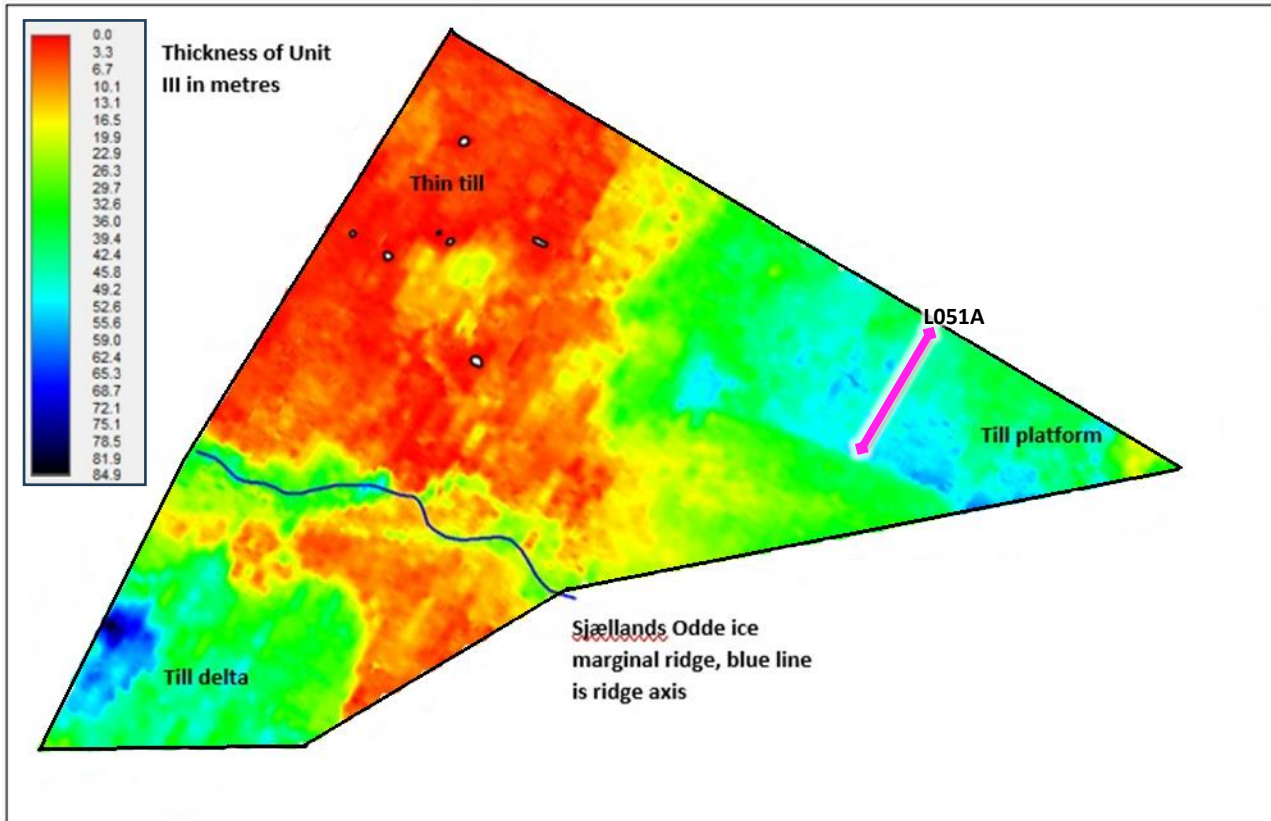


Figure 56: Thickness and distribution of Unit III Glacial deposits

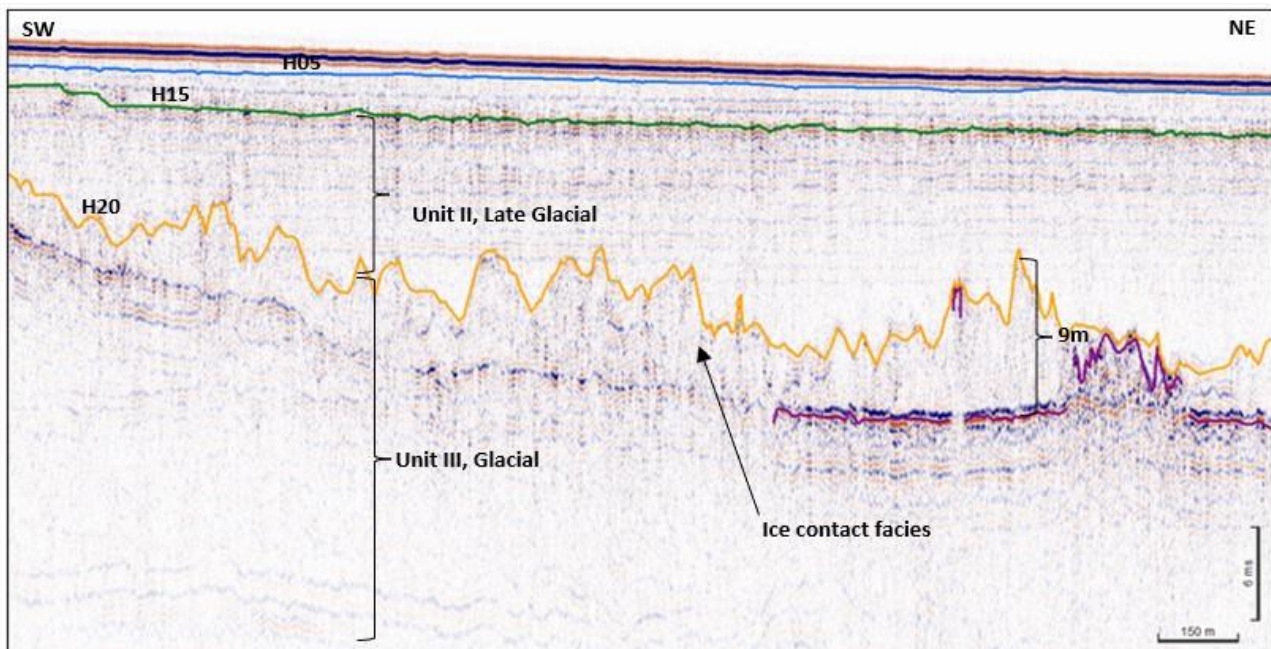
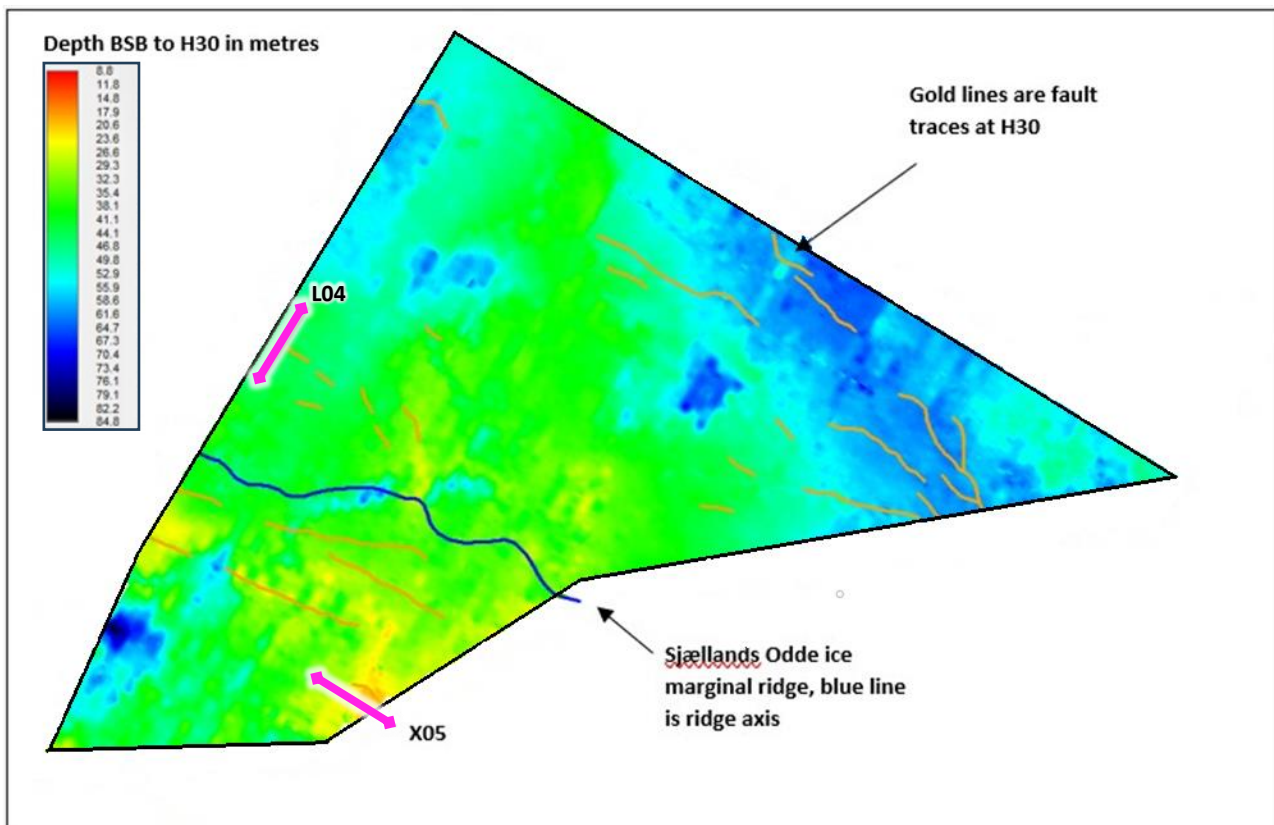


Figure 57: UHR data example, line L051A (location in Figure 56), Unit III, till platform/ice-contact facies

### Unit IV Bedrock

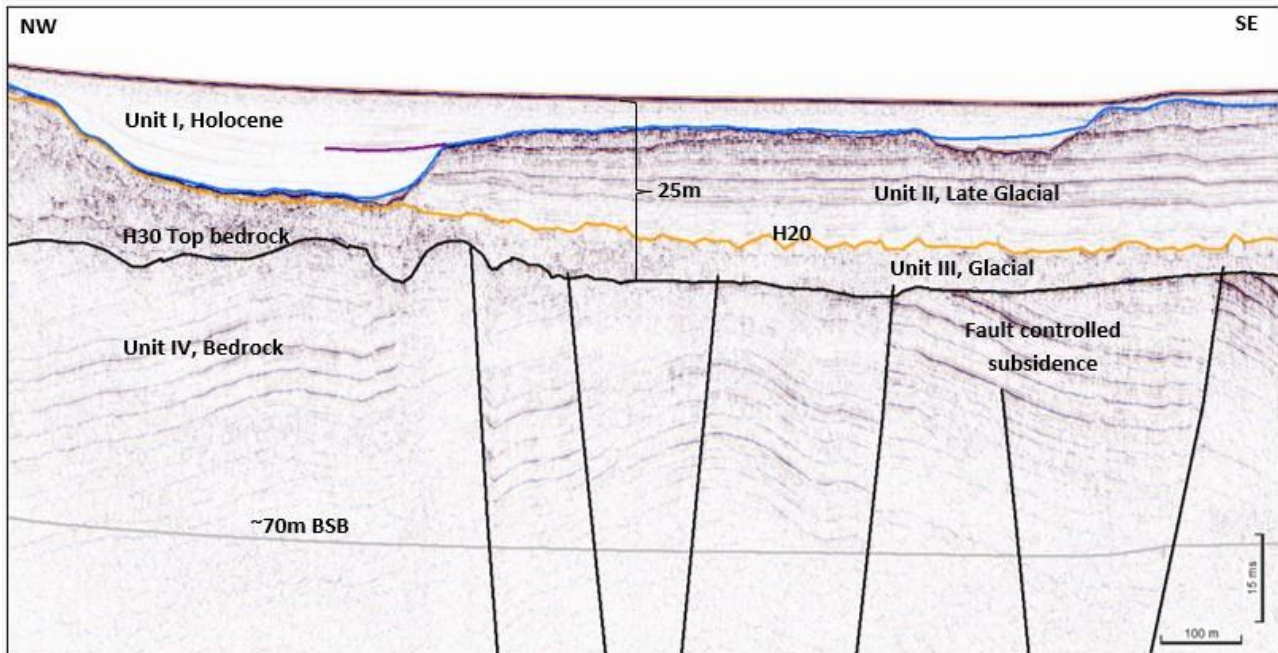
The GEUS desk study shows that the Grenå-Helsingborg Fault runs west-north-west to east-south-east through the centre of the area, in the approximate position of the Sjællands Odde ice marginal ridge. Numerous bedrock faults can be made out in the UHR and are mapped on a line-by-line basis. Those that trace from line to line are marked in gold on Figure 58 and strike roughly north-west to south-east. The desk study indicates that the bedrock will likely comprise Cretaceous carbonates and/or Jurassic clastics. These ancient faults were reactivated during the Jurassic/Cretaceous and, in this area, generated subsidence.

The top of the bedrock is generally 40-50 m below seabed, exceeding 60 m and reaching 80 m in the east of the area and over small parts of the far south-west and north. The upper surface of the bedrock is a gently dipping truncation surface with an angular unconformity between the Mesozoic rocks and their much younger overburden. Figure 58 shows the depth of the bedrock below seabed.

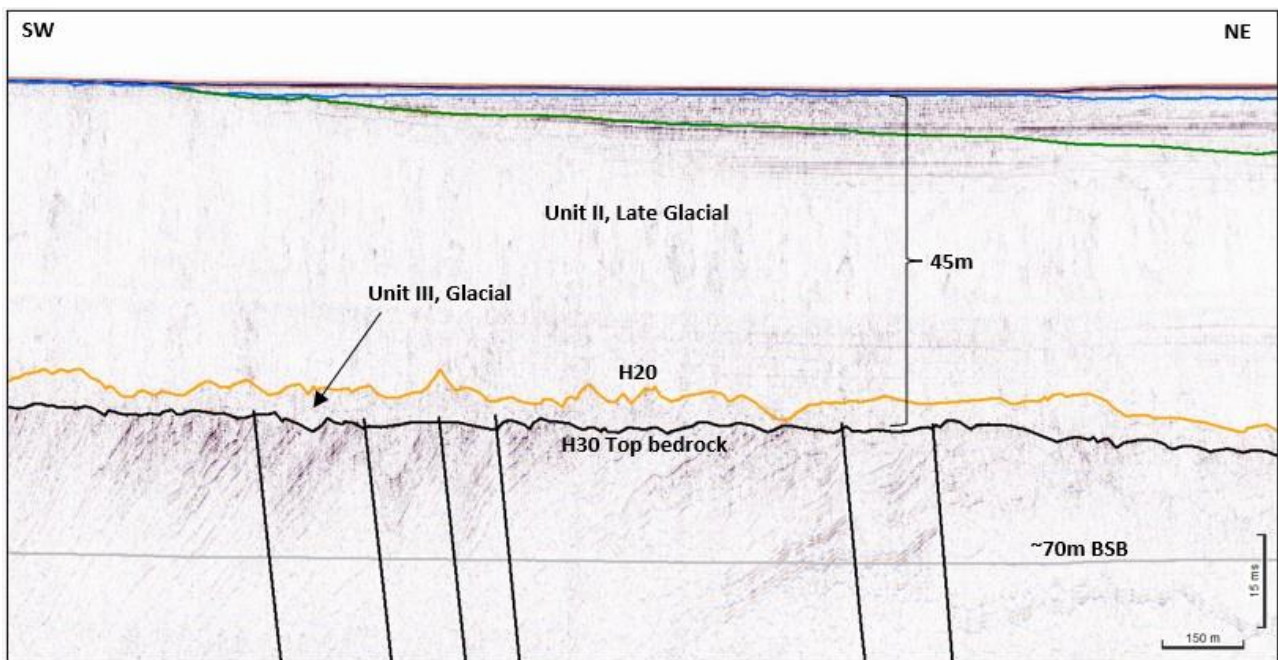


**Figure 58: Depth BSB to H30 (bedrock)**

The bedrock structure is well imaged in Figure 59 and Figure 60 as these lines are outside the area affected by shallow gas. In general, the bedrock is not imaged as good as these examples.



**Figure 59: UHR data example, line X05 (location shown in Figure 58), Unit IV, south of the area**



**Figure 60: UHR data example, line L04 (location shown in Figure 58), Unit IV, north-west of the area**

#### 9.2.4 Shallow geological installation constraints

The following considerations could be made regarding installation constraints based on assessment made from the geophysical dataset:

- Unit I sediments are very weak/soft. Their bearing capacity will be negligible and could cause retrieval difficulties related to settlement of seabed frames etc.
- Units I and II contain diffuse gas



- Unit III may have variable levels of overconsolidation
- Unit III may contain numerous cobbles and boulders
- Unit IV may have strength variations
- Unit IV may be weathered at the upper truncation surface
- Unit IV may locally be weakened by faulting and micro fractures

### **Cobbles and Boulders**

There are occasional indications of boulders within the sub-bottom profiler data (Figure 61). These data have been optimized to resolve the shallow stratigraphy and do not readily generate diffraction hyperbola, which are the usual seismic indication of point contacts in the sub-surface. A further complication is that the units most likely to contain boulders, Units II and III, have been deformed and compressed by ice confusing any returns from individual point contacts.

These circumstances, and the great volume of data, make line-by-line assessment of point contacts impractical and potentially inaccurate.

A probability (Boulder Factor) grid has been generated to indicate where boulders are more or less likely to be encountered. This is based on the thicknesses of Units I, II and III:

- The thickness of the post-glacial Unit I is multiplied by 1: There are rare indications of boulders which may have melted from floating ice.
- The thickness of glaciomarine Unit II is multiplied by 3: There are occasional indications of point diffractions and a greater influence of ice, there are indications of diffractions at seabed where it crops out.
- The thickness of Unit III is multiplied by 10: Though this unit has few direct point diffractions it contains what are interpreted to be ice contact tills, the type of facies most likely to contain erratics. The overall probability of encountering boulders is driven by the presence and thickness of the Unit III tills.

The resulting grid is a unitless value which has been generated as depth. It is a product of the total thickness of the Quaternary sequence (Figure 62). A similar grid could be depth limited to the top 5 or 10 metres, such a grid would show a strong response where the Unit III tills are close to the seabed.

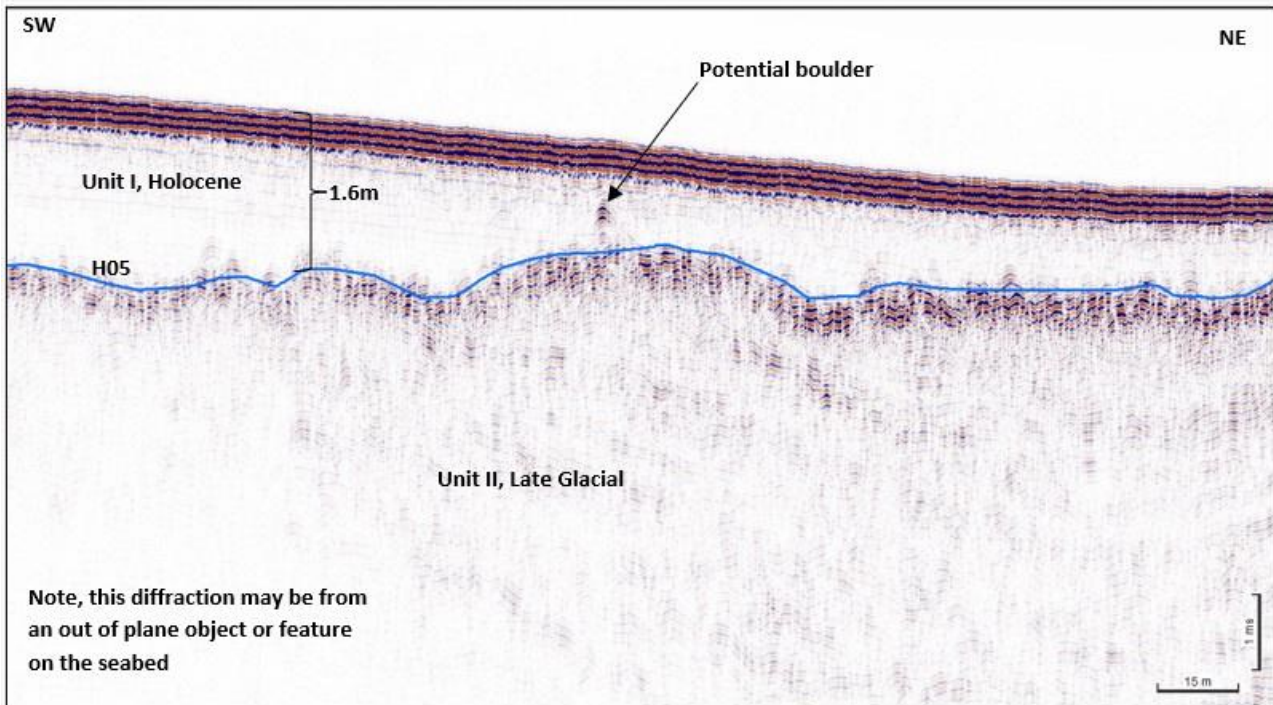


Figure 61: SBP data example, line L\_014, Unit I, rare point diffraction

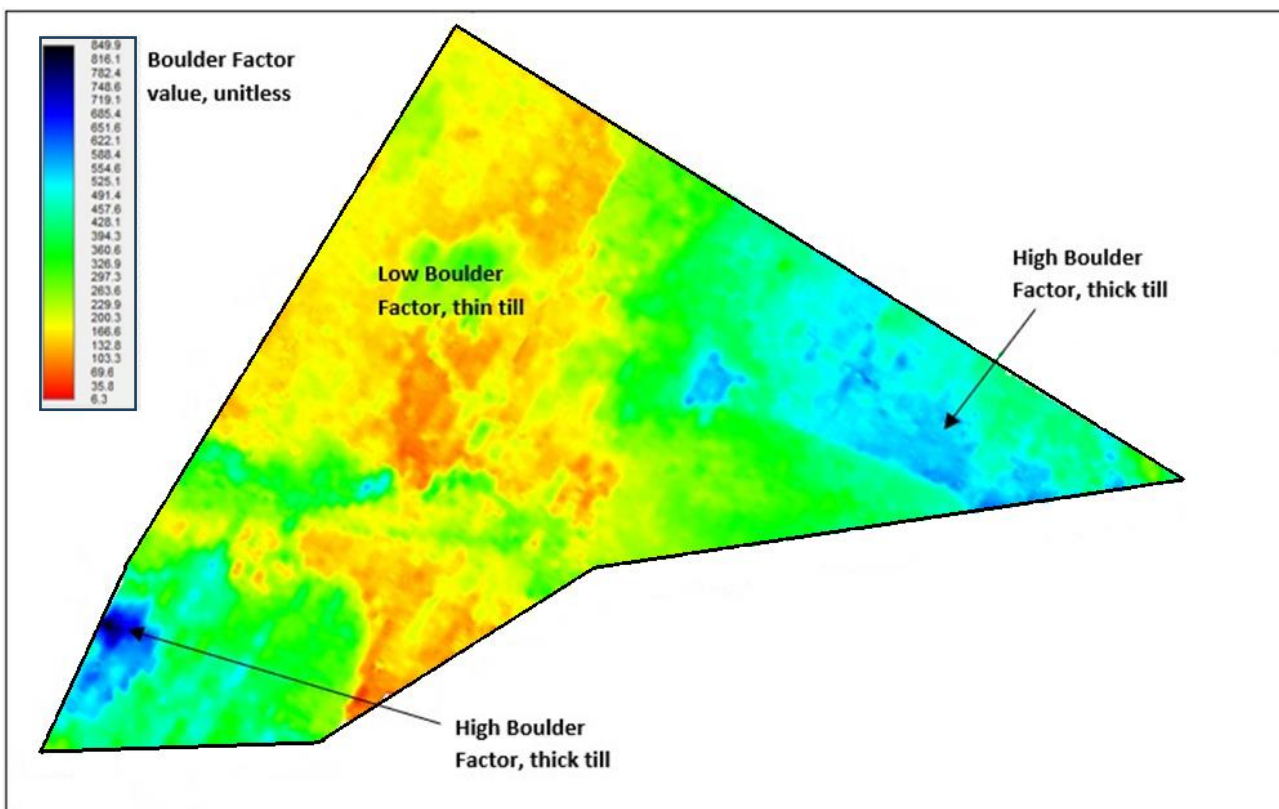


Figure 62: Boulder Factor, Quaternary

## **Gas**

Diffuse gas blanks the sub-bottom profiler data over much of the northern/central parts of the site (Figure 63 and Figure 64). It also influences the UHR data producing high amplitude reflections and a range of imaging problems such as blanking and internal multiples (Figure 65). A boundary has been drawn around the coherent areas of gas, based on the SBP data, but there are small areas scattered outside the boundary. The gas grids are of the depth to the top of the gas.

The gas appears to inhabit the bedded facies of Unit II and is likely to be decomposition gas from the decay of in-situ organic matter.

The consequences of the gas include:

- Blanking of seismic data
- Possible alteration of geotechnical properties of host sediments
- Safety impact on invasive operations
- Uncertainty over long term soil behavior around any installations

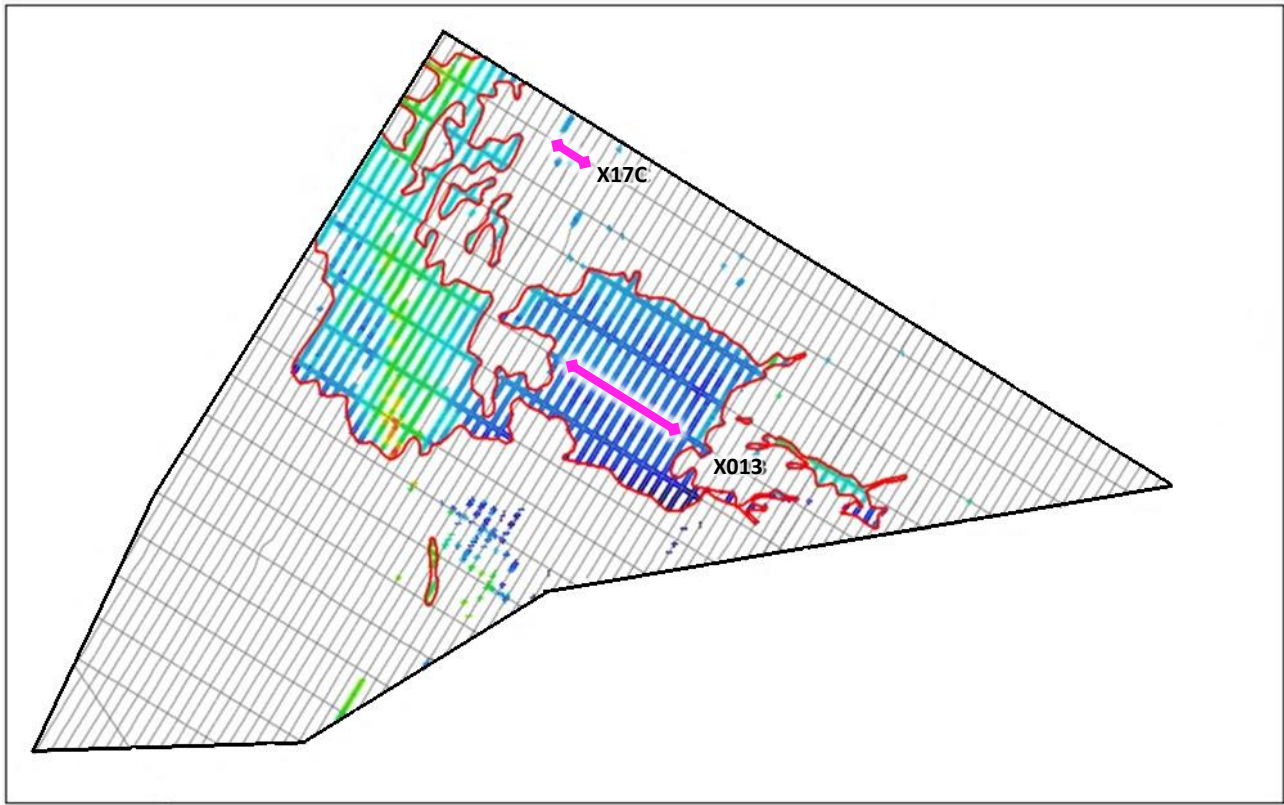


Figure 63: Gas, SBP geological survey

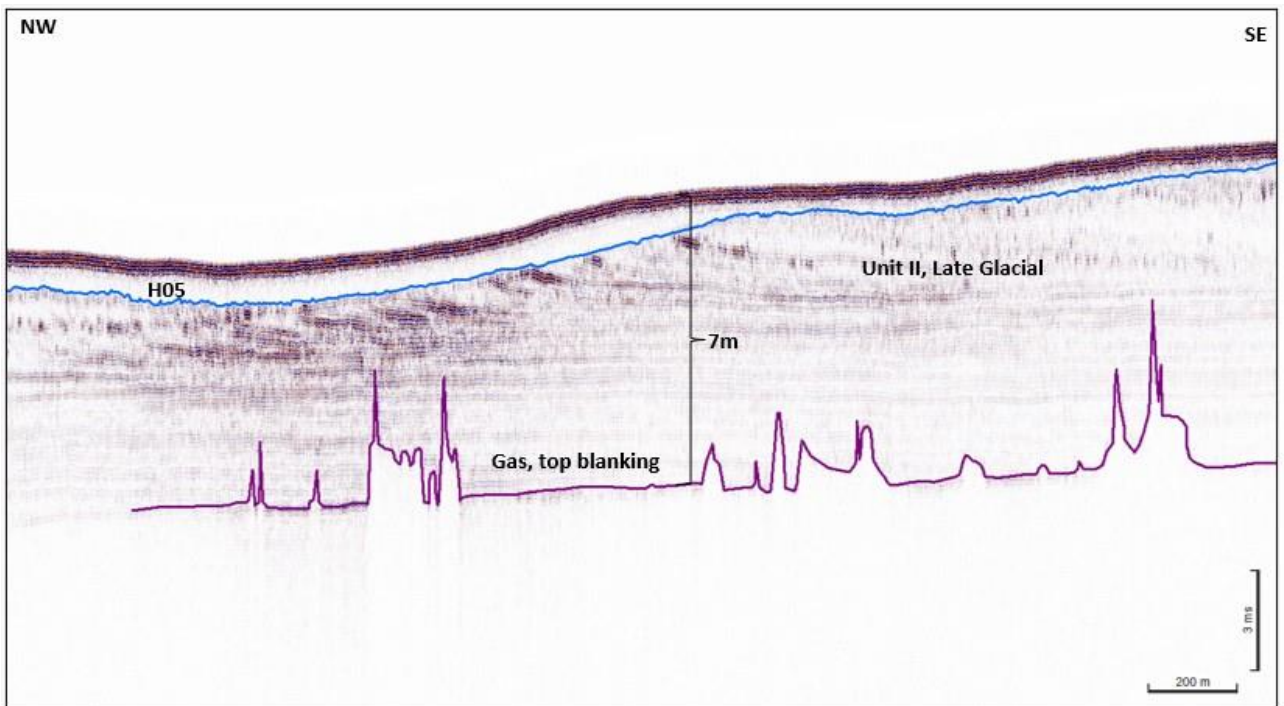
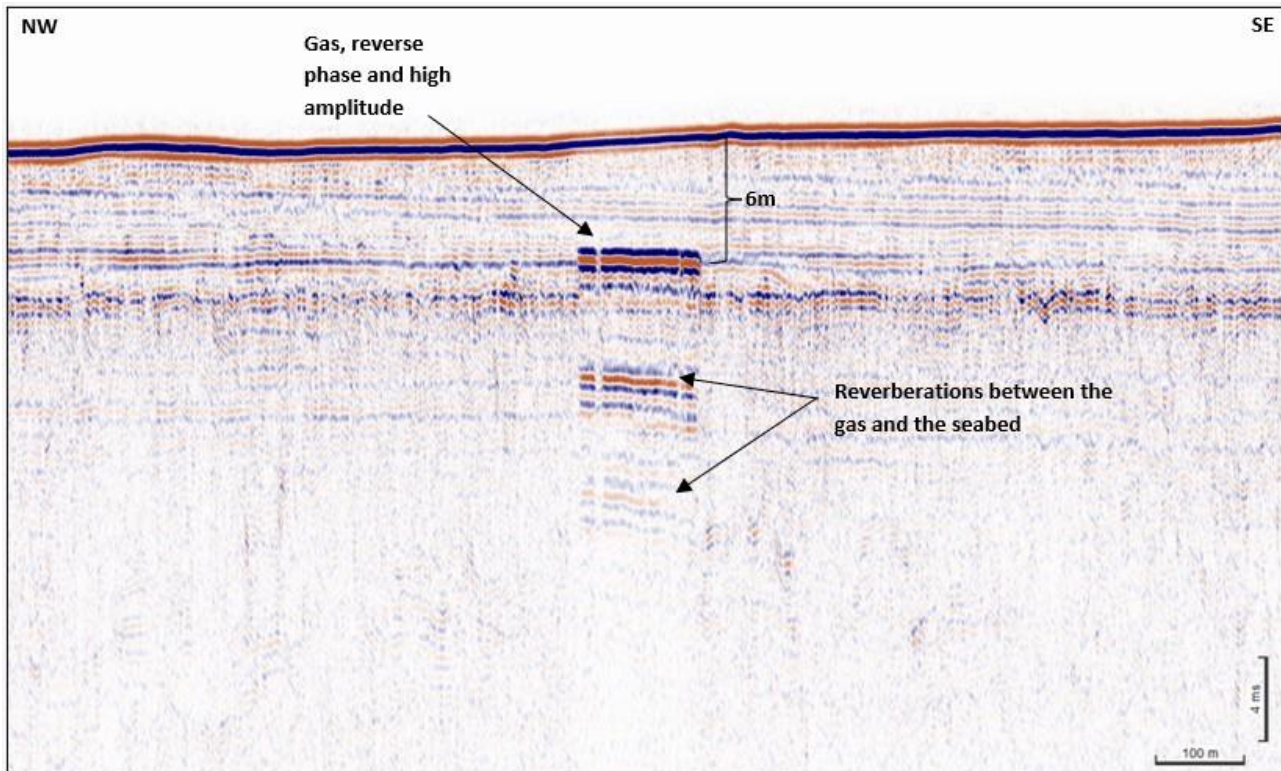


Figure 64: SBP data example, line X013 (location in Figure 63), Unit II, gas



**Figure 65: UHR data example, line X17C (location in Figure 63), Unit II, gas**

## 9.2.5 Sub-surface acoustic velocity model

### SBP depth data

The SBP depth data are based on the final time segy files. The water column and recorder delay are depth converted at the water velocity. This velocity interval extends from the top of the record to a point just above the picked water bottom. This small offset ensures that the seabed return signal is not distorted by the transition from one interval velocity to another.

The remainder of the record is converted at an assumed velocity of 1600 m/s. This is because these shallow penetrating data only image normally consolidated, uncompacted, sediments and there are no associated processing velocities to consider.

This sub-seabed interval velocity was also applied to the thickness conversion of the interpretation of the upper two units: the depth SBP data match the supplied thickness/depth grids for units I and II.

### UHR depth data

The UHR depth data have been built using an iterative approach. The limited range of acquisition offsets mean that there is little moveout in the raw data beyond 20-30 milliseconds below seabed. In turn, this means that the data are not especially sensitive to variations in velocity picking. This diminishes the consistency and strength of the relationship between velocity picks and the depth of primary reflections.

The time versions of the data have been depth converted with reference to a time grid of the base of the Quaternary sequence, based on interpretation of the final time data versions. This surface is the transition



from relatively young sediments to relatively ancient rocks. The surface has been used to apply and control an interval velocity ramp from lower velocities, above, and higher velocities in the deeper bedrock.

There may be small miss ties at the intersection of depth segy lines which are not present in the parent time versions of the lines. This is due to differences in depth conversion velocities which, in time, only influence signal characteristics rather than vertical position.

#### **Deployment of depth versions**

The depth segy lines are loaded into the Kingdom projects as multiversions of the parent time lines. All interpretation is of the time data. These time interpretations have been thickness and depth converted and can be displayed on the depth lines as grids. There may be minor misties between these depth grids and events in the depth segy, especially with the UHR data, as the two depth products have been generated by separate workflows.

---

## 10 COMPARISON BETWEEN SEABED AND SUB-SEABED FINDINGS

In the final stage of interpretation, surficial geology has been correlated to the SBP results.

Unit I Holocene sediments dominate the Hesselø South site (Figure 50), with thin parts observed where the Muddy Sands, Sands and Coarse gravel and sand surficial interpreted areas occur (Figure 37 and Figure 48), and thicker regions observed, where Sandy muds are mapped (Figure 37 and Figure 49).

In the southern part, the SSS interpreted 'Till/diamicton' regions (Figure 37), sufficiently correlate to the absence post glacial-marine Unit I and the periglacial-glaciomarine Unit II, although there are parts where a thin layer of Unit I or Unit II (<0.5 m) occurs, implying a subcrop/outcrop of glacial Unit III Till/diamicton (Figure 54 and Figure 55). The surficial interpreted 'Till/diamicton' west-east zone, in the central part of the site (Figure 37), adequately correlates to the top of H05-Unit I thickness grid. However, in this east-west zone, there is no Unit III outcrop, according to the SBP results, and Unit II glaciomarine sediments pinch out, showing significant thickness over the lower Unit III Till (Figure 53, Figure 54 and Figure 56). In those parts, which have been marked as Till/diamicton in the SSS (considering the reflectivity, the relief in the MBES, the texture and the grab samples), the sediments are most likely clay, sand, gravel and boulders. The latter implies a diamicton facies (without direct genetic -glacial- connotation) of different age, compared to the Unit III Till outcrops in the extreme south west. Those diamicton facies are most likely correlated to transitional glacial/glaciomarine ice-affected Unit II areas, slightly northwards to the Sjaellands Odde ice marginal ridge (Figure 53 and Figure 55).

## 11 CONCLUSIONS

Seabed levels across the Hesselø South site range from a minimum of 16.6 m MSL, near the south-western corner of the site, to a maximum of 35.3 m MSL, in the central western section.

A broad channel feature crosses the western side of the site. This feature is 750 - 3000 m wide and runs approximately north-south. Seabed levels within the channel range from 25.0 m MSL to 35.3 m MSL. To the east of the channel feature, seabed levels undulate very gently between 21.0 m MSL and 30.0 m MSL. Levels shoal very gently eastwards, towards a broad, low ridge feature, which stands up to 3.0 m high. To the east of the low ridge feature, seabed levels deepen very gently towards the east and north-east. To the west of the broad channel feature, seabed levels deepen very gradually towards the east, or east-northeast.

Typical slope gradients across the survey area range from  $<0.1^\circ$ -  $3.2^\circ$ . The highest slope values (very steep slopes;  $>15^\circ$ ) are related to the edges of seabed features such as boulders and wrecks, as well as on the sides of localised ridges and smaller elevated features.

Boulder fields are visible in the southwestern and central part of the site. The high-density boulder fields (Class 2) generally coincide with outcropping/subcropping areas of Till/diamicton, with intermediate density boulder fields (Class 1) surrounding the Class 2 boulder fields.

Sandwaves are seen in the southwestern part of the survey area. These features are orientated E-W, NW-SE and SW-NE, with wavelengths between 20 m and 130 m and heights between 0.1 and 1.0 m. Subordinate ripples are present between the sandwaves. These features are similarly orientated and have wavelengths between 0.5 m and 2 m.

Extensive fishing activities are noted, including numerous well-preserved trawl marks, mainly in the northern part of the area, as well as within the channel feature.

Six areas containing numerous, roughly circular, small depressions, between 0.1 m and 0.4 m deep and up to 5.0 m across, occur in the central-eastern part of the site. These six areas vary between 60 m and 1500 m in width and length. Similar features are seen along a SW-NE orientated line, in the south-eastern part of the site, and are possibly related to fishing, surveying or construction activities. An isolated depression, 6 to 8 m wide and 1.5 m deep, is seen in the southern part of the site. Disturbed seabed areas, possibly of anthropogenic origin (fishing, survey, construction activities) are also present.

An irregular, NW – SE orientated seabed mound, approximately 65 m long and up to 2.0 m high, is present in the central part of the site.

An area of unknown features is present in the northern part of the site. These are visible in the MBES data but are not recognizable in the SSS dataset. They could be interpreted as possible sandwaves, but no other evidence of other bedforms such as ripples is present. Alternatively, they could be possible erosional features/ice sculpted areas and a seabed expression of the H05 erosional surface, in an area where Unit II – periglacial-glaciomarine sediments are covered by a thin layer of Unit I Holocene deposits. The interpretation of those features is uncertain.

Three wrecks were found within the survey area. A total of 450 metallic features (either single or clusters) were identified within the survey area. Eight items, identified as varying lengths of soft rope, are present within the survey area. Three possible lengths of discarded cable were noted. A total of 464 items defined as



other contacts, possibly associated with fishing activities and the above-mentioned wrecks, are present within the survey area. A total of 453 sonar contacts were noted (either as single items or possible clusters of items). No subsea cables or pipelines are present within the Hesselø South site.

The geological foundation zone of the Hesselø South site extends to ~70 m below seabed. The rocks and sediments within this interval have been interpreted, with reference to the supplied GEUS desk study. There is generally a good correlation between the shallow geology imaged in this project's sub-seabed data, and the desk study.

In overview, the area has a glacial to post-glacial sequence of relatively recent sediments (Units I, II and III) overlying much older bedrock. The recent sediments are generally 40-50 m thick, though locally, they are interpreted to be much thicker.

**Unit I** is a package of Holocene deposits, comprising post-glacial silty, sandy CLAY, which is less than 1.5 m thick over large parts of the site. The interval includes a thin veneer of sandier seabed sediments, though these are interpreted to be very thin. The Holocene sediments are widely distributed over the study area. The Holocene is very thin or absent (unmapped) over an east-west trending glacial/glacio-marine ridge, which is present across the centre of the area and in the far south-west, where till is close to the seabed. Small pockets of Holocene sediments may occur in these areas and a <0.2 m thick seabed veneer may be present.

The Unit I deposits are thickest over a north-south trending, 1-2 km wide zone, situated in the central southern part of the area. Here the deposits partially infill a channel, which is still apparent at the seabed, and are up to 18 m thick and commonly over 5 m thick. The channel appears to have its origins during the late glacial/glaciomarine period. It does not correlate with any feature at the top of the bedrock. Here, some of the bedded deposits, included within the underlying Unit II (the Late Glacial division), may correspond with the earliest Holocene, the first ~2 000 years, prior to a short regression, caused by glacio-isostatic rebound.

The Late Glacial deposits of **Unit II** are very complex, due to the area's range of environmental conditions during the Late Weichselian and earliest Holocene. Some intervals show laminations indicative of clays and silts, others may represent sandy beach-type deposits. Locally, there are potential signs of late ice contact. The interval is mapped with horizon H20 at its base. This is generally at the top of deposits that show clear signs of ice contact; true glacial deposits. The relief at this surface strongly influences the thickness and distribution of the Late Glacial sediments.

In the extreme south-west, the Unit II glaciomarine sediments pinch out across a great thickening of the subcropping tills. Taken together, these two intervals form a delta-like complex of deposits, sourced from the south (the landward direction).

Further north, the Unit II deposits thin across an east to west trending till (Unit III) ridge. The GEUS desk study identifies this ridge as the Sjællands Odde ice marginal ridge. North of the till ridge, the glaciomarine deposits crop out and form a high. It is possible that the glaciomarine deposits to the north of the till ridge were pushed against the deeper till ridge during a later ice advance, perhaps by part of the Baltic Ice Stream. Unit II deposits in this area tend to have a more chaotic internal structure than those south of the till ridge.

Unit III (glacial deposits) occurs across most of the study area, and is absent over very small parts of the north of the site. Unit III is interpreted to have been deposited in association with the last major ice advance over the area, approximately 22 000 years ago. The till forms a relatively thin blanket over central and northern

areas, where it is less than 10 m thick. The till is arranged in a thick platform to the east and thickens considerably to the south, where it is at, or close to outcrop and comprises the entire post bedrock sequence.

An east-west trending till ridge runs across the site, just to the south of centre. This ridge generates an approximate 20 m thickness increase in Unit III and a similar reduction in the thickness of Unit II.

The upper part of Unit III is generally a glacial till, which has been subjected to direct ice contact, though the unit contains other facies, which may have been laid down in ice-marginal environments, during oscillations of the ice front. The ice-contact facies may comprise a clay-prone diamicton, which is likely to contain subordinate silt, sand, gravel, cobbles and boulders and will be overconsolidated. Consolidation levels may significantly vary over short distances. This sequence might be divided, perhaps separating the ice contact facies from the ice-marginal glaciomarine packages. It should be noted that even the glaciomarine intervals will have undergone some level of overconsolidation during the area's last ice advance.

The GEUS desk study shows that the Grenå-Helsingborg Fault runs west-north-west to east-south-east through the centre of the area, in the approximate position of the Sjællands Odde ice marginal ridge. Numerous bedrock faults are seen in the UHR data and strike roughly north-west to south-east. The desk study indicates that the bedrock will likely comprise Cretaceous carbonates and/or Jurassic clastics. These ancient faults were reactivated during the Jurassic/Cretaceous and, in this area, generated subsidence.

The top of the bedrock is generally 40-50 m below seabed, exceeding 60 m and reaching 80 m in the east of the area and over small parts of the far south-west and north. The upper surface of the bedrock is a gently dipping truncation surface, with an angular unconformity between the Mesozoic rocks and their much younger overburden.

The presence of gas and cobbles and/or boulders may constrain installation. Unit I and II sediments contain diffuse gas, while numerous cobbles and boulders may be present within Unit III.

## 12 OVERVIEW OF THE DIGITAL DELIVERABLES

### 12.1 GEOLOGICAL SURVEY

**Table 49: Overview of the digital deliverables for the geological survey**

Deliverable	Format	Data Location
<b>All sensors</b>		
Trackplots (line)	Shapefile	SN2023_004_F_ETRS89_UTM32N
Man-made objects (point)	Shapefile	SN2023_004_F_ETRS89_UTM32N
Man-made objects (line)	Shapefile	SN2023_004_F_ETRS89_UTM32N
Man-made objects (polygon)	Shapefile	SN2023_004_F_ETRS89_UTM32N
Seabed features (point)	Shapefile	SN2023_004_F_ETRS89_UTM32N
Seabed features (line)	Shapefile	SN2023_004_F_ETRS89_UTM32N
Seabed features (polygon)	Shapefile	SN2023_004_F_ETRS89_UTM32N
Seabed geology (polygon)	Shapefile	SN2023_004_F_ETRS89_UTM32N
Catalogue of Seabed objects	PDF	108_GEOPHYSICAL_REPORT - WPA&C
<b>SVP</b>		
SVP logfiles	Raw and excel	101_MBES - WPA&C
<b>SBP and UHRS</b>		
Processed SBP data and UHRS recordings (Depth and Time)	SEGY	104_SBP_2D_URHS - WPA
SBP and UHRS instrument tracks	Shapefile	SN2023_004_F_ETRS89_UTM32N
Boulder Factor	Encoded TIF	SN2023_004_R_ETRS89_UTM32N
Interpretation of post-processed seismic data	ASCII	104_SBP_2D_URHS - WPA
Horizon interpretation depth BSL gridded surface	ASCII	104_SBP_2D_URHS - WPA
	Encoded TIF	SN2023_004_R_ETRS89_UTM32N
Horizon interpretation depth below seabed gridded surface	ASCII	104_SBP_2D_URHS - WPA
	Encoded TIF	SN2023_004_R_ETRS89_UTM32N
Isochore gridded surface	ASCII	104_SBP_2D_URHS - WPA
	Encoded TIF	SN2023_004_R_ETRS89_UTM32N
Processing Project	Kingdom Project Files	104_SBP_2D_URHS - WPA
<b>Reports</b>		
Mob and Cal Report	PDF	Energinet SharePoint
Operations Report	PDF	Energinet SharePoint
Technical Report	PDF	Energinet SharePoint
<b>Charts</b>		
Overview	PDF	108_GEOPHYSICAL_REPORT - WPA&C
Trackplots	PDF	108_GEOPHYSICAL_REPORT - WPA&C
Sub-seabed Geology	PDF	108_GEOPHYSICAL_REPORT - WPA&C
<b>GIS</b>		
Trackplots (all sensors)	Shapefile	SN2023_004_F_ETRS89_UTM32N

Deliverable	Format	Data Location
Boulder Factor	Encoded TIF	SN2023_004_R_ETRS89_UTM32N
SBP Horizon BSL Grids H05	Encoded TIF	SN2023_004_R_ETRS89_UTM32N
SBP Horizon BSL Grids H20	Encoded TIF	SN2023_004_R_ETRS89_UTM32N
SBP Horizon BSL Grids H35 and H50	Encoded TIF	SN2023_004_R_ETRS89_UTM32N
SBP Horizon DBS Grids H05	Encoded TIF	SN2023_004_R_ETRS89_UTM32N
SBP Horizon DBS Grids H20	Encoded TIF	SN2023_004_R_ETRS89_UTM32N
SBP Horizon DBS Grids H35	Encoded TIF	SN2023_004_R_ETRS89_UTM32N
SBP Isochore Grids	Encoded TIF	SN2023_004_R_ETRS89_UTM32N

## 12.2 GEOPHYSICAL SURVEY

**Table 50: Overview digital deliverables for the geophysical survey**

Deliverable	Format	Data Location
<b>All sensors</b>		
Trackplots (line)	Shapefile	SN2023_004_F_ETRS89_UTM32N
Man-made objects (point)	Shapefile	SN2023_004_F_ETRS89_UTM32N
Man-made objects (line)	Shapefile	SN2023_004_F_ETRS89_UTM32N
Man-made objects (polygon)	Shapefile	SN2023_004_F_ETRS89_UTM32N
Seabed features (point)	Shapefile	SN2023_004_F_ETRS89_UTM32N
Seabed features (line)	Shapefile	SN2023_004_F_ETRS89_UTM32N
Seabed features (polygon)	Shapefile	SN2023_004_F_ETRS89_UTM32N
Seabed geology (polygon)	Shapefile	SN2023_004_F_ETRS89_UTM32N
Catalogue of Seabed objects	PDF	108_GEOPHYSICAL_REPORT - WPA&C
<b>MBES</b>		
Despiked, motion and tidal corrected point clouds	ASCII	101_MBES - WPA&C
Bathymetric average values gridded surface 0.25m, 1m and 5m	ASCII	101_MBES - WPA&C
	Encoded TIF	SN2023_004_R_ETRS89_UTM32N
Bathymetry Total Vertical Uncertainty values gridded surface 1m	ASCII	101_MBES - WPA&C
	Encoded TIF	SN2023_004_R_ETRS89_UTM32N
Bathymetry Contours 0.5m	Shapefile	SN2023_004_F_ETRS89_UTM32N
MBES Anomaly Points	Shapefile	SN2023_004_F_ETRS89_UTM32N
Vessel Tracks	Shapefile	SN2023_004_F_ETRS89_UTM32N
<b>SVP</b>		
SVP logfiles	Raw and excel	101_MBES - WPA&C
<b>Backscatter</b>		
Gridded 1m	Encoded TIF	SN2023_004_R_ETRS89_UTM32N
	ASCII	101_MBES - WPA&C
<b>SSS</b>		
Processed SSS data	HF XTF	102_SSS – WPC
	LF XTF	102_SSS – WPC
Navigation Files	ASCII	102_SSS – WPC
SSS mosaics HF	Single band TIF	SN2023_004_R_ETRS89_UTM32N

Deliverable	Format	Data Location
SSS mosaics LF	Single band TIF	SN2023_004_R_ETRS89_UTM32N
SonarWiz 7 Project	SonarWiz Project Files	102_SSS – WPC
Target Images	Single band TIF	SN2023_004_R_ETRS89_UTM32N
SSS Anomaly Points	Shapefile	SN2023_004_F_ETRS89_UTM32N
Magnetometer		
Processed Magnetometric Data	ASCII	103_MAG - WPC
Mag Anomaly Points	Shapefile	SN2023_004_F_ETRS89_UTM32N
Total Field Grid	Encoded TIF	SN2023_004_R_ETRS89_UTM32N
Residual Signal Grid	Encoded TIF	SN2023_004_R_ETRS89_UTM32N
Analytical Signal Grid	Encoded TIF	SN2023_004_R_ETRS89_UTM32N
Altitude Grid	Encoded TIF	SN2023_004_R_ETRS89_UTM32N
Oasis Montaj Project	Oasis Montaj Project	103_MAG - WPC
SBP and UHRS		
Processed SBP data and UHRS recordings (Depth and Time)	SEGY	104_SBP_2D_URHS - WPA
SBP and UHRS instrument tracks	Shapefile	SN2023_004_F_ETRS89_UTM32N
Boulder Factor	Encoded TIF	SN2023_004_R_ETRS89_UTM32N
Interpretation of post-processed seismic data	ASCII	104_SBP_2D_URHS - WPA
Horizon interpretation depth BSL gridded surface	ASCII	104_SBP_2D_URHS - WPA
	Encoded TIF	SN2023_004_R_ETRS89_UTM32N
Horizon interpretation depth below seabed gridded surface	ASCII	104_SBP_2D_URHS - WPA
	Encoded TIF	SN2023_004_R_ETRS89_UTM32N
Isochore gridded surface	ASCII	104_SBP_2D_URHS - WPA
	Encoded TIF	SN2023_004_R_ETRS89_UTM32N
Processing Project	Kingdom Project Files	104_SBP_2D_URHS - WPA
Grab Sampling		
Grab Sample Positions	Shapefile	SN2023_004_F_ETRS89_UTM32N
Grab Sample Classifications	Excel Doc	108_GEOPHYSICAL_REPORT - WPA&C
Grab Sample Lab Analysis	Excel Doc	108_GEOPHYSICAL_REPORT - WPA&C
Reports		
Mob and Cal Report	PDF	Energinet SharePoint
Operations Report	PDF	Energinet SharePoint
Technical Report	PDF	Energinet SharePoint
GIS		
Trackplots (all sensors)	Shapefile	SN2023_004_F_ETRS89_UTM32N
MBES Contours	Shapefile	SN2023_004_F_ETRS89_UTM32N
MBES Anomalies	Shapefile	SN2023_004_F_ETRS89_UTM32N
MBES Grid 0.25m, 1.0m and 5.0m	Shapefiles	SN2023_004_F_ETRS89_UTM32N
MBES THU Grid 1.0m	Shapefile	SN2023_004_F_ETRS89_UTM32N
MBES TVU Grid 1.0m	Shapefile	SN2023_004_F_ETRS89_UTM32N
Backscatter Grid 1.0m	Shapefile	SN2023_004_F_ETRS89_UTM32N
Boulder factor	Encoded TIF	SN2023_004_R_ETRS89_UTM32N
SBP Horizon BSL Grids H05	Encoded TIF	SN2023_004_R_ETRS89_UTM32N



<b>Deliverable</b>	<b>Format</b>	<b>Data Location</b>
SBP Horizon BSL Grids H20	Encoded TIF	SN2023_004_R_ETRS89_UTM32N
SBP Horizon BSL Grids H30	Encoded TIF	SN2023_004_R_ETRS89_UTM32N
SBP Gas BSL Grids	Encoded TIF	SN2023_004_R_ETRS89_UTM32N
SBP Horizon DBS Grids H05	Encoded TIF	SN2023_004_R_ETRS89_UTM32N
SBP Horizon DBS Grids H20	Encoded TIF	SN2023_004_R_ETRS89_UTM32N
SBP Horizon DBS Grids H30	Encoded TIF	SN2023_004_R_ETRS89_UTM32N
SBP Gas DBS Grids	Encoded TIF	SN2023_004_R_ETRS89_UTM32N
SBP Isochore Grids	Encoded TIF	SN2023_004_R_ETRS89_UTM32N
<b>Charting</b>		
Trackplots and sampling locations	PDF	108_GEOPHYSICAL_REPORT - WPA&C
Bathymetry	PDF	108_GEOPHYSICAL_REPORT - WPA&C
Backscatter	PDF	108_GEOPHYSICAL_REPORT - WPA&C
Seabed Surface Classification	PDF	108_GEOPHYSICAL_REPORT - WPA&C
Seabed Objects	PDF	108_GEOPHYSICAL_REPORT - WPA&C
Seabed Features	PDF	108_GEOPHYSICAL_REPORT - WPA&C
Sub-seabed Geology	PDF	108_GEOPHYSICAL_REPORT - WPA&C

---

## REFERENCES

- Gardline 2021. Geotechnical Report, Preliminary Investigation, Hesselø OWF. Volume II: Measured and Derived Geotechnical Parameters and Final Results – Interim CPT Report. Project no. 11596. Client reference 20/07944, rev. 2, date 22.11.2021.
- Fugro. Geophysical Results Report. Energinet Denmark Hesselø Geophysical Survey | Denmark, Inner Danish Sea, Kattegat. F172145-REP-GEOP-001 02 | 13 August 2021. Final
- Jensen, J. B., Bennike, O., 2020; General geology of the southern Kattegat, the Hesselø wind farm area, Desk Study. Report for Energinet Eltransmission A/S. GEUS.
- Jensen, J. B., Petersen, K. S., Konradi, P., Kuijpers, A., Bennike, O., Lemke, W. & Endler, R. 2004: Neotectonics, sea-level changes and biological evolution in the Fennoscandian Border Zone of the southern Kattegat Sea. *Boreas*, Vol. 31, pp. 133–150. Oslo.
- Bendixen, C., Jensen, J.B. Boldreel, L. O., Claousen, O. R., Seidenkrantz, M.-S., Nyberg, J., Hübscher, C. 2015 - The Holocene Great Belt connection to the southern Kattegat, Scandinavia: Ancylus Lake drainage and Early Littorina Sea transgression. *Boreas* 10.1111/bor.12154.
- Bendixen, C., Boldreel, L. O., Jensen, J. B., Bennike, O., Hübscher, C., Clausen, O. R. 2017: Early Holocene estuary development of the Hesselø Bay area, southern Kattegat, Denmark and its implication for Ancylus Lake drainage. *Geo Mar Lett*.
- Lykke-Andersen, H, Seidenkrantz, M.-S. & Knudsen, K. L. 1993. Quaternary sequences and their relations to the pre-Quaternary in the vicinity of Anholt, Kattegat, Scandinavia. *Boreas*, bind 22, nr. 4, s. 291-298
- Rambøll 2021. Geotechnical Data Report. Hesselø OWF Supplementary VC – Gilleleje.
- Jensen, P., Aagaard, I., Burke, R. A., Dando, P. R., Jørgensen, N. O., Kuijpers, A., Laier, T., O’Hara, S. C. M., Schmaljohann, R. 1992. ‘Bubbling reefs’ in the Kattegat: submarine landscapes of carbonate cemented rocks support a diverse ecosystem at methane seeps. *Marine Ecology Progress Series* Vol. 83 pp. 103-112
- General Geology of the Southern Kattegat, the Hesselø wind farm area. Desk Study. Jørn Bo Jensen
- Chester K. Wentworth. A Scale of Grade and Class Terms for Clastic Sediments: University of Iowa, 1922
- Robert L. Volk. The distinction between Grain Size and Mineral Composition in Sedimentary-Rock Nomenclature; *Journal of Geology*, Vol 62, Number 4, July 1954



---

**APPENDIX A. HESSELØ SOUTH – UHR SEISMIC PROCESING REPORT**





---

**APPENDIX B. SURFICIAL GEOTECHNICAL GROUND-TRUTHING REPORT**